MULTI SHOOTER LOCALIZATION WITH ACOUSTIC SENSORS

A THESIS SUBMITTED TO
THE GRADUATE SCHOOL OF NATURAL AND APPLIED SCIENCES
OF
MIDDLE EAST TECHNICAL UNIVERSITY

BY

ÇAĞLAR AKMAN

IN PARTIAL FULFILLMENT OF THE REQUIREMENTS
FOR
THE DEGREE OF MASTER OF SCIENCE
IN
ELECTRICAL AND ELECTRONICS ENGINEERING

SEPTEMBER 2017

Approval of the thesis:

MULTI SHOOTER LOCALIZATION WITH ACOUSTIC SENSORS

Submitted by **ÇAĞLAR AKMAN** in partial fulfillment of the requirements for the degree of **Master of Science in the Department of Electrical and Electronics Engineering, Middle East Technical University** by,

Prof. Dr. Gülbin Dural Ünver,
Dean, Graduate School of **Natural and Applied Sciences**   _____

Prof. Dr. Tolga Çiloğlu
Head of Department, **Electrical and Electronics Engineering**   _____

Prof. Dr. Mehmet Kemal Leblebicioğlu
Supervisor, **Electrical and Electronics Engineering, METU**   _____

Examining Committee Members:

Prof. Dr. Tolga Çiloğlu
Electrical and Electronics Engineering, METU   _____

Prof. Dr. Mehmet Kemal Leblebicioğlu
Electrical and Electronics Engineering, METU   _____

Assist. Prof. Dr. Elif Vural
Electrical and Electronics Engineering, METU   _____

Assist. Prof. Dr. Sevinç Figen Öktem
Electrical and Electronics Engineering, METU   _____

Assist. Prof. Dr. Ahmet Güneş
Mechatronics Engineering, ATILIM UNIVERSITY   _____

Date: _06.09.2017_

I hereby declare that all information in this document has been obtained and presented in accordance with academic rules and ethical conduct. I also declare that, as required by these rules and conduct, I have fully cited and referenced all material and results that are not original to this work.

Name, Last name: **Çağlar AKMAN**

Signature   : _____

ABSTRACT

MULTI SHOOTER LOCALIZATION WITH ACOUSTIC SENSORS

AKMAN, Çağlar

M.S, Department of Electrical and Electronics Engineering

Supervisor: Prof. Dr. Mehmet Kemal Leblebicioğlu

September 2017, 104 pages

This thesis proposes a generalized estimation framework for acoustic based shooter localization system relying on time of arrival (ToA) and direction of arrival (DoA) of gunshot acoustic events, namely muzzle blast and shockwave. This framework is valid in case both acoustic events are present or one of them is missing. Furthermore, it provides a solution not only for a single shooter but also for simultaneous multiple shooters. As regards to details, this thesis proposes a DoA estimation method based on beamforming for simultaneous multi shooter detection in reverberant environment. A system calibration method for adjusting microphone positions in the microphone array and estimating local speed of sound to enhance shooter localization accuracy is also proposed in this thesis. Finally, this thesis proposes an architecture and a hardware design for the implementation of this acoustic based shooter localization system.

Keywords: Shooter Location Estimation, Simultaneous Multiple Acoustic Source Detection, Beamforming, Acoustic System Calibration, Acoustic Embedded System Design

ÖZ

AKUSTİK ALGILAYICILAR İLE ÇOKLU ATIŞ KONUM TESPİTİ

AKMAN, Çağlar

Yüksek Lisans, Elektrik ve Elektronik Mühendisliği Bölümü

Tez Yöneticisi: Prof. Dr. Mehmet Kemal Leblebicioğlu

Eylül 2017, 104 sayfa

Bu tez, atış kaynaklı namlu sesi ve şok dalgasından elde edilen varış zamanı ve varış yönü bilgilerinden faydalanan akustik tabanlı atış konum tespiti yöntemi sunmaktadır. Bu sunulan yöntem hem her iki akustik olayın hem de akustik olaylardan birinin eksik olduğu durumda geçerlidir. Bu yöntem sadece tek atış kaynağı için değil ayrıca eş zamanlı ve çoklu atış kaynak tespitine de olanak sağlamaktadır. Bu bağlamda, eş zamanlı ve çoklu atış kaynak tespiti için hüzme oluşturma temelli bir varış zamanı tespit yöntemi bu tezde anlatılmaktadır. Bunların yanı sıra, bu tezde atış konum tespiti doğruluğunun arttırılması için mikrofon dizinindeki mikrofon pozisyonlarını doğru olarak ayarlamak ve ortam ses hızını tahmin etmek için sistem kalibrasyon yöntemi sunulmaktadır. Ayrıca, akustik tabanlı atış konum tespitine yönelik olarak donanım mimari ve tasarımı bu tez içinde sunulmaktadır.

Anahtar Kelimeler: Atış Konum Tespiti, Eşzamanlı Çoklu Akustik Kaynak Tespiti, Hüzme Oluşturma, Akustik Sistem Kalibrasyonu, Akustik Gömülü Sistem Tasarımı

To My Wife

ACKNOWLEDGEMENTS

I wish to express my deepest gratitude to my supervisor Prof. Dr. Mehmet Kemal Leblebicioğlu for his guidance, advice, criticism, and insight throughout the research.

I would also like to thank Dr. Tolga Sönmez for his encouragement and guidance throughout the research. I gratefully acknowledge him for his very valuable advice and criticism to this thesis.

Finally, and most importantly, none of this could have happened without my wife Emine, love of my life. I would like to thank her for standing beside me throughout my life and this research. She offered her support, encouragement, patience, and love at every moment of this research. Her tolerance of my long hour studies, while she was taking care of our home and our children, qualifies her a very special person. This accomplishment would not have been possible without her. I would also thank my sons Kuzey and Rüzgar for making life enjoyable and meaningful. Thank you all, I am so glad I have you all in my life.

TABLE OF CONTENTS

LIST OF TABLES

TABLES

LIST OF FIGURES

FIGURES

LIST OF ABBREVIATIONS

AoA	:	Angle of Arrival
BF	:	Beamforming
DoA	:	Direction of Arrival
DSBF	:	Delay-and-Sum **BF**
GCC	:	Generalized Cross Correlation
LMS	:	Least Mean Square
MB	:	Muzzle Blast
PSBF	:	Phase Shift Beamformer
SNR	:	Signal to Noise Ratio
SPL	:	Sound Pressure Level
SRP	:	Steered Response Power
SW	:	Shockwave
TDoA	:	Time Difference of Arrival
ToA	:	Time of Arrival
UCA	:	Uniform Circular Array
ULA	:	Uniform Linear Array
WB-SRPBF	:	Wide Band Steered Response Power Beamformer

CHAPTER 1

INTRODUCTION

The security is a prominent need throughout the history of humanity. It is true not only for the individuals but also for the countries; therefore, the governments allocate funds for military and civil security systems. Regular security systems basically consist of wide area surveillance, perimeter protection, and distributed intrusion detection subsystems. Security system solutions vary and extend to enhance situational awareness according to the resultant requirements for threat analysis.

Shooter detection and localization systems are auxiliary subsystems for security systems. The main purpose of these systems is to provide security units to take an action before or after attacks in daylight and in night darkness even if attackers are not in the line of sight. Such systems are required for military facilities, camps, and special operations forces as well as civil critical facilities, carrying a high potential risk of armed attack. There is a study gathering and reviewing the historical development of shooter localization systems through technological improvements (Aguilar, 2013).

An ordinary gunshot generates several acoustic and optic signatures. An acoustic signature called muzzle blast and associated optic signature called muzzle flash are caused by high-pressure gases as the projectile leaves the barrel. When the muzzle velocity is over the local speed of sound then projectile creates another acoustic signature called shockwave as it travels in the trajectory. In addition, a projectile has a thermal signature since the bullet is much hotter than the local ambient temperature. Shooter localization systems in the literature utilize optics and acoustics to detect and process those signatures to estimate range, direction, and geolocation of shooter.

There are several optic-based shooter localization systems in the literature. The VIPER counter sniper system deploys middleware IR sensors to detect muzzle flash and use

acoustic detectors to detect muzzle blasts for verification purpose (Moroz, Pierson, Ertem, & Burchick Sr., 1999). IR imaging is used for processing thermal signature of the bullet to detect trajectory and to trace back to the origin corresponding to the shooter location (Agurok, Falicoff, Alvarez, & Shatford, 2012).

Most common methods in the literature are based on processing acoustic signatures since those systems can be easily deployed to the area of interest by a single microphone array or a sensor network of microphone arrays and have estimation results with high accuracy in azimuth and elevation. In fact, such systems are commercially available and they provide various size and type of system solutions such as fixed, vehicle mounted and wearable (Magand, Donzier, & Molliex, 2004; Raytheon Corp, 2017).

Acoustic shooter localization systems fundamentally differ from each other in terms of acoustic signals in consideration, acoustic signal processing method, and location estimation framework. While some systems make use of only muzzle blast (Page & Sharkey, 1995) or only shockwave (Sallai, et al., 2013; Danicki, The shock wave-based acoustic sniper localization, 2006), many of them take into account both of those signals in order to estimate shooter direction and range with respect to shooter location estimation framework (Lédeczi, et al., 2005; Lindgren, Olof, Fredrik, & Habberstad, 2010).

Estimation framework of acoustic shooter location systems fundamentally relies on the continuous measurement of acoustic signals by spatially distributed microphones with known locations. Signal processing of acoustic events in those measurements leads to Direction of Arrival (DoA) or Angle of Arrival (AoA) information that is involved in calculations of shooter localization according to the geometry proposed by the estimation framework. There are several DoA and AoA estimation techniques based on Time Difference of Arrival (TDoA) and beamforming in the literature which can be preferred according to the type of application (Brandstein & Ward, 2013).

The success of shooter localization systems relies on several performance parameters of the estimation framework. One of the parameters is how to handle the detection of

acoustic events. It might not be possible to measure and detect both muzzle blast and shockwave signals due to the field of view (FOV) at the sensor location or signal to noise ratio (SNR). Thus, a shooter location system providing an estimation framework which is still valid in the absence of one of those acoustic events is better than that of expecting both of those acoustic events. Another parameter is the performance of signal processing methods because it is important for detecting required features of the acoustic events with high precision. The final parameter is the accuracy of DoA or AoA estimation of muzzle blast and shockwave. This estimation relies on the accuracy of signal processing as well as the accurate measurement of the system parameters such as microphone locations, the speed of sound, and the bullet speed. Thus, precise measurement of those parameters is critical to the success of shooter localization.

In addition to the performance of shooter localization systems, it is also important to analyze expectations of the end users from a shooter localization in real life. Shooter attacks may vary from a single shot of a sniper waiting in ambush to simultaneous and multiple shots in a siege. Furthermore, these attacks can occur in open terrain as well as in urban area which causes more reflections and reverberations than open terrain due to surrounding buildings. Most of the studies focus on the reverberation-free single shot case, but there are several studies involving multiple shooters and reverberation problems by applying sensor fusion on the distributed microphone array sensor network (Lédeczi, et al., 2005; Osborne, Bar-Shalom, George, & Kaplan, 2014).

In consideration of mentioned essentials of shooter localization and requirements of the system solution, the objective of the thesis is to propose a method for simultaneous multi shooter localization in a reverberant environment with acoustic sensors. Thus, the thesis defines an optimization based shooter localization framework and proposes a beamformer based DoA estimation method for simultaneous multi shooter localization and reflection elimination. In addition, the thesis studies the effects of system parameters such as microphone positions and the speed of sound in the accuracy of shooter localization and defines a TDoA based system calibration model for calibration of system parameters to enhance the accuracy of shooter localization.

The thesis finally proposes a system architecture and corresponding hardware design for acoustic based shooter localization system.

The thesis firstly describes characteristics and acoustic properties of gunshot related acoustic events, namely muzzle blast and shockwave in Chapter 2 for clarifying the acoustic based shooter localization concept. The effect of environment on gunshot acoustics in terms of change in speed of sound and reverberation is also provided in this chapter. Furthermore, the ideal mathematical expressions for both of the acoustic events based on the characteristics defined in Chapter 2 are provided in APPENDIX A and APPENDIX B. The method of converting those signals to more realistic signals by adding noise and reverberation is also described in APPENDIX C. In fact, all simulations in regard to signal detection throughout the thesis are performed with simulated muzzle blast and shockwave signals.

The thesis defines an optimization based estimation framework using ToA and DoA of muzzle blast and shockwave signals for wireless sensor network of microphone arrays in Chapter 3. In fact, there are several shooter location estimation frameworks in the literature. For example, Damarla, Kaplan & Whipps (2010) have studied shooter localization with asynchronous microphones instead of microphone arrays and they have proposed a localization method based only on time difference between ToA's of muzzle blast and shockwave. This method does not have a synchronization problem since only independent ToA's are processed, but it lacks directional information since time difference of ToA's of muzzle blast and shockwave provide information about the range. Besides, there is another study in the literature proposing a method considering both ToA and DoA of available muzzle blasts and shockwaves for localization by fusing available muzzle blast and shockwave information at different sensors in the sensor network (Völgyesi, Balogh, Nadas, Nash, & Ledeczi, 2007). This method consists of separate calculations to estimate shooter location and projectile trajectory. The localization method in the thesis fuses all available ToA's and DoA's of muzzle blasts and shockwaves at sensors in the field and utilize an optimization-based framework rather than stepwise calculations to estimate shooter location, projectile trajectory, and projectile speed. Moreover, the framework is valid if both

muzzle blast and shockwave signals are present as well as if one of the acoustic events is missed. Furthermore, it provides an estimation of shooter location estimation both for single sensor and sensor network cases. The performance and simulation results of shooter location estimation framework are present in the thesis for single sensor and sensor network of microphone arrays.

In Chapter 4, the thesis examines both TDoA and beamforming techniques for estimating DoA of acoustic events. In fact, conventional TDoA based DoA estimation technique is used for self-system calibration method described in Chapter 5. There are several TDoA based DoA estimation methods in the literature (Brandstein & Ward, 2013). This method has been studied due to its low computational demand and it is an appropriate technique for calibrating separate microphone locations of an array within the system calibration method described in the thesis. The beamforming based DoA estimation method called *Wide Band Steered Response Power Beamformer* (WB-SRPBF) is used for localization of simultaneous multi shooter and reflection elimination in a reverberant environment. There are quite a few studies in the literature on the solution of multi shooter localization problem with beamforming technique in the literature. Ramos et al (2011) have studied delay-and-sum beamformer in the time domain for multi shooter localization and reflection elimination with a tetrahedral microphone array; however, the method requires high computational power. The beamformer method proposed in this thesis is frequency based and utilize narrowband phase-shift beamformer by dividing the band into equal sub-bands to enhance computational power and the method is performed under intense muzzle blast and shockwave signals. Simulation and performance results of WB-SRPBF based DoA estimation methods are also involved in the thesis.

In Chapter 5, the thesis defines a system model and system parameters based on the location estimation framework described in Chapter 3. According to the system model, the thesis analyzes the effects of the measurement errors of the system parameters such as microphone locations and the speed of sound in the performance and accuracy of shooter location estimation. Consequently, the thesis proposes a system calibration model derived from the system model and a corresponding TDoA based calibration

method utilizing measurements of a controlled shot to enhance the performance of shooter localization. Danicki (2009) has studied a calibration method for microphone positions based on ToA measurement of shockwave at each acoustic sensor corresponding to several controlled shots. The calibration method proposed in this thesis utilizes both DoA of muzzle blast and shockwave estimated by corresponding TDoA's to calibrate microphone positions and the speed of sound to enhance the accuracy of shooter location estimation. The calibration of the system parameters and the location estimation simulations with respect to uncalibrated and calibrated system parameters are provided in the thesis.

In addition, the thesis proposes a system architecture and a hardware design in Chapter 6. There are several studies involving hardware design in the literature (Lédeczi, et al., 2005; Sallai, Lédeczi, & Völgyesi, 2011). The hardware design proposed in the thesis utilizes digital signal processor (DSP) based processing unit, MEMS microphones. In addition, it involves accelerometer, magnetometer and GPS for self-positioning and self-orientation so that the hardware architecture can be applied to stationary, vehicle-mounted or wearable systems. The hardware platform also utilizes a wireless communication unit to establish a sensor network for shooter localization.

All the simulations demonstrating the performance of shooter location estimation framework, WB-SRPBF based DoA estimation for simultaneous multiple shots, reflection elimination, and shooter localization enhancement with system calibration are provided in Chapter 7, respectively. All simulations involve proper noise levels, error models, and effect of reflections in order to emulate more realistic conditions.

Finally, the conclusion related the work described in the thesis is provided in Chapter 8. This chapter also involves possible future work and further improvements for the methods and work proposed in the thesis.

CHAPTER 2

ACOUSTIC PROPERTIES OF GUNSHOT

2.1 Overview of Gunshot Acoustics

Acoustic based shooter localization systems rely on bullet physics and measurements of gunshot acoustic events namely muzzle blast and shockwave. Muzzle blast is due to the explosion of gases at the barrel. Shockwave is caused by the supersonic motion of a projectile in the air. The characteristics of muzzle blast and shockwave are described in section 2.2 and 2.3, respectively. Shooter localization systems measure and process the acoustic signals by microphone array with known geometry to estimate parameters such as Time of Arrival (ToA), Time Difference of Arrival (TDoA) and Direction of Arrival (DoA) required for shooter location estimation framework. Acoustic events associated to a gunshot, simulated as described in APPENDIX A and APPENDIX B, are illustrated in Figure 2.1 for two microphones in an array.
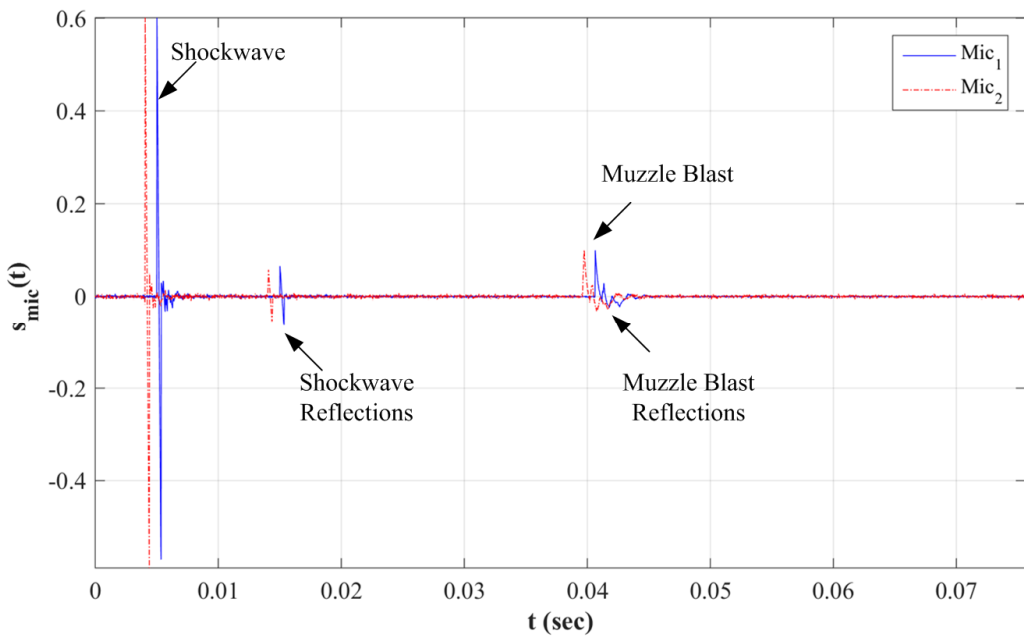
Figure 2.1: Gunshot Acoustic Events – Muzzle Blast and Shockwave

Figure 2.1 shows that there is a time difference between arrivals of same signals called TDoA due to spatially distributed microphones in the array. This time difference is used to estimate DoA as described in Chapter 4 in shooter localization. Figure 2.1 also shows that shockwave arrives at microphones before muzzle blast as muzzle blast propagates at the speed of sound from shooter location to the sensor while the shockwave, caused by a projectile moving at supersonic speed on the trajectory, propagates at speed of sound from a point on the trajectory to the sensor. This situation provides a time separation of those signals according to their features. ToA of muzzle blast is directly proportional to the distance from the shooter to the sensor. ToA of shockwave is the sum of travelling time of the projectile from the shooter to the shockwave detachment point on the trajectory and the time it takes from the trajectory to the sensor. The sound pressure level (SPL) also depends on the distance and it is inversely proportional to it. In detail, SPL of muzzle blast decreases as the distance between shooter and sensor increases and SPL of shockwave decreases as the distance between trajectory and shooter location increases. This situation determines the detection zones for the acoustic events as described in section 3.2.1.

The measurements of acoustic events of gunshot also depend on the characteristics of the gun used in a gunshot, the environmental conditions, and the properties of terrain in which measurements are performed. For instance, weapon characteristics such as projectile caliber, length, and speed determine the shape of shockwave (Whitham, 1952). In addition, the environmental conditions such as wind, pressure, temperature, and humidity affect the speed of sound which is an important parameter in shooter localization. Moreover, reverberant environments due to solid surfaces cause multiple recordings of acoustic signals called reflections as shown in Figure 2.1. Further details of environmental effects on acoustic events are provided in section 2.4.

Shooter localization systems should consider not only the typical characteristics of muzzle blast and shockwave signal but also effects of environmental conditions for signal analysis and detection. The detection methods for muzzle blast and shockwave are described in Chapter 4. The success of signal detection is important to extract information required by shooter location estimation framework.

2.2 Muzzle Blast

An ordinary gunfire creates an acoustic event called muzzle blast caused by high-pressure gases at the barrel as the projectile leaves. This signal propagates at speed of sound from shooter location to outward in a spherical shape. Sound pressure level of muzzle blast, approximately 150 dB near the muzzle, is inversely proportional to the distance between the shooter and the sensor; furthermore, it is stronger in the direction of shot (Maher & Shaw, 2008). In this thesis, muzzle blast waves are assumed to be planar waves since the range from sensor to the shooter is assumed to be long as in the far field. This is a valid assumption because the distance between shooter and sensor locations is much greater than the wavelength of gunshot acoustics.

Muzzle blast is an impulsive signal with a time duration of 3–5 msec and has frequency spectrum in between 300 Hz and 1 KHz (Mays, 2001). The signature of muzzle blast can be expressed as Friedlander-Reed wave model (Fransler, Thompson, Carnahan, & Patton, 1993). The analytical expression depending on Friedlander-Reed model of muzzle blast is provided in Appendix A. Figure 2.2 illustrates an ideal muzzle blast and its spectrum derived from the analytical expression.
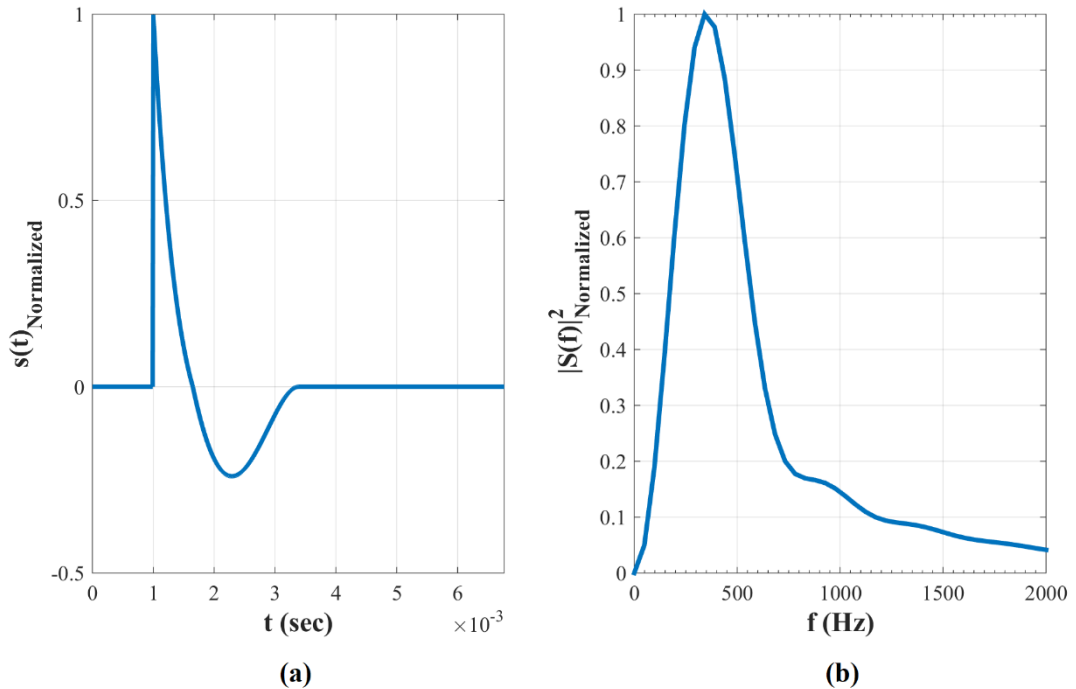
Figure 2.2: An Ideal Muzzle Blast Signal in Time (a) and Frequency (b) Domains

Ideal muzzle blast signature can be converted to a more realistic signal by applying additive white noise for simulating random processes in real world and reverberation as described in Appendix C, for simulating reflections and multipath effects. Figure 2.3 illustrates an example of more realistic muzzle blast signal involving white noise and reflections.
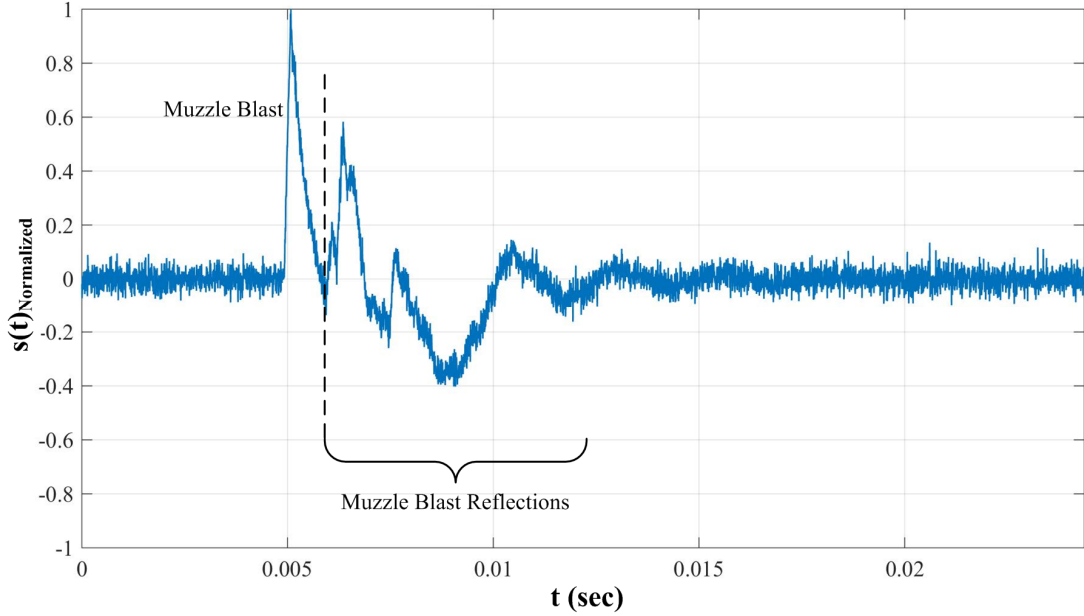
Figure 2.3: Muzzle Blast Signal with SNR of 10dB and Reflections

Shooter localization relying only on muzzle blast signals have two main deficiencies. First, muzzle blast SPL can be suppressed by a silencer, which causes the signal to be missed due to low SNR. The second deficiency is the directional property of muzzle blast. In detail, muzzle blast is highly subject to reflections and diffractions due to surrounding objects. For example, a sensor deployed in the field might measure only the diffracted muzzle blast signal due to solid surfaces around if there is an obstacle hindering the shooter from the field of view of the sensor and there are solid surfaces around. In such a case, DoA estimation would be incorrect since it is done according to the reflected signal. This problem can be resolved by deploying multiple sensors in the field. Furthermore, acoustic shooter localization systems consider both muzzle blast and shockwave for accurate shooter location estimation, in case the gunfire is a supersonic shot.

2.3 Shockwave

Shockwave is another acoustic event associated with a supersonic shot. The shot is called supersonic when the projectile travels at a higher speed than the speed of sound. The supersonic projectile generates conic shape shockwaves due to the sound barrier as it travels on the trajectory in the air (Whitham, 1952). The shape of shockwave cone can be described by the ratio of the speed of projectile v to the local speed of sound c which is called Mach number M as a dimensionless quantity shown in (1).

$$M = \frac{v}{c} \tag{1}$$

The projectile propagating at speed of v forms the vertex of the cone, shockwaves traveling at speed of c escapes the bullet trajectory with an angle of θ_M. This can be described geometrically as shown in Figure 2.4 and formulated as (2); thus, shockwave cone angle θ_M can be calculated as (3) from the geometry.
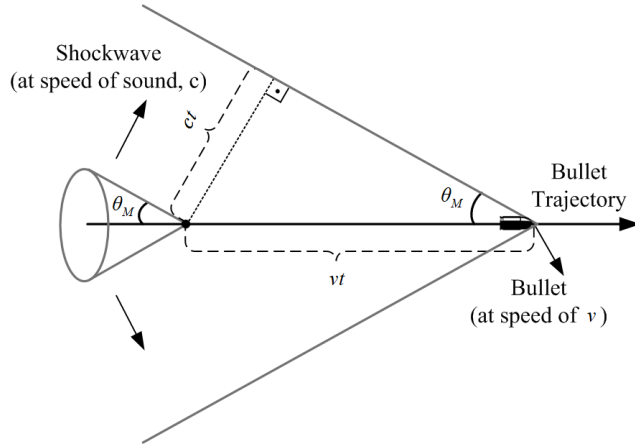
Figure 2.4: Shockwave Cone Geometry and Cone Angle

$$\sin(\theta_M) = \frac{ct}{vt} \tag{2}$$

$$\theta_M = \arcsin(1/M) \tag{3}$$

$$M > 1, \ 0 < \theta_M < \pi/2$$

Equation (3) is valid under certain assumptions such that shockwave is a plane wave; the projectile has a constant velocity and trajectory is a straight line. Although those

assumptions are valid for an accurate shooter localization, there are more realistic approaches involving bullet deceleration and curvilinear projectile trajectory in the literature (Danicki, The shock wave-based acoustic sniper localization, 2006). The thesis also assumes that shockwaves are plane waves likewise muzzle blasts and projectile travels at a constant speed on a straight trajectory.

Equation (3) also states that the speed of projectile changes the shape of shockwave cone; in turn, DoA of shockwave which is an essential parameter in the estimation of trajectory and shooter location. Hence, a prior knowledge of bullet velocity should be provided to shooter localization framework or this parameter should be estimated by the framework. The speed of sound should also be known by the framework not only for trajectory estimation but also for shooter localization. Further details of the proposed estimation framework are provided in Chapter 3.

Shockwave signals have a distinctive shape of 'N' due to short rising times around 1 μsec at the beginning and end of the signal (Whitham, 1952). It is an impulsive signal likewise muzzle blast. However, it has a shorter time duration than muzzle blast of 200–500 μsec and has a frequency band in between 1 KHz and 10 KHz (Lédeczi, et al., 2005). Figure 2.5 illustrates an example of ideal shockwave signal and its power spectrum derived from the analytical expression described in Appendix B. Figure 2.6 shows more realistic shockwave involving noise and reflections.

(a)   (b)
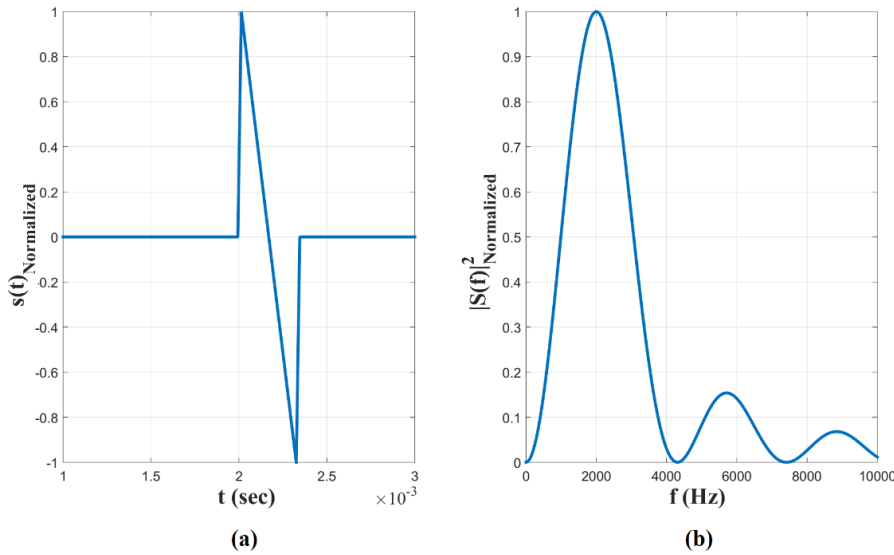
Figure 2.5: An Ideal Shockwave Signal in Time (a) and Frequency (b) Domains

12
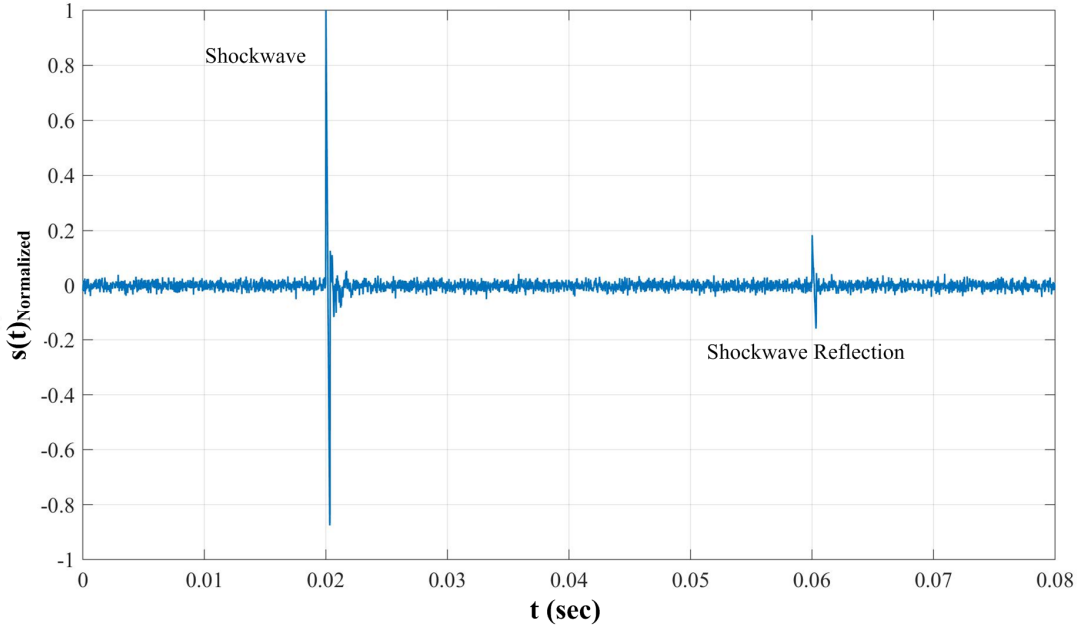
Figure 2.6: Shockwave Signal with SNR 10dB, and reflection

Shockwaves provide much more information than the muzzle blast signal. While muzzle blast signal gives information only about shooter location, shockwave provides information about shooter location as well as projectile trajectory and weapon type. Whitham (1952) has related shockwave wavelength T to caliber Φ and length l of weapon, Mach number M, speed of sound c and the closest distance between the trajectory and measurement point which is called miss point distance d_{MP} as (4). Bullet speed and miss distance can be calculated with the method of shooter location and projectile trajectory estimation as described in Chapter 3. There are several studies about caliber and weapon type estimation by using Whitham's equation (4) and bullet deceleration model shown in (5) (Völgyesi et al., 2007; Sallai et al., 2011). The thesis does not focus on the caliber and weapon type estimation and assumes a straight bullet path in shooter localization.

$$T = \frac{1.82 M d_{MP}^{1/4} \Phi}{c\left(M^2 - 1\right)^{3/8} l^{1/4}} \approx \frac{1.82 \Phi}{c}\left(\frac{M d_{MP}}{l}\right)^{1/4} \tag{4}$$

$$v_{Muzzle} = \sqrt{v^2 - 2ar} \tag{5}$$

v_{Muzzle} : Bullet velocity at muzzle a : Bullet decceleration
v : Average bullet velocity r : Range to shooter

13

2.4   Effects of Environment on Acoustic Events

Acoustic signals are subject to the environment. The main effects of environmental conditions on acoustic events of a gunshot can be categorized under two topics, namely reflections and change in local speed of sound.

Muzzle blast and shockwave signals are reflected due to solid surfaces and surrounding obstacles. Ground as a solid surface is the main source of reflection in open terrain and urban areas. Moreover, urban areas have much more obstacles causing in diffraction and reflection of acoustic waves. Acoustic sensors measure original signals as well as reflected signals; hence, the quality of signal detection decreases. There are several studies for detection and elimination of effects of reflection in the literature. For example, Libal and Spyra (2014) have proposed wavelet bases classification to classify muzzle blast and shockwave as well as reflections. Another example in the literature is eliminating the effect of reverberation by fusing ToA measurements of acoustic events and searching a consistent function between ToA's and estimated shooter location (Lédeczi, et al., 2005). This thesis proposes beamforming method for DoA estimation which can also be used to eliminate reflections. Elimination of reflections can be achieved by searching steered response power (SRP) above a predefined threshold. Furthermore, a fusion of DoA's and ToA's estimated by multiple sensors within a common output function in terms of shooter location is used to eliminate effects of reflection, further details and corresponding simulations are provided in section 7.4.

Shooter localization methods use the speed of sound as a system parameter which is completely dependent on environmental parameters such as temperature, humidity, pressure, and air density (Bohn, 1988). In fact, this thesis assumes dry air for practical calculation of the local speed of sound so the speed of sound can be calculated as (6).

$$c = c_0 \sqrt{1 + \frac{\vartheta}{273.15}} \tag{6}$$

ϑ : Ambient Temperature (^0C)

c_0 : Local speed of sound at 0^0C (331.3 m/s)

CHAPTER 3

ESTIMATION FRAMEWORK

3.1   Derivation of the Estimation Framework

The shooter localization framework relies on DoA's and ToA's of muzzle blast and shockwave signals to estimate shooter location and trajectory of the projectile. The formulation of the framework is derived from the geometry depicted in Figure 3.1. The geometry is constructed according to the acoustic properties described in Chapter 2 with the assumptions that the projectile is propagating at a constant speed on a straight trajectory and both of acoustic events are planar waves with respect to the sensor. In detail, the geometry consists of the allocation of sensor nodes and shooter, projectile trajectory, propagation, DoA and associated ToA of shockwave and muzzle blast and assistive geometric parameters. Figure 3.1 illustrates the geometry of estimation framework for a single sensor, this geometry can be generalized for the multi sensor case. Table 3.1 lists the detailed description of parameters in the geometry.
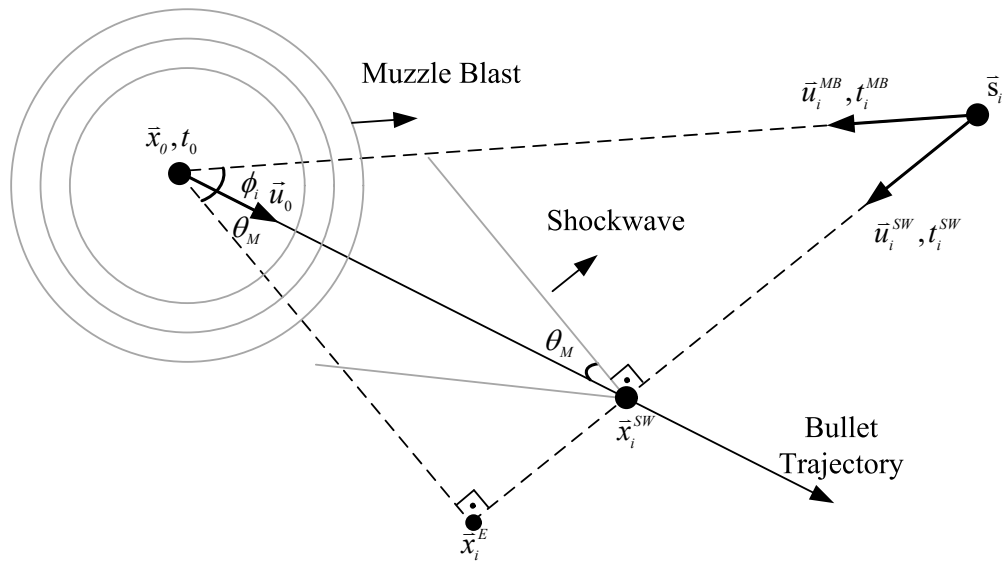
Figure 3.1: Geometry of Estimation Framework with respect to i^{th} Sensor

Table 3.1: Description of Parameters in Geometry of Estimation Framework[1]

$\vec{s}_i$	Location of i$^{\text{th}}$ sensor
t_0	Shot Time
t_i^{MB}	ToA of muzzle blast at i$^{\text{th}}$ sensor
t_i^{SW}	ToA of shockwave at i$^{\text{th}}$ sensor
$\vec{u}_i^{MB}$	DoA unit vector of muzzle blast with respect to i$^{\text{th}}$ sensor
$\vec{u}_i^{SW}$	DoA unit vector of shockwave with respect to i$^{\text{th}}$ sensor
$\vec{u}_0$	Unit vector of bullet trajectory
$\vec{x}_0$	Location of shot in Cartesian coordinates
$\vec{x}_i^{E}$	Location of imaginary edge for assistive purpose
$\vec{x}_i^{SW}$	Detachment point of shockwave with respect to i$^{\text{th}}$ sensor
θ_M	Shockwave cone angle
ϕ_i	Miss angle, angle between i$^{\text{th}}$ sensor location and the closest point on trajectory to the sensor with respect to the shooter location

Muzzle blast waves propagate omnidirectional at the speed of sound from the shooter location to outward as it is shown in Figure 3.1. Thus, DoA of muzzle blast with respect to i$^{\text{th}}$ sensor points to the shooter location and expressed as (7). The corresponding ToA can be expressed by calculating the time passed by muzzle blast propagating from the shooter location $\vec{x}_0$ to the sensor location $\vec{s}_i$ as (8).

$$\vec{u}_i^{MB} = \frac{\vec{x}_0 - \vec{s}_i}{\left\| \vec{x}_0 - \vec{s}_i \right\|_2} \tag{7}$$

$$t_i^{MB} = \frac{\left\| \vec{x}_0 - \vec{s}_i \right\|_2}{c} + t_0 \tag{8}$$

---

[1] All locations in the estimation geometry illustrated in Figure 3.1 are in 3D Cartesian coordinates.

ToA of shockwave (9) relies on both the time passed for the projectile moving at speed of v from the shooter location to shockwave detachment point $\vec{x}_i^{SW}$ and the time passed for shockwaves propagating at the speed of sound c from detachment point to sensor.

$$t_i^{SW} = \frac{\left\| \vec{x}_0 - \vec{x}_i^{SW} \right\|_2}{v} + \frac{\left\| \vec{x}_i^{SW} - \vec{s}_i \right\|_2}{c} + t_0 \tag{9}$$

If projectile speed v is expressed in terms of Mach number M and speed of sound c as (1), and if M is expressed in terms of shockwave cone angle θ_M as (2), then (10) is obtained as an expression of ToA of shockwave.

$$t_i^{SW} = \frac{\left\| \vec{x}_0 - \vec{x}_i^{SW} \right\|_2}{c} \sin(\theta_M) + \frac{\left\| \vec{x}_i^{SW} - \vec{s}_i \right\|_2}{c} + t_0 \tag{10}$$

Equation (10) can be converted to (11) by geometric operations in accordance with the geometry shown in Figure 3.1.

$$\left\| \vec{x}_i^E - \vec{x}_i^{SW} \right\|_2 = \left\| \vec{x}_0 - \vec{x}_i^{SW} \right\|_2 \sin(\theta_M)$$

$$t_i^{SW} = \frac{\left\| \vec{x}_i^E - \vec{x}_i^{SW} \right\|_2}{c} + \frac{\left\| \vec{x}_i^{SW} - \vec{s}_i \right\|_2}{c} + t_0$$

$$\left\| \vec{x}_i^E - \vec{s}_i \right\|_2 = \left\| \vec{x}_i^E - \vec{x}_i^{SW} \right\|_2 + \left\| \vec{x}_i^{SW} - \vec{s}_i \right\|_2$$

$$t_i^{SW} = \frac{\left\| \vec{x}_i^E - \vec{s}_i \right\|_2}{c} + t_0$$

$$\left\| \vec{x}_i^E - \vec{s}_i \right\|_2 = \left\| \vec{x}_0 - \vec{s}_i \right\|_2 \sin(\theta_M + \phi_i)$$

$$t_i^{SW} = \frac{\left\| \vec{x}_0 - \vec{s}_i \right\|_2}{c} \sin(\theta_M + \phi_i) + t_0 \tag{11}$$

DoA of shockwave with respect to i^{th} sensor points to detachment point of shockwave $\vec{x}_i^{SW}$ rather than the shooter location and is expressed as (12).

$$\vec{u}_i^{SW} = \frac{\vec{x}_i^{SW} - \vec{s}_i}{\left\| \vec{x}_i^{SW} - \vec{s}_i \right\|_2} \tag{12}$$

Shockwave detachment point $\bar{x}_i^{SW}$ can be calculated as (13) in accordance with the geometry proposed in Figure 3.1.

$$\bar{x}_i^{SW} = \frac{\left\|\bar{x}_0 - \bar{s}_i\right\|_2 \cos\left(\theta_M + \phi_i\right)}{\cos\left(\theta_M\right)} \bar{u}_0 + \bar{x}_0 \tag{13}$$

Substituting expression of detachment point (13) in (12) results in the expression of DoA of shockwave (14) in terms of shooter location, sensor location, cone angle and miss angle.

$$\bar{u}_i^{SW} = \frac{\left\|\bar{x}_0 - \bar{s}_i\right\|_2 \cos\left(\theta_M + \phi_i\right)\bar{u}_0 + \left(\bar{x}_0 - \bar{s}_i\right)\cos\left(\theta_M\right)}{\left\|\left\|\bar{x}_0 - \bar{s}_i\right\|_2 \cos\left(\theta_M + \phi_i\right)\bar{u}_0 + \left(\bar{x}_0 - \bar{s}_i\right)\cos\left(\theta_M\right)\right\|_2} \tag{14}$$

Both DoA and ToA of shockwave involve miss angle ϕ as a parameter. Miss angle is defined as the angle between projectile trajectory and the line joining the shooter and the sensor. Thus, miss angle is a dependent parameter and can be expressed as (15) in terms of locations of shooter and sensor projectile trajectory. The limits of miss angle are defined as (15) rather than $(0, \pi)$ which is the limits of *arccos* since it is an acute angle. This angle is used as a parameter in the estimation framework in case shockwave signal is detected by the sensor. The relation between detection zones and miss angle is described in section 3.2.1.

$$\cos\left(\phi_i\right) = \frac{\bar{s}_i - \bar{x}_0}{\left\|\bar{s}_i - \bar{x}_0\right\|_2} \bullet \bar{u}_0 \tag{15}$$

$$\phi_i = \arccos\left(\frac{\bar{s}_i - \bar{x}_0}{\left\|\bar{s}_i - \bar{x}_0\right\|_2} \bullet \bar{u}_0\right) \quad , \quad 0 < \phi_i < \frac{\pi}{2} - \theta_M$$

The shooter estimation framework is constructed by the equations of DoA's and ToA's of muzzle blast and shockwave formulated as (7), (8), (11), and (14) for each sensor. The framework consists of measured and estimated parameters. Sensor locations, ToA's and DoA's are measured parameters since sensor locations can be measured with a GPS and both ToA's and DoA's are measured in the signal detection phase described in Chapter 4. The speed of sound can be assumed as a known parameter since it can be calculated according to (6) by measuring the ambient temperature with

a temperature sensor. On the other hand, shooter location, shot time, projectile trajectory and Mach number are unknown parameters which are to be estimated. As a result, a constrained nonlinear optimization problem can be obtained by rearranging ToA's and DoA's $(\vec{u}_i^{MB}, t_i^{MB}, \vec{u}_i^{SW}, t_i^{SW})$ calculated in signal detection phase and expressions for ToA's and DoA's $(\widehat{\vec{u}_i^{MB}}, \widehat{t_i^{MB}}, \widehat{\vec{u}_i^{SW}}, \widehat{t_i^{SW}})$ as in (7), (8), (11), and (14). This constrained nonlinear optimization problem is called as the generalized shooter location estimation framework (16). Minimizing the cost function J leads to shooter location, shot time, projectile trajectory, and Mach number.

$$
f_{1i} = \widehat{\vec{u}_i^{MB}} - \vec{u}_i^{MB} = \frac{\vec{x}_0 - \vec{s}_i}{\left\| \vec{x}_0 - \vec{s}_i \right\|_2} - \vec{u}_i^{MB}
$$

$$
f_{2i} = \widehat{t_i^{MB}} - t_i^{MB} = \frac{\left\| \vec{x}_0 - \vec{s}_i \right\|_2}{c} + t_0 - t_i^{MB}
$$

$$
f_{3i} = \widehat{t_i^{SW}} - t_i^{SW} = \frac{\left\| \vec{x}_0 - \vec{s}_i \right\|_2}{c} \sin(\theta_M + \phi_i) + t_0 - t_i^{SW}
$$

$$
f_{4i} = \widehat{\vec{u}_i^{SW}} - \vec{u}_i^{SW} = \frac{\left\| \vec{x}_0 - \vec{s}_i \right\|_2 \cos(\theta_M + \phi_i) \vec{u}_0 + (\vec{x}_0 - \vec{s}_i) \cos(\theta_M)}{\left\| \left\| \vec{x}_0 - \vec{s}_i \right\|_2 \cos(\theta_M + \phi_i) \vec{u}_0 + (\vec{x}_0 - \vec{s}_i) \cos(\theta_M) \right\|_2} - \vec{u}_i^{SW}
$$

$$
\phi_i = \arccos(\frac{\vec{s}_i - \vec{x}_0}{\left\| \vec{s}_i - \vec{x}_0 \right\|_2} \bullet \vec{u}_0) \quad , \quad 0 < \phi_i < \frac{\pi}{2} \tag{16}
$$

$$
\min_{x_o, t_0, u_{,0}, M} J = \sum_{i=1}^{N} \left\| f_{1i} \right\|_2^2 + \left| f_{2i} \right|^2 + \left| f_{3i} \right|^2 + \left\| f_{4i} \right\|_2^2 \quad N : \text{Number of sensors}
$$

subject to

$$
\left\| \vec{x}_0 \right\|_2 < R_{Max}
$$
$$
t_0 > 0
$$
$$
\left\| \vec{u}_0 \right\|_2 < 1
$$
$$
1 < M < \frac{v_{Max}}{c}
$$

The constraints of the optimization problem are determined according to performance expectations for a shooter localization system. First, the constraint of shooter location $\vec{x}_0$ can be determined with respect to the detection range of the shooter localization. For example, R_{Max} might be set up to 1000 m depending on the performance values in the literature (Millet & Baligand, 2006). The constraint of shot time is determined simply such that it is a positive value. The constraint for direction of trajectory implies

that the direction vector should be a unit vector. Finally, the constraint of Mach number is determined such that shot is supersonic $M > 1$, and it is less than a predefined maximum limit which is the ratio of maximum bullet speed to measured local speed of sound. The minimum and maximum bullet speed v_{Max} can be determined as approximate values among muzzle velocities for common rifles given in publicly available online ballistics tables. For instance, it can be assumed as 1000 m/sec.

3.2 Estimation Framework Related to Acoustic Events

Outputs of the estimation framework can be categorized into two groups as principal and supplementary estimations. Shooter location and projectile trajectory are principle estimations since they provide information about where the shooter is and to where the shooter aims. On the other hand, shot time and projectile speed are supplementary estimations which are used in localization and trajectory estimation. The framework is able to output those estimations under certain conditions.

The generalized shooter location estimation framework (16) is valid in case both muzzle blast and shockwave are detected or one of them is missed because of low SNR level or sensor location avoiding signal detection as described in section 3.2.1. However, outputs of estimation framework vary with respect to the type of detected signals since the formulas related to the missed signal are removed from the estimation framework. In fact, there are three combinations of detection which can be grouped as detection of only muzzle blast, only shockwave and both muzzle blast and shockwave. Further details are provided in succeeding sections.

3.2.1 Detection Zones of Muzzle Blast and Shockwave

Detection of acoustic signals depends on the range from sensor location to the location of the acoustic source since SPL of the acoustic source is inversely proportional to distance. In the concept of shooter localization, while the range from sensor location to shooter location affects muzzle blast, the range from sensor location to projectile trajectory affects shockwave in terms of detection due to low SNR levels. Furthermore, the detection of those acoustic events depends on the geometric allocation of the

sensor, the shooter, and the trajectory line. In detail, a sensor deployed in the field may not sense shockwave not only due to SNR level but also since shockwaves never arrive at sensor due to the orientation of the trajectory line. Detection zones for muzzle blast and shockwave signals with respect to a sensor in the field are illustrated in Figure 3.2. A sensor in the shaded region can detect both of muzzle blast and shockwave, but a sensor positioned outside can only detect muzzle blast because while muzzle blast propagates in all directions, shockwave propagates from a point on trajectory $\vec{x}_i^{SW}$ with an angle of θ_M.
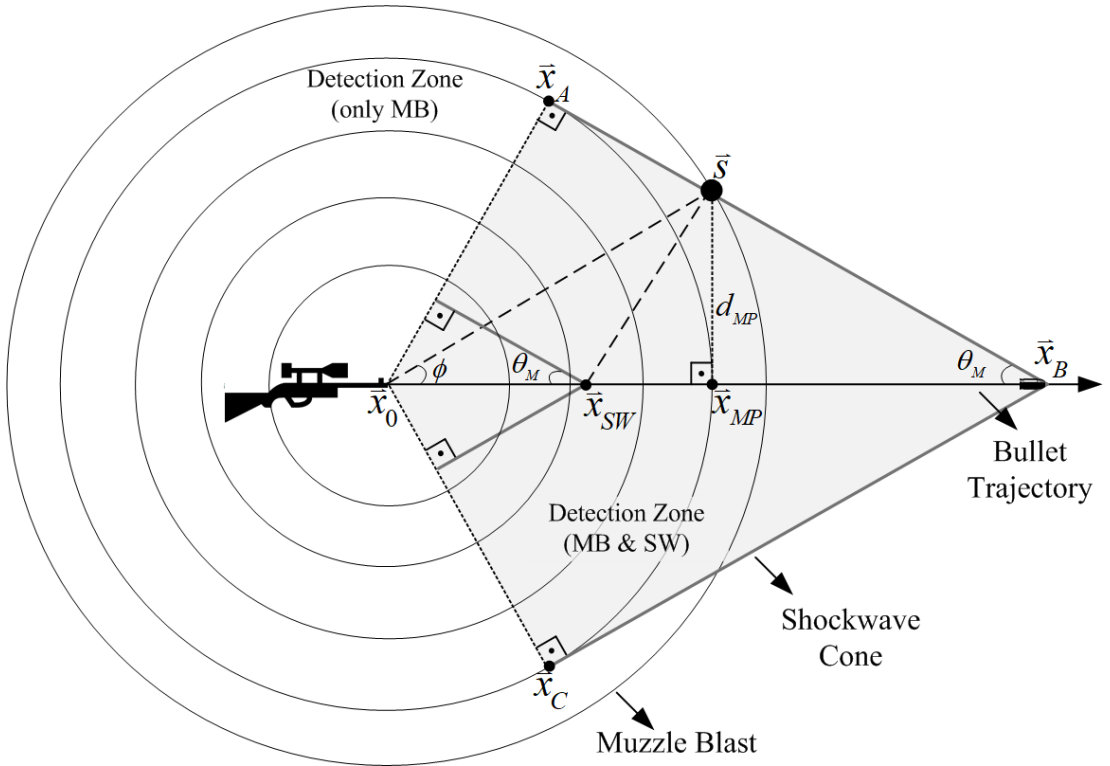
Figure 3.2: The Zones of Muzzle Blast and Shockwave in Gunshot Field

In Figure 3.2, the zone for both of muzzle blast and shockwave detection is defined as the region between the shooter location $\vec{x}_o$, cone tip of shockwave $\vec{x}_B$ and tangency points of shockwave cone front wave and muzzle blast wave $\vec{x}_A$ and $\vec{x}_C$, respectively. This region can also be defined by the miss angle ϕ, which is defined as an acute angle between trajectory and imaginary line from shooter location to sensor location. If location of the sensor approaches to tangency points then miss angle increases and if location of the sensor approaches to trajectory line the miss angle decreases. The range

of values of miss angle is defined as (17). Negative values of miss angle are not taken into consideration since it is used as a geometric angle rather than an oriented angle in the estimation framework.

$$0 \le \phi \le \frac{\pi}{2} - \theta_M \qquad (17)$$

Miss angle ϕ is also used to calculate miss distance d_{MP} which is the distance between the sensor location and the closest point on the trajectory to the sensor. Miss distance is used for caliber and weapon type estimation as (4) described in Chapter 2.

$$d_{MP} = \left\| \bar{s} - \bar{x}_0 \right\|_2 \sin(\phi) \qquad (18)$$

The miss distance can vary from 0–50 m but miss distance is about 20 m for reliable detection without ground interaction (Stoughton, 1997). Stoughton (1997) has also proposed a method for shockwave measurement at longer miss distances.

As a result, a sensor positioned in the field can always detect muzzle blast if it is not hindered by an obstacle or suppressed by a silencer or attenuated due to long range. However, trajectory line should lay in the shockwave detection zone defined by miss angle and miss distance so that a sensor can detect a shockwave generated by a supersonic projectile. Hence, acoustic based shooter localization systems should take into consideration the detection zones in the estimation process.

3.2.2 Only Muzzle Blast Detection

If only muzzle blast signal is detected by a sensor node then the generalized estimation framework (16) turns into (19) consisting of only muzzle blast dependent parameters. In this case, estimation framework can only output shooter location and shot time but it cannot estimate projectile trajectory and speed since there is no information bearing shockwave at the sensor. Furthermore, if there is a single sensor, the framework can only provide DoA of muzzle blast, but it cannot estimate the shooter location and shot time. A minimum number of two sensors are required for an estimation. As the number of the sensors increases, the accuracy of the location estimation increases. Simulation

results of shooter location and shot time estimation in case of detection of only muzzle blast signal are provided in section 7.2.1.

$$
\begin{aligned}
f_{1i} &= \widehat{\vec{u}_i^{MB}} - \vec{u}_i^{MB} &&= \frac{\vec{x}_0 - \vec{s}_i}{\left\| \vec{x}_0 - \vec{s}_i \right\|_2} - \vec{u}_i^{MB} \\
f_{2i} &= \widehat{t_i^{MB}} - t_i^{MB} &&= \frac{\left\| \vec{x}_0 - \vec{s}_i \right\|_2}{c} + t_0 - t_i^{MB} \\
&\min_{x_o, t_0} J = \sum_{i=1}^{N} \left\| f_{1i} \right\|_2^2 + \left| f_{2i} \right|^2 \quad N \geq 2 \\
&\text{subject to} \\
&\qquad\qquad \left\| \vec{x}_0 \right\|_2 < R_{Max} \\
&\qquad\qquad t_0 > 0
\end{aligned}
\tag{19}
$$

Shooter localization and shot time estimation has a common output function (20) which should be satisfied by all sensors in terms of shooter location and shot time.

$$
\vec{x}_0 = \vec{s}_i + c \left(t_i^{MB} - t_0 \right) \vec{u}_i^{MB}
\tag{20}
$$

This common output function can be utilized to reduce wrong estimations due to reflected signals measured by multiple sensors in the field. In detail, if the difference between shooter location and shot time estimations of each sensor are in a predefined convergence limits, then they can be labeled as valid estimations. Otherwise, if those estimations are not in the predefined limits and far from each other, then they can be labeled as invalid. Further details of reflection elimination are provided in section 7.4.

3.2.3   Only Shockwave Detection

If a sensor node only detects shockwave and misses muzzle blast, then it lacks direct information about shooter direction since DoA of muzzle blast pointing shot direction is absent. Instead, a sensor node has information about trajectory line and projectile. Hence, the generalized estimation framework (16) is altered to (21) excluding muzzle blast dependencies. Simulation results of projectile trajectory and speed estimation for the only shockwave detection case are provided in section 7.2.2.

23

If there is a single sensor in the field then framework cannot output any estimation the system has only DoA and ToA information of shockwave signal. If there are two or more sensors in the field and trajectory lays in between sensors then framework can estimate the speed of projectile and trajectory. Shooter location and shot time cannot be estimated with the framework (21) since a gun might have been fired at any point on the projectile trajectory which is consistent with the estimated projectile speed and trajectory. In framework (21), constraints of shooter location and shot time are involved just for consistency, in other words, the solutions for shot time and shooter location are not unique but they have consistency with respect to each sensor.

$$f_{3i} = \widehat{t_i^{SW}} - t_i^{SW} = \frac{\|\bar{x}_0 - \bar{s}_i\|_2}{c} \sin(\theta_M + \phi_i) + t_0 - t_i^{SW}$$

$$f_{4i} = \widehat{\bar{u}_i^{SW}} - \bar{u}_i^{SW} = \frac{\|\bar{x}_0 - \bar{s}_i\|_2 \cos(\theta_M + \phi_i)\bar{u}_0 + (\bar{x}_0 - \bar{s}_i)\cos(\theta_M)}{\|\|\bar{x}_0 - \bar{s}_i\|_2 \cos(\theta_M + \phi_i)\bar{u}_0 + (\bar{x}_0 - \bar{s}_i)\cos(\theta_M)\|_2} - \bar{u}_i^{SW}$$

$$\phi_i = \arccos\left(\frac{\bar{s}_i - \bar{x}_0}{\|\bar{s}_i - \bar{x}_0\|_2} \cdot \bar{u}_0\right) \quad , \quad 0 < \phi_i < \frac{\pi}{2}$$

$$\min_{u_0, M} J = \sum_{i=1}^{N} |f_{3i}|^2 + \|f_{4i}\|_2^2 \quad N \geq 2 \tag{21}$$

subject to

$$\|\bar{x}_0\|_2 < R_{Max}$$
$$t_0 > 0$$
$$\|\bar{u}_0\|_2 < 1$$
$$1 < M < \frac{v_{Max}}{c}$$

There is not an explicit common output function for only shockwave detection case not like (20) in only muzzle blast detection case. The optimization (21) results in a common projectile trajectory and speed in which all sensors in the field agree.

3.2.4 Both Muzzle Blast and Shockwave Detection

If the sensors in the field detect and measure both of muzzle blast and acoustic signals then framework (16) is used without any change. If there is a single sensor then the shooter location and the shot time can be estimated by using ToA's and DoA' of

muzzle blast and shockwave signals. However, estimation of projectile trajectory and shot time requires more than one sensor deployed in the field under appropriate conditions. For a trajectory estimation, trajectory line should pass between sensor locations. Simulation results of the case of both muzzle blast and shockwave detection for single and multiple sensors are provided in section 7.2.3.

From the geometry in Figure 3.1, shooter location can be expressed as (22) in terms of muzzle blast dependent parameters.

$$\vec{x}_0 = \vec{s}_i + c\left(t_i^{MB} - t_0\right)\vec{u}_i^{MB} \tag{22}$$

Another similar equation (23) can be obtained for the imaginary edge point $\vec{x}_i^E$ which can be interpreted as imaginary acoustic source location.

$$\vec{x}_i^E = \vec{s}_i + c\left(t_i^{SW} - t_0\right)\vec{u}_i^{SW} \tag{23}$$

This imaginary edge point can also be expressed in terms of shooter location, sensor location and DoA's of muzzle blast and shockwave as (24).

$$\vec{x}_i^E - \vec{s}_i = \left(\left(\vec{x}_0 - \vec{s}_i\right) \bullet \vec{u}_i^{SW}\right)\vec{u}_i^{SW} \tag{24}$$

Substituting (22) and (23) in (24) in terms of imaginary edge, sensor and shooter locations results in (25), an expression involving shot time in terms of known parameters. As a result, shot time can be expressed in terms of DoA's and ToA's of muzzle blast and shockwave signals by applying straightforward calculations (26).

$$c\left(t_i^{SW} - t_0\right)\vec{u}_i^{SW} = c\left(t_i^{MB} - t_0\right)\left(\vec{u}_i^{MB} \bullet \vec{u}_i^{SW}\right)\vec{u}_i^{SW} \tag{25}$$

$$\cancel{c}\left(t_i^{MB} - t_0\right)\left(\vec{u}_i^{MB} \bullet \vec{u}_i^{SW}\right)\cancel{\left(\vec{u}_i^{SW} \bullet \vec{u}_i^{SW}\right)}_1 - \cancel{c}\left(t_i^{SW} - t_0\right)\cancel{\left(\vec{u}_i^{SW} \bullet \vec{u}_i^{SW}\right)}_1 = 0$$

$$\left(t_i^{MB} - t_0\right)\left(\vec{u}_i^{MB} \bullet \vec{u}_i^{SW}\right) - \left(t_i^{SW} - t_0\right) = 0$$

$$t_0\left(1 - \left(\vec{u}_i^{MB} \bullet \vec{u}_i^{SW}\right)\right) = t_i^{SW} - t_i^{MB}\left(\vec{u}_i^{MB} \bullet \vec{u}_i^{SW}\right)$$

$$t_0 = \frac{t_i^{SW} - t_i^{MB}\left(\vec{u}_i^{MB} \bullet \vec{u}_i^{SW}\right)}{1 - \left(\vec{u}_i^{MB} \bullet \vec{u}_i^{SW}\right)} \tag{26}$$

Shooter location can be expressed as (27) by substituting (26) in (22) in terms of shot time. Consequently, both shooter location and shot time can be expressed in terms of ToA and DoA of muzzle blast and shockwave.

$$\vec{x}_0 = \vec{s}_i + c \left(t_i^{MB} - \frac{t_i^{SW} - t_i^{MB} \left(\vec{u}_i^{MB} \bullet \vec{u}_i^{SW} \right)}{1 - \left(\vec{u}_i^{MB} \bullet \vec{u}_i^{SW} \right)} \right) \vec{u}_i^{MB}$$

$$\vec{x}_0 = \vec{s}_i + c \left(\frac{t_i^{MB} - t_i^{SW}}{1 - \left(\vec{u}_i^{MB} \bullet \vec{u}_i^{SW} \right)} \right) \vec{u}_i^{MB} \tag{27}$$

Both expressions for shooter location and shot time are also common output functions for the framework (16). In other words, all DoA and ToA measurements by each sensor in the field should satisfy expression (26) and (27). Wrong estimations due to reflections can be eliminated with this common output function likewise the procedure applied with (20) in only muzzle blast detection case.

3.2.5   Properties of the Estimation Framework

The estimation framework described in this chapter is modelled so that it is valid even if one of the acoustic events is absent among recordings. However, type of estimated parameters varies depending on the present signal. All simulations regarding the type of detected signals and number of sensors in the field are provided in section 7.2.

While muzzle blast provides information about shooter location, shockwave provides projectile specific information. Thus, shot location and time can be estimated if muzzle blast is present and trajectory line and projectile speed can be estimated if shockwave is present in the recordings. The number of sensors in the field is also important for the estimation framework. A single sensor can only output ToA and DoA of the signals detected, in fact, a minimum number of two sensors are required for an estimation. In fact, there is a special case such that if both muzzle blast and shockwave signals are detected, then shooter location and shot time estimations are possible even if there is a single sensor in the field. However, there is still need of multiple-sensors in the field to estimate projectile trajectory even if both acoustic events are detected.

CHAPTER 4

TIME AND DIRECTION OF ARRIVAL ESTIMATION

4.1 Overview

Acoustic shooter localization requires precision in ToA and DoA measurements, used as essential information in the estimation framework. There are several approaches in the literature for muzzle blast and shockwave detection which can be grouped as time and frequency methods. Lédeczi, et al., (2005) proposes time domain analysis utilizing zero-crossing coder for detection and feature extraction of muzzle blast and shockwave among possible candidates. On the other hand, frequency domain based methods use wavelet analysis to classify acoustic events (Libal & Spyra, 2014; Mays, 2001). Those two methods are not superior with respect to each other, both aim to obtain ToA's and DoA's of muzzle blast and shockwave signals in precision.

Each microphone in the array continuously measures and records acoustic signals around. Recordings of each microphone are processed to detect and identify muzzle blast and shockwave and then to extract ToA and DoA of corresponding signals. This signal processing phase can be modeled by a block diagram as depicted in Figure 4.1.
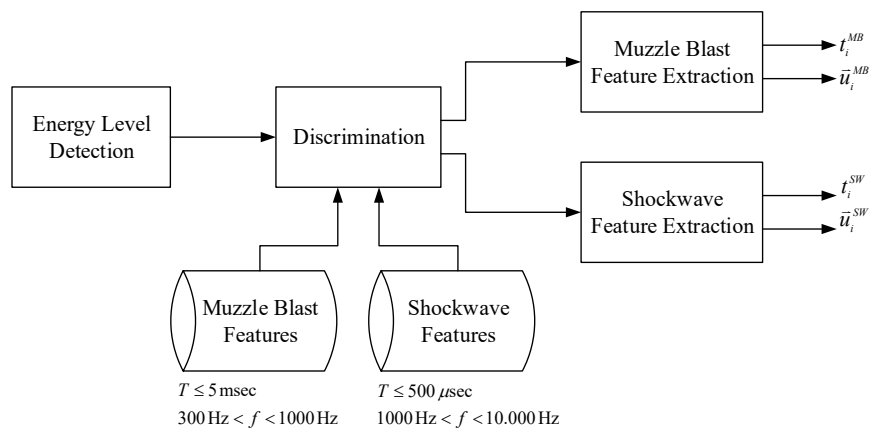
Figure 4.1: Block Diagram of Acoustic Event Analysis in a Sensor Node

Both muzzle blast and shockwave signals are transient impulsive signals with sharp rising and falling edges within a time interval. Hence, energy level detection in terms of peak detection above an amplitude threshold and time interval detection in which oscillations occur can be used to detect a list of acoustic event candidates. Resultant candidate list involves both muzzle blast and shockwave, as well as, other irrelevant impulsive signals.

After detection of acoustic event candidates in recordings of each microphone in the array, the candidate list can be narrowed down with respect to distinguishing features of muzzle blast and shockwave signals as described in Chapter 2. A candidate is simply eliminated if it does not match the required features. Furthermore, if a candidate is not measured by each microphone in the array, then it is discarded since a valid acoustic event should be measured by each microphone. In the end of discrimination process, the candidate list is narrowed down to valid signals and each valid signals are labeled as muzzle blast or shockwave.

Finally, each identified acoustic events are further processed to extract ToA and DoA to use in the estimation framework. ToA of an acoustic signal can be measured as the start time of the first edge of that signal recorded by the reference microphone in the array. DoA estimation can be realized with two different methods based on TDoA and beamforming. In TDoA technique, time differences between occurrences of the acoustic events at each microphone are calculated to estimate DoA by means of the speed of sound and the microphone array geometry. On the other hand, beamforming technique basically searches for directions maximizing steered response power to estimate DoA. Both methods aim to estimate ToA and DoA of the signals used in the estimation framework, but they are comparable in terms of real-time applications and robustness. While TDoA technique is preferred in real-time applications because of its high speed of computation, beamforming technique is preferred in applications requiring high precision due to its high accuracy of localization.

This thesis involves both of those methods. While TDoA technique, described in section 4.2, is used for system calibration method, provided in Chapter 5 and single

shooter localization, beamforming method is used for both single and multiple shooter location estimations and elimination of reflection as described in section 4.3.

4.2 TDoA Technique

TDoA technique is simply measuring time differences between ToA's of acoustic events recorded by spatially distributed microphone pairs and estimating corresponding DoA of the acoustic event providing that speed of sound is known (Brandstein & Ward, 2013). When an acoustic event occurs, it is measured by each microphone in the array with different ToA's depending on the spatial distribution of microphones. In detail, while a reference microphone measures a signal at a time, another microphone measures the same occurrence with a certain delay related to DoA of the wave, relative locations of microphones and speed of sound.

Figure 4.2 depicts a two-dimensional geometrical view of plane waves arriving at two microphones positioned at different locations with distance r on same axis, as an example. In this thesis, TDoA technique is used with an assumption that both muzzle blast and shockwave signals are plane waves due to the assumption that source location is adequately far from the sensors in the field. Otherwise, planar wave lines in Figure 4.2 should be replaced with curvilinear waves and all calculations should be revised with respect to near field assumption.
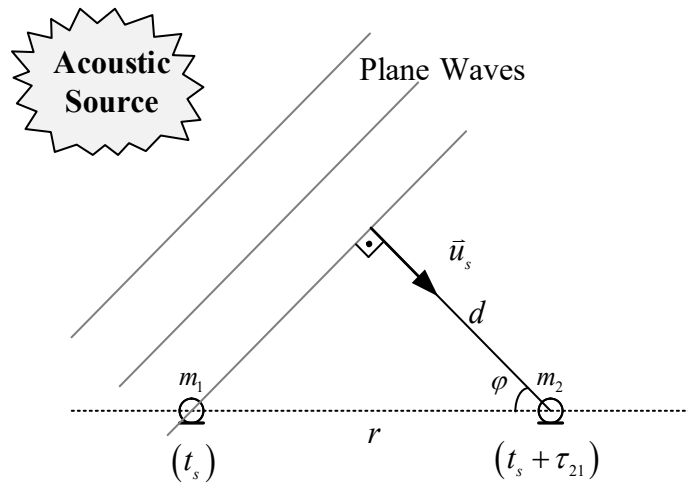
Figure 4.2: TDoA Based DoA Estimation

Figure 4.2 shows that when a plane wave propagating in the direction of $\vec{u}_s$ arrives at microphone m_1, there is still distance d for acoustic waves travelling to arrive at next microphone m_2. This distance can be expressed in terms of DoA of acoustic source and relative location vector between microphones as (28).

$$d = r \cdot \cos(\varphi)$$

$$d = \left(\left(\bar{m}_2 - \bar{m}_1 \right) \bullet \vec{u}_s \right) \tag{28}$$

Consequently, the time delay between microphones can be simply calculated as (29).

$$\tau_{21} = \frac{d}{c}$$

$$\tau_{21} = \frac{1}{c} \left(\left(\bar{m}_2 - \bar{m}_1 \right) \bullet \vec{u}_s \right) \tag{29}$$

If (28) and (29) are expanded for multiple microphones which are spatially distributed in three-dimensional microphone array, then TDoA's can be expressed as (30) with respect to reference microphone m_1.

$$\tau = \frac{1}{c} \left(A_{Diff} \, \vec{u}_s^{\,T} \right)$$

$$
\underbrace{\begin{bmatrix} \tau_{21} \\ \tau_{31} \\ . \\ . \\ . \\ \tau_{m1} \end{bmatrix}}_{R^{(m-1)x1}} = \frac{1}{c} \underbrace{\begin{bmatrix} x_2 - x_1 & y_2 - y_1 & z_2 - z_1 \\ x_3 - x_1 & y_3 - y_1 & z_3 - z_1 \\ . & . & . \\ . & . & . \\ x_m - x_1 & y_m - y_1 & z_m - z_1 \end{bmatrix}}_{R^{(m-1)x3}} \underbrace{\begin{bmatrix} u_{sx} \\ u_{sy} \\ u_{sz} \end{bmatrix}}_{R^{3x1}} \tag{30}
$$

τ : TDoA's with respect to reference microphone

A_{Diff} : Microphone positions with respect to reference microphone

$\vec{u}_s$: DoA of acoustic source, $\vec{u}_s = \begin{bmatrix} u_{sx} & u_{sy} & u_{sz} \end{bmatrix}$

m_1 : Reference microphone

m_n : Microphone at location (x_n, y_n, z_n)

τ_{n1} : TDoA between m_n and m_1

TDoA's are expressed as (30) in terms of relative microphone locations, DoA's and speed of sound. In acoustic shooter localization systems, TDoA's can be measured, but DoA is not known. DoA of an acoustic source can be estimated as the solution to the least squares optimization problem (31) derived from (30).

$$\min_{\bar{u}_s} J = \left\| \frac{1}{c}\left(A_{Diff}\, \bar{u}_s^{\,T}\right) - \tau \right\|_2^2 \tag{31}$$
$$\text{subject to}$$
$$\left\| \bar{u}_s \right\|_2 = 1$$

The solution of the optimization problem (31) can be obtained by means of Moore-Penrose pseudo inverse as (32) (Penrose, 1955).

$$\bar{u}_s^{\,T} = \tilde{A}\,\tau \tag{32}$$
$$\tilde{A} : \text{Moore-Penrose pseudo inverse of } \left(\frac{1}{c}A_{Diff}\right)$$

As (61) and (62) states that TDoA's, microphone array geometry and speed of sound are required in DoA estimation. In fact, the speed of sound can be calculated by measuring ambient temperature and applying to (6). Relative locations of microphones can be extracted from known array geometry. TDoA's are obtained by differences between ToA's of signals at each microphone, as a challenging problem.

An array of four noncoplanar microphones has been shown adequate for acoustic source localization (Alameda-Pineda, Horaud, & Mourrain, 2013). An example of non-coplanar tetrahedral shape microphone array used is shown in Figure 4.3.

Figure 4.4 illustrates an example of recorded signals by each microphone in the array shown in Figure 4.3. In this example, acoustic source is a simulated muzzle blast, as described in Appendix A, with DoA of 60° in azimuth and 30° in elevation and speed of sound is assumed to be 340 m/s. The spherical coordinate system used in this thesis is described in APPENDIX D. Time delays between microphones are observed in the recordings illustrated in Figure 4.3. In detail, waves arrive at m_3 first and m_2 latest as expected according to given DoA.
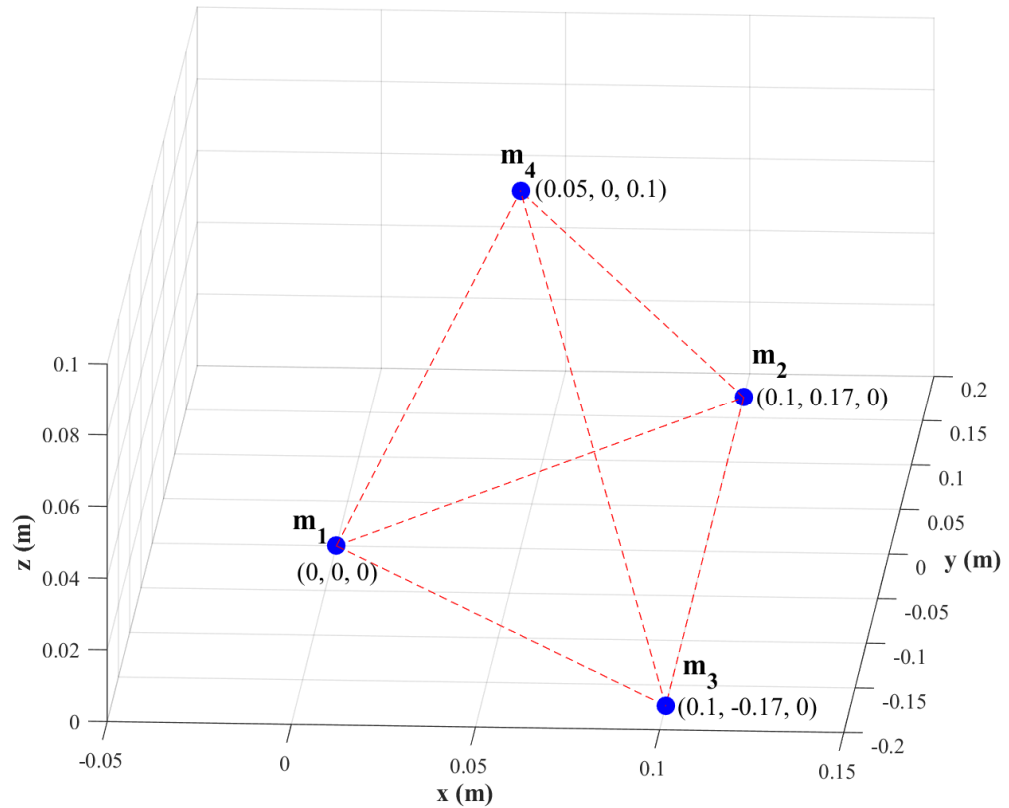
Figure 4.3: Tetrahedral Microphone Array for TDoA Based DoA Estimation
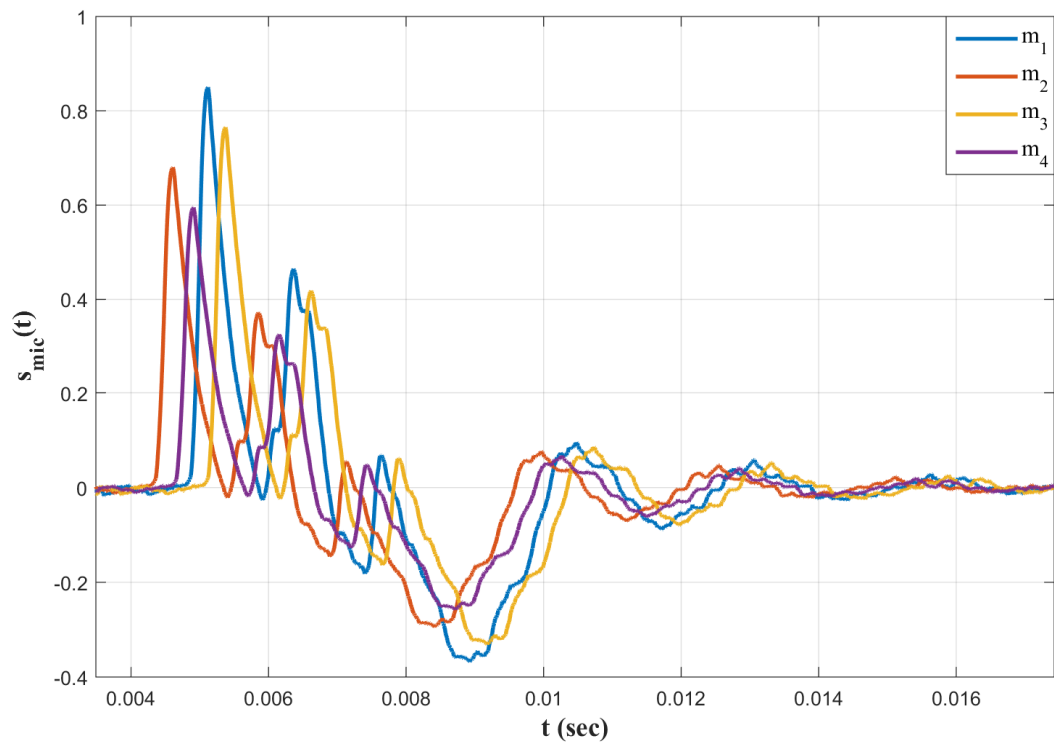
Figure 4.4: Recorded Signals by the Microphone Array in Figure 4.3

TDoA's can be estimated by methods of generalized cross-correlation (GCC) known in the literature (Svaizer, Matassoni, & Omologo, 1997). In detail, the time delay between a microphone pair maximizing GCC of that pair is set as TDoA between the pair of microphones. If this process is repeated for each microphone pair then solution set of those linear equations is obtained by minimizing the least squared error. Finally, resultant TDoA can be rearranged by setting delays of each microphone with respect to predefined reference microphone. This is important since ToA of the acoustic signal is set as estimated ToA of the reference microphone.

In TDoA based shooter localization systems, ToA is obtained by extracting start time of the first edge of acoustic events in the recording of reference microphone and then TDoA is obtained by cross-correlation between microphone recordings to estimate DoA of the acoustic event. Finally, those ToA and DoA values are used in the estimation framework described in section 3.2 for shooter localization.

TDoA based shooter localization method requires accuracy in time measurement and precision in microphone geometry. In fact, it is preferred in real-time applications due to low demand of computational process. However, the efficiency of this technique might decrease due to low SNR, strong reflections, and high reverberation. Hence, this thesis proposes another DoA estimation method based on beamforming technique for multiple shooter detections even in a reverberant environment. TDoA based technique is used in the system calibration where a controlled experiment is conducted to caliber microphone locations as described in Chapter 5. In this controlled shot, SNR level or reverberation can be adjusted so that system calibration can be performed.

4.3   Beamforming Technique

Beamforming technique is kind of a spatial filtering which enhances signals in desired directions and attenuates signals in other directions (Van Veen & Buckley, 1988). It can be applied for both received and transmitted signals in a variety of applications from tracking and searching for an object with phased-array RADAR (Brookner, 1985) to source localization in SONAR (Kneipfer, 1992) and directional transmission and reception in communication (Adams, Horowitz, & Senne, 1980). The main purposes

of beamforming technique are to increase SNR for plane wave signals, to resolve and discriminate plane waves arriving from varying directions and finally estimate the directions of arriving plane waves. There are several beamforming techniques in the literature varying from non-adaptive beamforming methods such as delay-and-sum beamforming (DSBF), interpolation and phase-shift to adaptive beamforming.

Mucci (1984) has compared the efficiency of several non-adaptive beamformers with respect to their spectral characteristics and hardware requirements. According to his study, phase-shift beamformer is the most efficient method among the others but efficient for narrowband applications; on the other hand, conventional DSBF is the least complex method and applicable for wideband signals but demands high hardware requirements in terms of memory and sampling rate. In shooter localization concept, Ramos et al (2011) has studied time domain SRP technique with array of four microphones placed 25 cm apart from each other and high sampling rate of 96 KHz for DoA estimation in gunshot acoustics, and they later (2013) have studied background noise reduction to enhance acoustic event detection in acoustic shooter localization. However, Mucci (1984) has shown that this method requires high computational power.

This thesis utilizes a frequency domain wide band steered response power (SRP) based on the concept of phase-shift beamformer (PSBF), which is called as wideband steered response power beamformer (WB-SRPBF) in this thesis. In detail, the method utilizes narrow bandpass filters at different bands and Hilbert transformation. The thesis uses this method for several reasons. First, it is a robust method and it can be applied to near real-time applications due to its moderate computational demand; however, TDoA technique is still more adequate for real-time applications than beamformer method. In fact, both Hilbert transform and narrow bandpass filters are involved in the method to increase computational speed. In detail, Hilbert transformation is used to obtain an analytical signal and to remove the negative frequency side; furthermore, the bulk of narrow bandpass filters are used to reduce the computation required to process full band. Second, it can be used for wideband signals like shockwave with a bandwidth of about 10 KHz and muzzle blast with a moderate bandwidth of about 1

KHz. Finally, it requires an appropriate sampling rate of 52 KHz. Besides, this technique is applied not only for a single shot but also for simultaneous multiple shots even in noisy and reverberant environments. Resultant simulations and tests of the beamformer method are provided in section 7.3.

In this method, a microphone array with proper geometry electronically scans azimuth and elevation angles for muzzle blast and shockwave. The spherical coordinate system used in this thesis is described in APPENDIX D. Continuous measurements of SRP levels in steered angles are compared with a predefined threshold value to obtain a list of candidate acoustic events arriving from that direction. The list of candidates which are also associated with estimated DoA is narrowed down according to features of muzzle blast and shockwave, as described in Chapter 2.

The resultant list of acoustic events which are labeled as muzzle blast and shockwave signals might still involve both original and reflected signals, although most of the attenuated reflections have already been eliminated in power level comparison. Those remainder reflections can be eliminated by the common output functions described in section 3.2 for each type of detected acoustic events. Figure 4.5 depicts a block diagram of WB-SRPBF applied to gunshot acoustics.
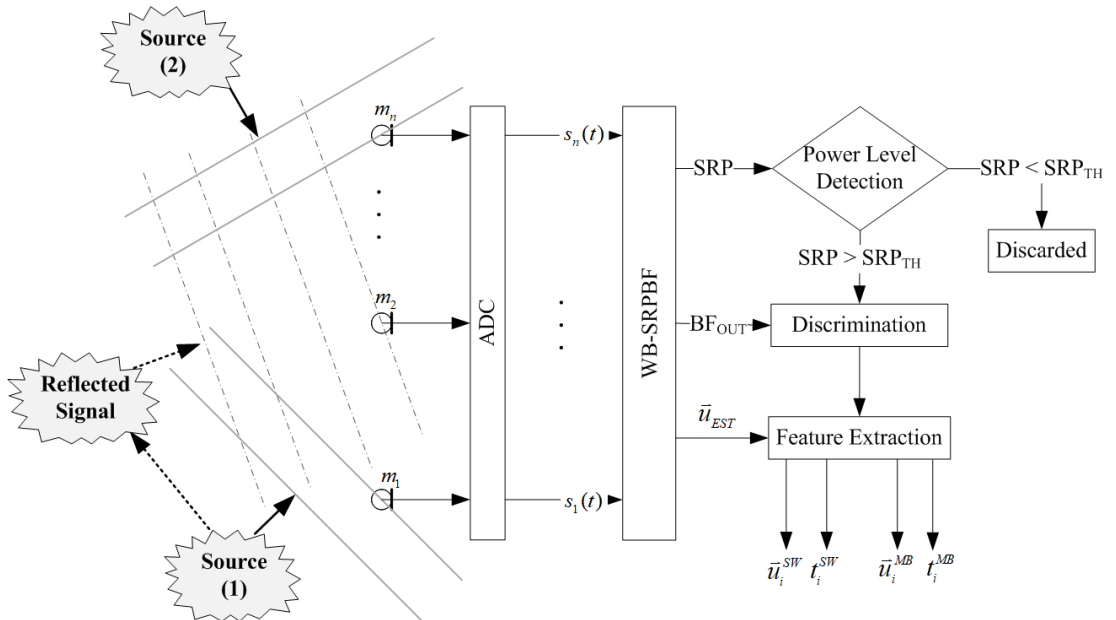
Figure 4.5: WB-SRPBF Block Diagram for Gunshot Acoustics

WB-SRPBF is a hierarchical method in which narrowband SRP of beamformer at predefined frequencies are calculated in sub-blocks and then SRP of each sub-block is summed up to obtain overall SRP. Block diagram of a single sub-block of WB-SRPBF is shown in Figure 4.6.
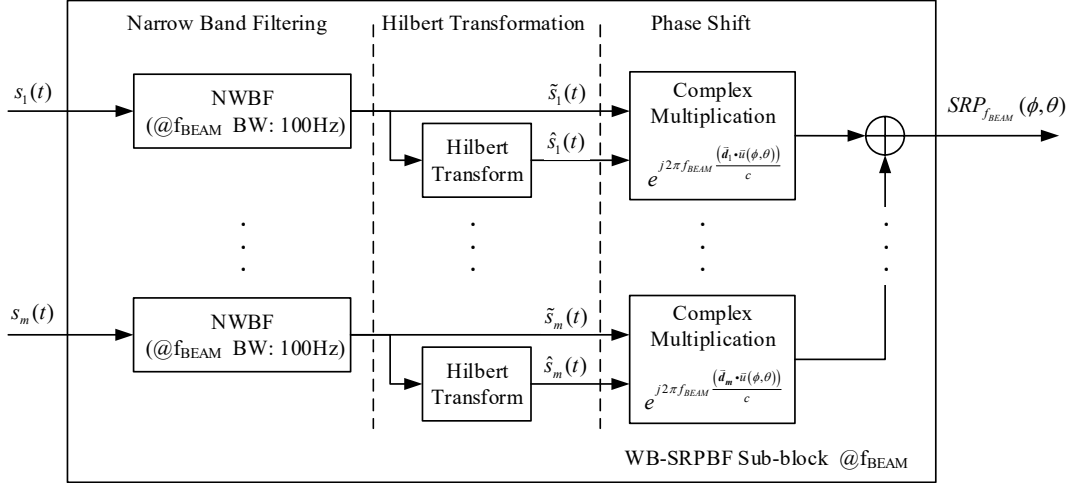
Figure 4.6: Block Diagram of Single Sub-Block of WB-SRPBF @ f$_{BEAM}$

WB-SRPBF sub-blocks relies on phase-shift beamformer concept. In detail, each sub-block is assigned with a fixed operating frequency f_{BEAM} starting from 300 Hz to 10 KHz with 100 Hz increments. Furthermore, narrow band pass filters in each sub block is assigned with a central frequency equal to operating frequency of the corresponding sub-block and a bandwidth of 100 Hz. Consequently, there are plenty of sub-blocks operating as PSBF at different bands between 300 Hz-10 KHz, which involves both muzzle blast and shockwave signals. Besides, the upper limit of the bandwidth can be set as 3-4 KHz to reduce the computation time because frequency components of shockwave is intense in between 1-4 KHz and muzzle blast bandwidth is between 300 Hz and 1 KHz. These limits are still appropriate for and accurate DoA estimation.

Each signal processed in WB-SRPBF shown in Figure 4.6 has a number of samples corresponding to a time window of 10 msec so that window size is adequate for both muzzle blast having a duration of 3–5 msec and shockwave having a duration about 200–500 μsec. Furthermore, each window overlaps with a half-length of window size to guarantee to detect the signals not fitting the frame.

36

As shown in Figure 4.6, signal recorded in each microphone is filtered by narrowband filter with central frequency of f_{BEAM} and a fixed bandwidth f_{BW} as (33). The reason of using narrow band filter is to divide wideband into sub bands to process each sub bands instead of whole bandwidth. There are hardware efficient implementations in the literature (Awasthi & Raj, 2014), most efficient method can be implemented according to requirements of the application.

$$\tilde{s}_i[n] = h_f[n] * s_i[n] \tag{33}$$

$$h_f[n] = \cos(2\pi f_{BEAM} n) \frac{\sin(2\pi f_{BW} n/2)}{2\pi f_{BW} n/2}$$

The filtered signal $\tilde{s}_i[n]$ is altered to analytical signal $\boldsymbol{S}_i[n]$ by Hilbert transformation as (34) so that negative frequency components are discarded.

$$\boldsymbol{S}_i[n] = \tilde{s}_i[n] + j\,\hat{s}_i[n] \tag{34}$$

$$\hat{s}_i[n] = h_{HILBERT}[n] * \tilde{s}_i[n]$$

$$h_{HILBERT}[n] = \begin{cases} \dfrac{1 - e^{j\pi n}}{\pi n} & for \quad n \neq 0 \\ 0 & for \quad n = 0 \end{cases}$$

All analytical signals corresponding to each channel form a matrix as (35).

$$\boldsymbol{S} = \begin{bmatrix} \boldsymbol{S}_1 \\ \boldsymbol{S}_2 \\ \vdots \\ \boldsymbol{S}_{N_M} \end{bmatrix}, \quad \boldsymbol{S} \in \Re^{N_M x N_S} \tag{35}$$

N_M : Number of Microphones
N_S : Number of Samples

Then, phase shift corresponding to the set of steering angles at frequency f_{BEAM} is applied to analytical signal matrix $\boldsymbol{S}$ to find SRP at f_{BEAM}. The formulation and derivation of classical beamformer are available in the literature (Dougherty, 2008).

According to the classical beamformer formulations, cross-spectral matrix (CSM) is obtained from the analytical signal $\boldsymbol{S}$ as (36).

$$CSM = \mathbf{S} \cdot \mathbf{S}^T \tag{36}$$

CSM is converted to trimmed-CSM (37) by setting each diagonal term to 0. Allen et al., (2013, pp. 83-86) have shown that diagonal terms of CSM do not aid beamformer; instead, result in harm since they introduce channel noise to beamformer sum.

$$\overline{CSM}_{i,j} = \begin{cases} CSM_{i,j} & i \neq j \\ 0 & i = j \end{cases} \tag{37}$$

SRP corresponding to steered angles and f_{BEAM} is calculated as (38).

$$SRP\left(f_{BEAM},\phi,\theta\right) = w U^T\left(f_{BEAM},\phi,\theta\right)\overline{CSM}\,U\left(f_{BEAM},\phi,\theta\right)w \tag{38}$$

Weight vector w is assumed to be uniform (39) for N_M number of microphones.

$$w = \frac{1}{N_M}\mathbf{1}^{N_M x1} \tag{39}$$

Steering vector is set as (40) with respect to steering angle and f_{BEAM} for M number of microphones.

$$U\left(f_{BEAM},\phi,\theta\right) = \begin{bmatrix} e^{j2\pi f_{BEAM}\frac{\left(\bar{m}_1 \cdot \bar{u}(\phi,\theta)\right)}{c}} \\ e^{j2\pi f_{BEAM}\frac{\left(\bar{m}_2 \cdot \bar{u}(\phi,\theta)\right)}{c}} \\ \vdots \\ e^{j2\pi f_{BEAM}\frac{\left(\bar{m}_M \cdot \bar{u}(\phi,\theta)\right)}{c}} \end{bmatrix} \tag{40}$$

$\bar{m}_i$: Position Vector i[th] Microphone

$\bar{u}(\phi,\theta)$: Unit Vector of Direction defined by (ϕ,θ)

$$\bar{u}(\phi,\theta) = \begin{bmatrix} \cos(\theta)\cos(\phi) \\ \cos(\theta)\sin(\phi) \\ \sin(\theta) \end{bmatrix}$$

Equation (38) gives SRP map for corresponding steering angles at f_{BEAM}. This process is repeated with varying f$_{BEAM}$ from 300 Hz to 10 KHz with 100 Hz increments and

each resultant SRP value is summed to obtain overall SRP of beamformer as shown in Figure 4.7.
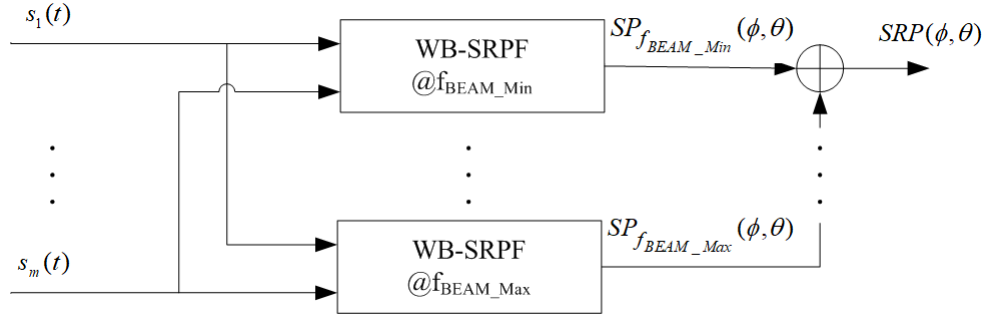
Figure 4.7: Block Diagram of Overall SRP Calculation in WB-SRPBF

DoA of a signal can be estimated as the azimuth and the elevation angles (ϕ, θ) maximizing $SRP_{normalized}(\phi, \theta)$ map as (41).

$$\max_{\phi, \theta} J = SRP_{normalized}(\phi, \theta) \tag{41}$$

Equation (41) can be altered to (42) by searching peak values above a predefined threshold so that WB-SPRBF is able to detect DoA's of multiple signal sources. In fact, the threshold can be adjusted such that the signals corresponding to the shots performed in an expected estimation range are detected with the WB-SRPBF method.

$$\boldsymbol{SRP}_{peaks} = peak_{\phi, \theta}\left(SRP_{normalized}(\phi, \theta)\right), \quad \forall \boldsymbol{SRP}_{peaks} \geq P_{TH} \tag{42}$$

$$DoA_{EST} = \begin{bmatrix} \phi_1 & \theta_1 & 1 \\ \phi_2 & \theta_2 & 1 \\ \vdots & \vdots & \vdots \\ \phi_n & \theta_n & 1 \end{bmatrix}, \quad \begin{matrix} \phi \in \phi_{peaks} \\ \theta \in \theta_{peaks} \end{matrix}$$

N_E : Number of Valid Estimations

Estimated DoA's (42) might include original signals as well as reflections. If the power level of the reflected signal is below the threshold then it is discarded during the estimation process; however, if it exceeds the threshold level than it cannot be simply discarded. In such cases, wrong estimations can be eliminated with common output

functions of estimation framework as described in Chapter 3. Simulations regarding the elimination of reflection are provided in section 7.4.

When DoA's are estimated with respect to (42), corresponding delays ΔT_i can be calculated as (43). The output of beamformer regarding to each estimated DoA is obtained by summing all delayed microphone signals as (44).

$$\Delta T_i\left(\phi_k,\theta_k\right)=\frac{-\left(\vec{m}_i\bullet\vec{u}_k\left(\phi_k,\theta_k\right)\right)}{c}, \quad k\in[1,N_E] \tag{43}$$

$$s_{out\_k}[n]=\sum_{i=1}^{N_M}w_i s_i\left[n-\Delta T_i\left(\phi_k,\theta_k\right)\right], \quad \left(\phi_k,\theta_k\right)\in DoA_{EST} \tag{44}$$

s_i : Microphone Signal

w_i : Microphone Beamformer Weight

ϕ_k : Steering Angle in Azimuth

θ_k : Steering Angle in Elevation

$\vec{u}_k$: Steering Unit Vector

$\vec{m}_i$: Position Vector of ith Microphone

N_M : Number of Microphones

N_E : Number of Valid Estimations

The beamformer output (44) can also be expressed in terms of source signal $x_s[n]$. In fact, when a signal source arrives at a microphone array then each microphone records the same signal with a delay $\Delta\tau_i$ as (45). Thus, recorded signals by each microphone can be expressed as (46).

$$\Delta\tau_i\left(\phi_s,\theta_s\right)=\frac{\left(\vec{m}_i\bullet\vec{u}_s\left(\phi_s,\theta_s\right)\right)}{c} \tag{45}$$

$$s_i[n]=x_s\left[n-\Delta\tau_i\left(\phi_s,\theta_s\right)\right], \quad 1\leq i\leq N_M \tag{46}$$

x_s : Source Signal

ϕ_s : Azimuth Angle of Arrival of Source

θ_s : Elevation Angle of Arrival of Source

$\vec{u}_s$: Unit Vector of DoA of Source

Equation (41) has a local maximum if delays ΔT_i with respect to steered angles in (44) are equal to delays $\Delta\tau_i$ due to arrival angles of source signal. In other words, estimated

arrival angles are equal to actual arrival angles of source so that beamformer results in local maximum in SRP map at corresponding angles. Hence, the beamformer output maximizing SRP map can be obtained as (47).

$$\text{If } \phi_k = \phi_s \text{ and } \theta_k = \theta_s, \text{then}$$

$$\Delta\tau_i\left(\phi_s,\theta_s\right) = \frac{\left(\vec{m}_i \cdot \vec{u}_s\left(\phi_s,\theta_s\right)\right)}{c}$$

$$\Delta T_i\left(\phi_s,\theta_s\right) = \frac{-\left(\vec{m}_i \cdot \vec{u}_s\left(\phi_s,\theta_s\right)\right)}{c}$$

$$\Delta\tau_i\left(\phi_s,\theta_s\right) = -\Delta T_i\left(\phi_s,\theta_s\right)$$

Then,

$$s_i\left[n\right] = x\left[n - \Delta\tau_i\left(\phi_s,\theta_s\right)\right]$$

$$s_{out\_k} = \sum_{i=1}^{N_M} w_i x\left[n - \cancel{\Delta\tau_i\left(\phi_s,\theta_s\right)} - \cancel{\Delta T_i\left(\phi_s,\theta_s\right)}\right]$$

$$s_{out\_k}\left[n\right] = \sum_{i=1}^{N_M} w_i x\left[n\right], \quad k \in \left[1, N_E\right] \tag{47}$$

Since each microphone weight is set uniformly as (39), (47) turns into (48).

$$s_{out\_k}\left[n\right] = \sum_{i=1}^{N_M} w_i x\left[n\right], \quad k \in \left[1, N_E\right]$$

$$w_i = \frac{1}{N_M}$$

$$s_{out\_k}\left[n\right] = x\left[n\right] \tag{48}$$

In shooter localization framework described in Chapter 3, both DoA and ToA are required. In fact, DoA is estimated with beamformer technique and ToA is estimated from the beamformer output.

Equation (48) holds for the ideal case such that estimated DoA value is exactly equal to the actual value of DoA. In fact, the accuracy of ToA estimation strictly depends on the accuracy of DoA estimation since ToA is extracted from the beamformer output signal and time shifts in the beamformer strictly depend on DoA. The angular difference between estimated DoA and actual DoA leads to erroneous time shift in microphone signals, in turn, erroneous ToA estimation as (49).

If $\phi_k = \phi_s + \phi_{err}$ and $\theta_k = \theta_s + \theta_{err}$, then

$$\Delta\tau_i(\phi_s,\theta_s) = \frac{\left(\bar{m}_i \bullet \bar{u}_s(\phi_s,\theta_s)\right)}{c}$$

$$\Delta T_i(\phi_k,\theta_k) = \frac{-\left(\bar{m}_i \bullet \bar{u}_k(\phi_k,\theta_k)\right)}{c}$$

$$\Delta T_i(\phi_k,\theta_k) = \frac{-\left(\bar{m}_i \bullet \bar{u}_k(\phi_s,\theta_s)\right)}{c} + \frac{-\left(\bar{m}_i \bullet \bar{u}_e(\phi_e,\theta_e)\right)}{c}$$

$$\Delta\tau_i(\phi_s,\theta_s) = -\Delta T_i(\phi_s,\theta_s) - \Delta T_i(\phi_e,\theta_e)$$

$$s_i[n] = x\left[n - \Delta\tau_i(\phi_s,\theta_s)\right] \quad , \quad (\phi_s,\theta_s) \in DoA_{ACT}$$

$$s_{out\_k}[n] = \sum_{i=1}^{N_M} w_i s_i\left[n - \Delta T_i(\phi_k,\theta_k)\right] \quad , \quad (\phi_k,\theta_k) \in DoA_{EST}$$

$$s_{out\_k} = \sum_{i=1}^{N_M} w_i x\left[n - \Delta T_i(\phi_e,\theta_e)\right]$$

$$s_{out\_k}[n] = x\left[n - \Delta T_i(\phi_e,\theta_e)\right] \tag{49}$$

If a microphone is set as a reference in the microphone array and its location is further set as the origin, then corresponding time delay of reference microphone becomes zero and delays in recordings of other microphones are measured with respect to the reference microphone. Furthermore, the output signal of beamformer becomes equal to the signal measured by the reference microphone as (50).

$$\bar{m}_{ref} = \begin{bmatrix} 0 & 0 & 0 \end{bmatrix}$$

$$\Delta\tau_{ref}(\phi_s,\theta_s) = \frac{\left(\bar{m}_{ref} \bullet \bar{u}_s(\phi_s,\theta_s)\right)}{c}$$

$$\Delta\tau_{ref}(\phi_s,\theta_s) = 0$$

$$s_{ref}[n] = x_s\left[n - \Delta\tau_{ref}(\phi_s,\theta_s)\right]$$

$$s_{ref}[n] = x_s[n] \tag{50}$$

The beamformer output is analyzed in discrimination process shown in Figure 4.5 and labeled as muzzle blast or shockwave. Then, ToA is extracted for beamformer output associated with estimated DoA. Finally, ToA and DoA values for muzzle blast and shockwave signals are utilized in the estimation framework described in Chapter 3 for shooter localization.

For an illustration purpose of ToA estimation, Figure 4.8 depicts an example topology for a microphone array consisting of 9 omnidirectional microphones which can be used in WB-SRPBF technique described in this section. In simulations provided in section 7.3, the number of microphones is set as 4, 8, 16 and 32. In fact, microphone array of 16 and 32 are selected for multiple shooter localization. This example is provided just for illustration purpose of ToA estimation in ideal and non-ideal cases.
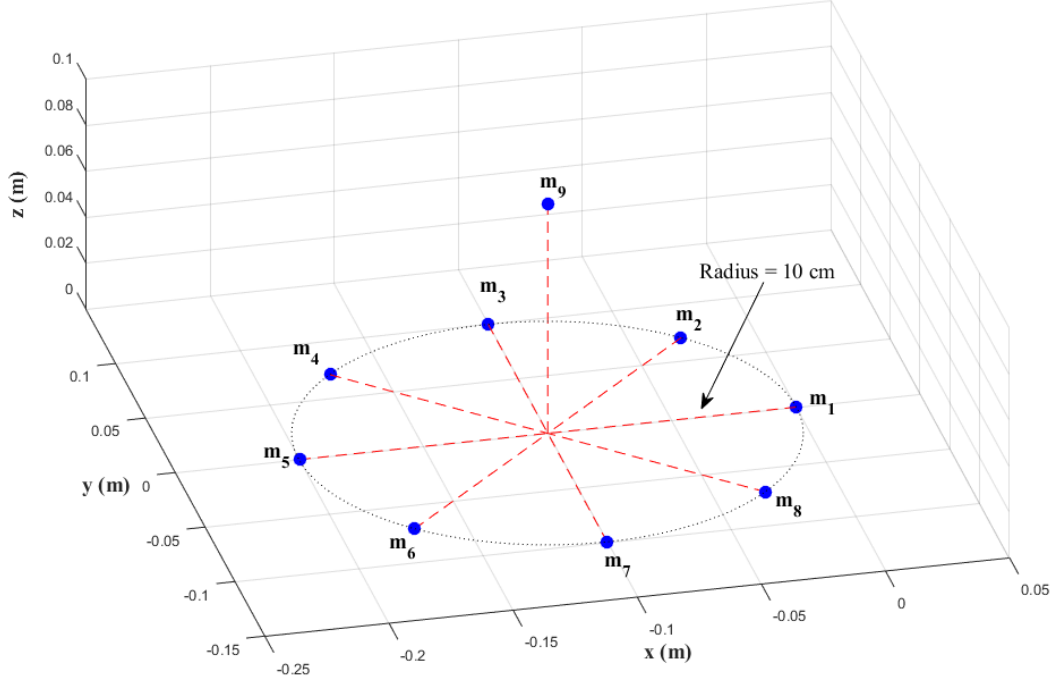
Figure 4.8: Microphone Array for WB-SRPBF Based DoA Estimation

The array consists of 9 discrete omnidirectional microphones. In detail, 8 microphones are uniformly distributed on a circle with a radius of 10 cm to form a uniform circular array (UCA) so that the array can scan 360° in azimuth. The angle between each successive microphone of UCA in the horizontal plane is 45° relative to the array center at (-0.1, 0, 0). There is also one more microphone populated 10 cm above the center of the circular array to form a non-coplanar microphone array for increasing accuracy of estimation in elevation angle.

Recorded signals by each microphone on the array corresponding to a single acoustic source arriving at the microphone array with an angle of 120° in azimuth and 15° in

elevation is illustrated in Figure 4.9. For this example, acoustic source is selected as a shockwave signal simulated as described in APPENDIX B.
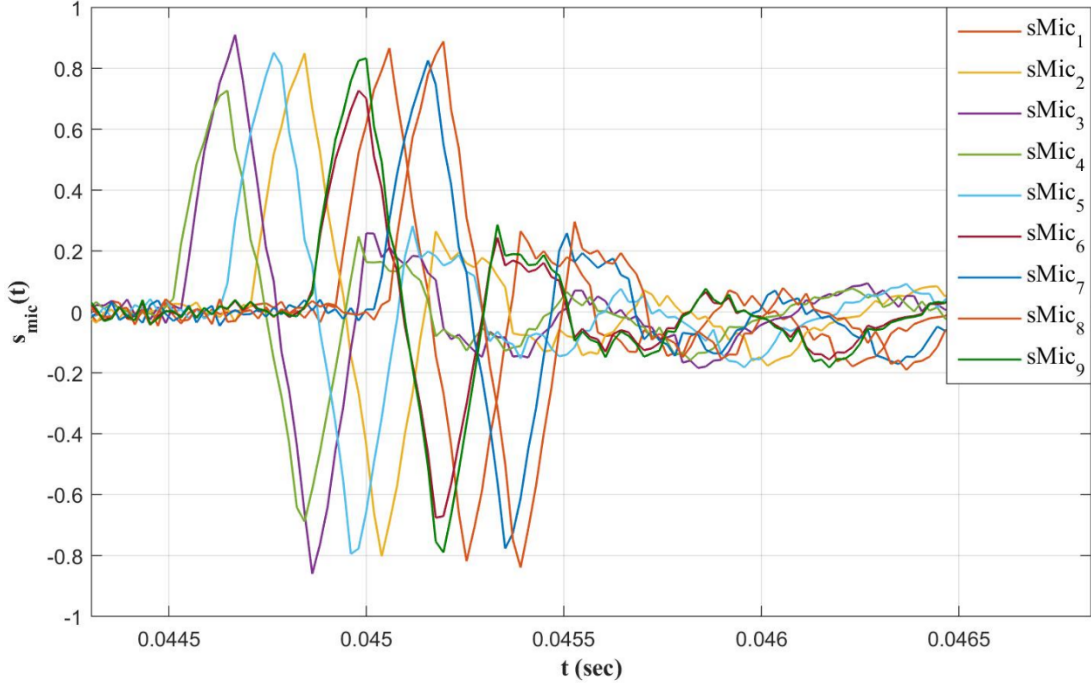
Figure 4.9: Signals Recorded by the Microphone Array in Figure 4.8

If DoA of the source signal is estimated with the WB-SRPBF method, then each TDoA can be calculated according to equation (43) and beamformer output can be obtained as described in (44). The WB-SRPBF output regarding microphone array geometry shown in Figure 4.8 and the arriving signal is depicted in Figure 4.10 for an ideal case, where estimated DoA is equal to the actual DoA. Then, the output of beamformer is equal to signal recorded by the reference microphone (50) as depicted in Figure 4.10. This figure for the ideal case such that actual DoA is equal to estimated DoA. If there is an error in DoA estimation then there will be a time shift corresponding to the angular error and beamforming output is different than the signal recorded by reference microphone. Figure 4.11 depicts beamformer output corresponding to an angular error of 5° in DoA estimation. This error value is the maximum angular error found in simulations provided in 7.3.2. This time shift is still appropriate for accurate shooter localization.
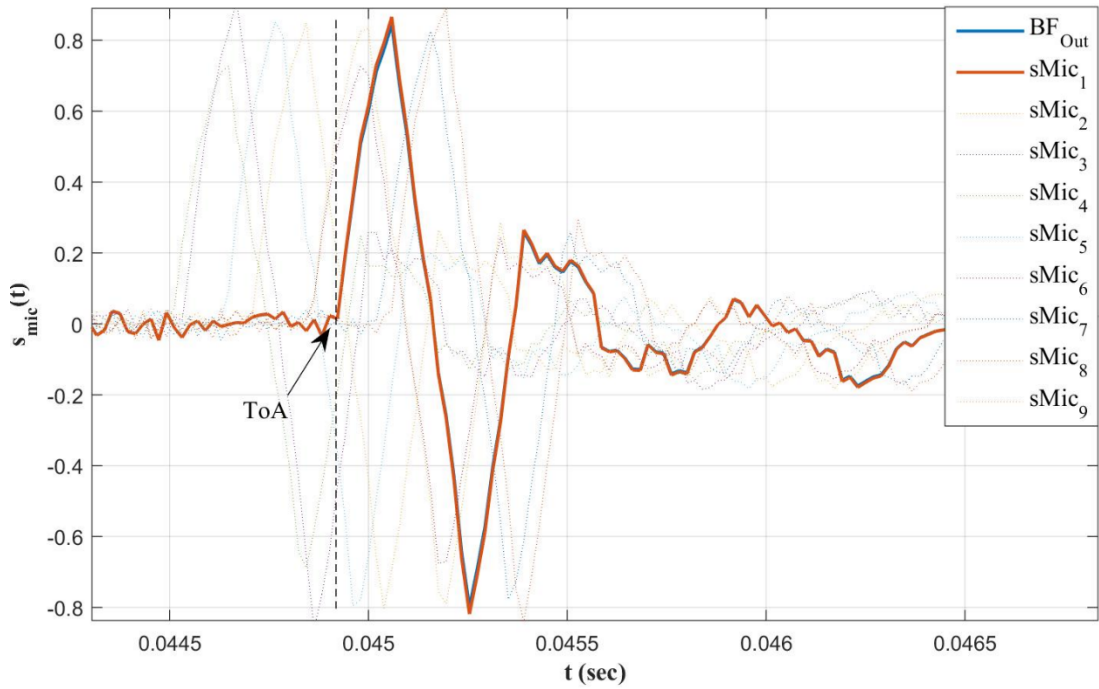
Figure 4.10: WB-SRP Beamformer Output for Ideal Case
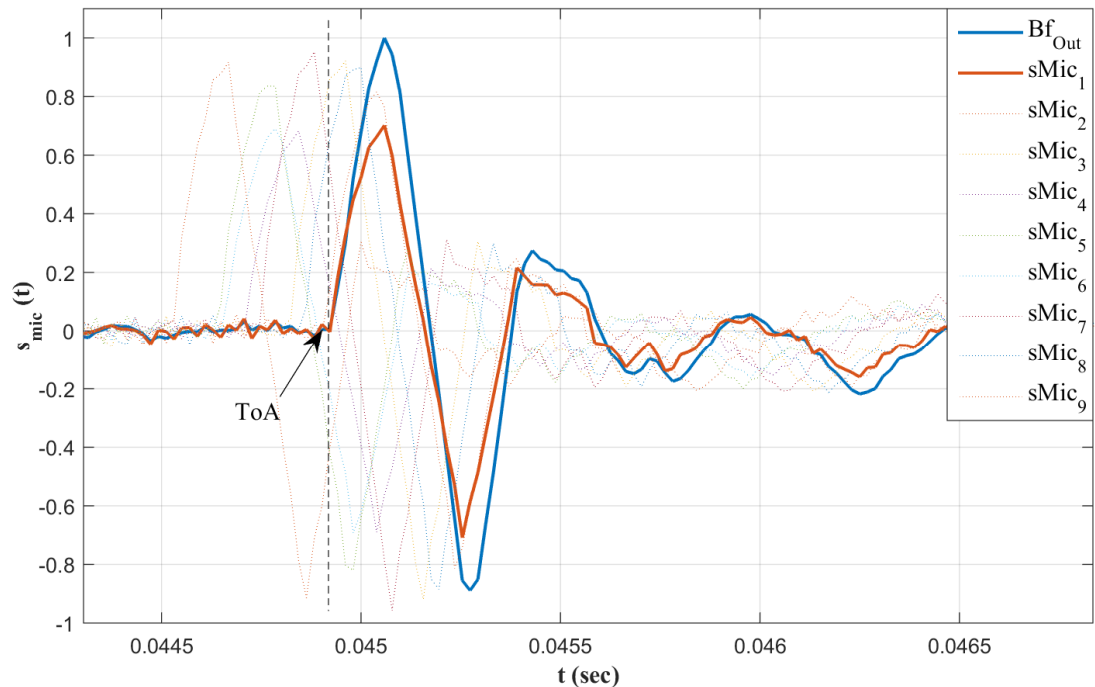
Figure 4.11: WB-SRP Beamformer Output for Erroneous DoA Estimation

DoA is estimated with WB-SRPBF and ToA is obtained by analyzing beamformer output signal then DoA and ToA are used in the estimation framework described in

Chapter 3. Further simulations and tests for WB-SRBF based DoA estimation in shooter localization are provided in section 7.3.

4.4 Comparison of TDoA and Beamforming Techniques

TDoA based and WB-SRPBF based shooter localization systems have a difference in terms of application requirements. For instance, while TDoA technique requires low computational power, WB-SRPBF process takes longer time because of successive computations such as filters and complex multiplications even if those computations are performed in parallel threats. On the other hand, WB-SRPBF provides more robust estimation results than TDoA based shooter localization systems and it has also the capability of multiple shot detection. Table 4.1 lists general comparison between TDoA and beamforming techniques.

Table 4.1: Comparison of TDoA and WB-SRPBF

Parameter	TDoA	WB-SRPBF
Computational Requirement	Low – Moderate	High
Real-Time Applications	Appropriate	Inappropriate Appropriate for near-real time
Number of Microphones	Low	Moderate – High The number of microphones and aperture size increase as required angular resolution of detection decreases.
Multiple Shot Detection	Inappropriate	Appropriate
Reverberation Detection	Inappropriate	Appropriate (at moderate reverberation levels)

CHAPTER 5

SYSTEM MODEL AND CALIBRATION

5.1   System Model

Acoustic based shooter location estimation framework can be modelled as a functional system which relates ToA and DoA values extracted from the recorded signals to outputs of the estimation framework by means of known parameters such as speed of sound, sensor location, and microphone locations. Acoustic based shooter localization system can be modelled as depicted in Figure 5.1.
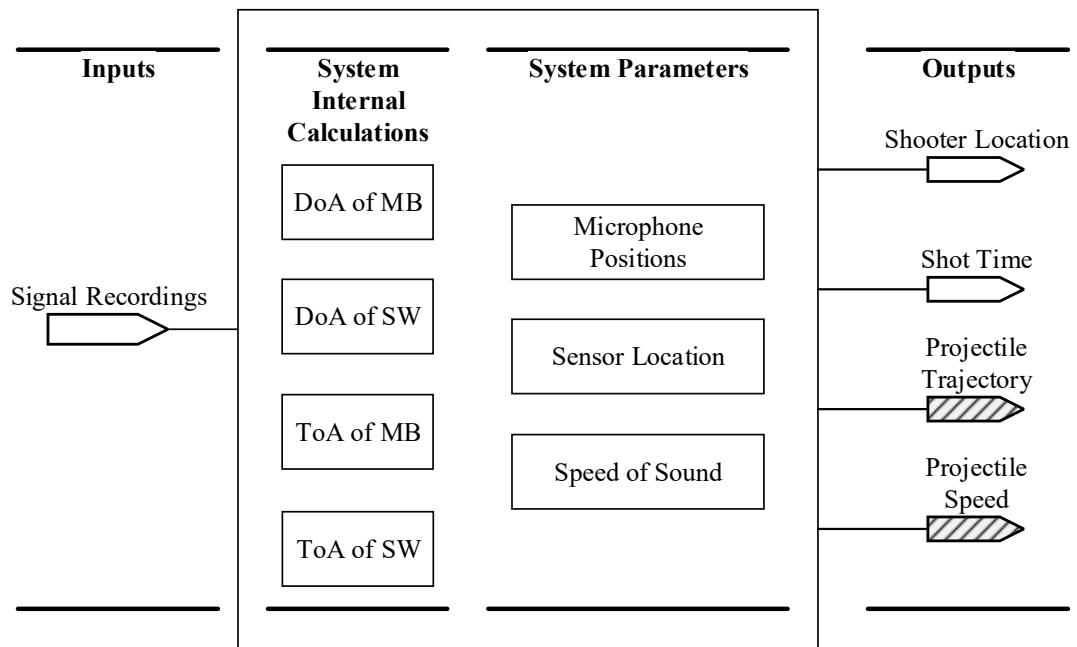
Figure 5.1: Acoustic Shooter Localization System Model

According to the system model, signal recordings are inputs and shooter location, shot time, projectile trajectory and projectile speed are outputs. In fact, projectile speed and trajectory are available in case of the multi sensor network and trajectory passing between sensors. Besides, parameters such as speed of sound, microphone locations,

and sensor location are called system parameters because they are independent and both internal calculations and system outputs are dependent on those parameters. For example, DoA estimation directly depends on microphone locations and sound speed in both TDoA (31) and WB-SRPBF (38) methods. ToA calculation is also an internal calculation, but it depends on timing error rather than system parameters. Furthermore, outputs of the system also rely on each system parameter since they are calculated by means of calculated DoA and ToA values, sensor location and speed of sound.

5.2 Effects of System Parameters

As described in section 5.1, the independent parameters are the speed of sound, microphone locations and sensor locations which are also called system parameters. Furthermore, they are constants for the system; however, they are measured with some measurement tools. For example, the speed of sound might be calculated by applying temperature value measured by a temperature sensor to equation (6), sensor location might be measured by GPS and relative locations of each microphone might be measured by a tape. Hence, the accuracy of each system parameter depends on the tolerance of measurement tools. The assumptions for measurement errors are listed in Table 5.1. There is a further study in the literature that analyzes the sensitivity of the shooter localization for various types of parameters with respect to numbers of sensors in the field. (Ozugur, Sonmez, Basli, & Leblebicioglu, 2015)

Table 5.1: Assumptions for Error Models in Measurement of System Parameters

System Parameter	Assumed Error Models
Sensor Location	Microphone location measurement error is modelled as a zero-mean normal distribution with a variance of 3 meter $- N(0,3)$.
Microphone Location	Measurement of microphone locations is modelled as a zero-mean normal distribution with a variance of 3 mm $- N(0,0.003)$.
Speed of Sound	Measurement error of temperature sensor is modelled as a zero-mean normal distribution with a variance of 5°C $- N(0,5)$.

Figure 5.2, Figure 5.3 and Figure 5.4 depict the effect of measurement error of each parameter separately in shooter localization, respectively. Each plot corresponds to 500 Monte Carlo simulations involving measurement errors described in Table 5.1. In simulations, shot location is at (500m–400m–60m) and the sensor is located at the origin. Furthermore, it is assumed that the sensor measures both muzzle blast and shockwave related parameters and only mentioned measurement error is introduced to shooter localization while the other parameters are set to ideally correct values.
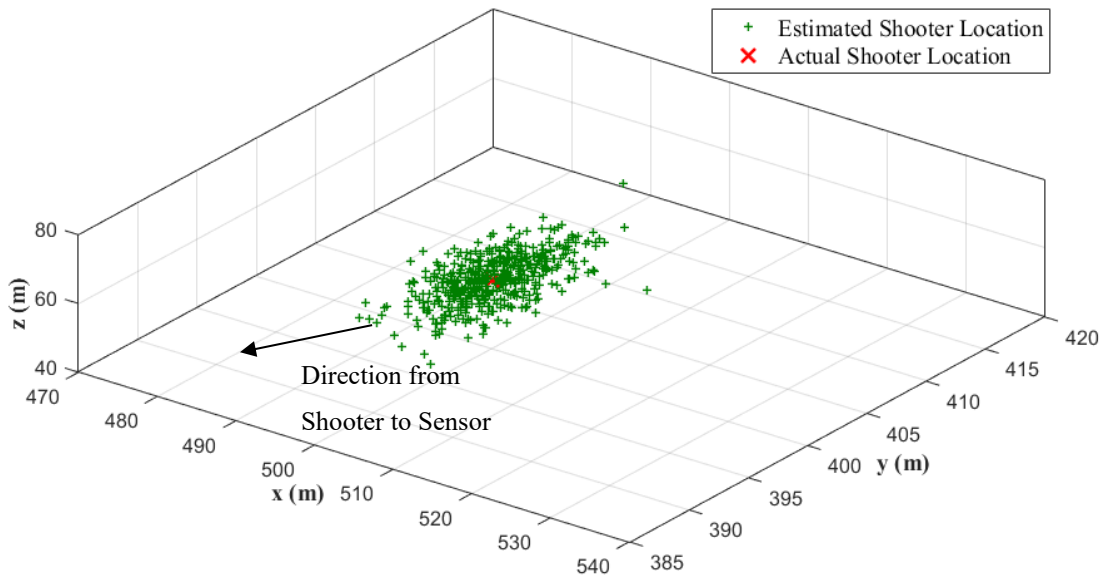
Figure 5.2: Effect of Sensor Location Error in Shooter Localization
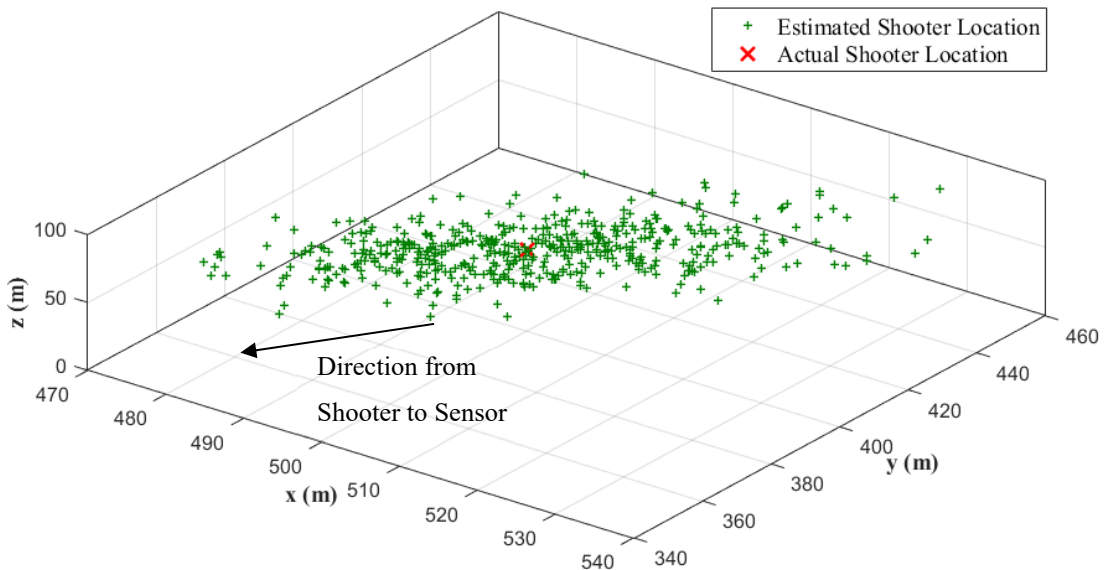
Figure 5.3: Effect of Microphone Position Error in Shooter Localization

49
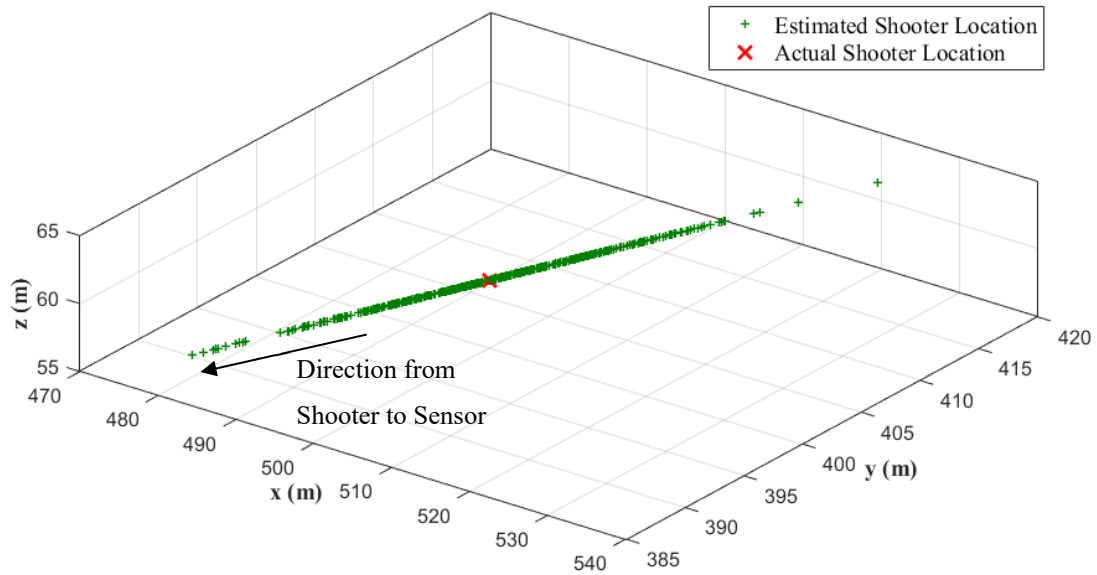
Figure 5.4: Effect of Speed of Sound Error in Shooter Localization

Figure 5.5 illustrates the resultant shooter location estimation in case all measurement errors of system parameters are applied together. In detail, each measurement error described in Table 5.1 is introduced to shooter localization while other required parameters are set with true values.
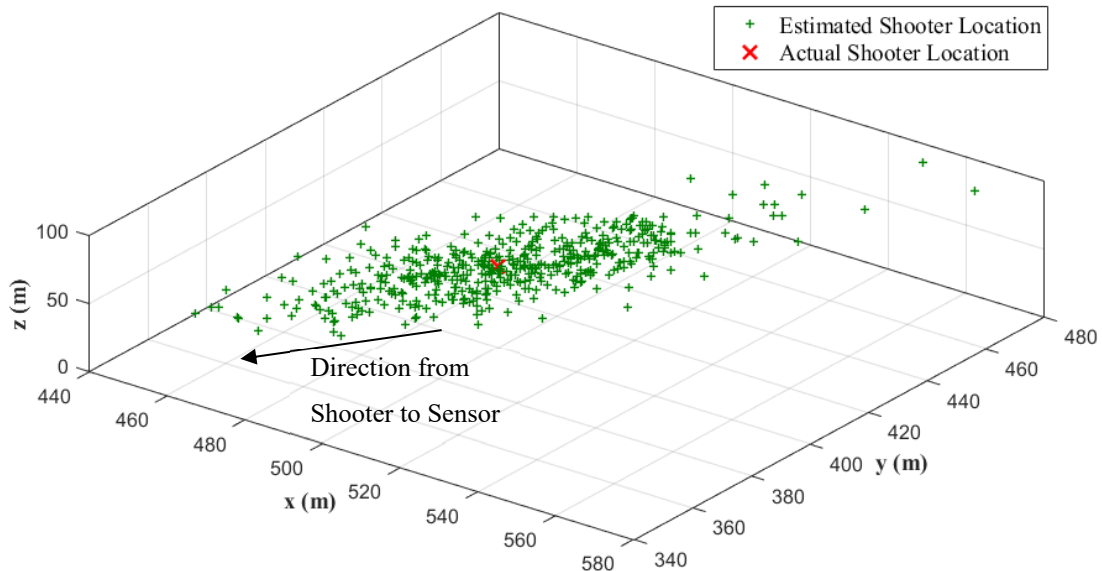
Figure 5.5: Overall Effect of System Parameters in Shooter Localization

Table 5.2: Effect of System Parameters in Shooter Localization

System Parameter	Associated Error	Standard Deviation Error in Shooter Localization (m)		
		X – Coord	Y – Coord	Z – Coord
Sensor Location	$N(0,3)$	3.002	3.143	2.975
Microphone Location	$N(0,0.003)$	11.359	17.223	10.981
Speed of Sound	$N(0,5)$	6.203	4.962	0.7443
Overall Error of System Parameters		15.454	20.3815	12.6203

Shooter localization errors corresponding to each measurement error of system parameters are listed in Table 5.2 for the shooter location estimation. Erroneous location estimations due to measurement error of sensor location directly equal to the assumed error model of sensor location since sensor position is a parameter added as a reference point in shooter localization as shown in equation (20) and (27). On the other hand, error in microphone locations results in large scattering in shooter location estimation. As shown in Table 5.2, normally distributed error with a standard deviation of 3 mm in locations of microphones results in scattered location estimations on an average of 10 m. Shooter location estimation is affected by the locations of microphones since DoA's are essential in shooter localization as shown in (27) and they strictly depend on microphone locations as shown in equations (31) and (38). However, error in the speed of sound leads shooter location estimations to scatter along the direction from shooter to the sensor rather than in all directions. It is because the speed of sound is a scaling factor in shooter location estimation and DoA estimation.

It can be stated that microphone locations and speed of sound have a significant effect on shooter localization accuracy. Thus, a calibration method is proposed in this thesis to calibrate system parameters to enhance the accuracy of shooter location estimation.

5.3 System Calibration Model

As described in section 5.2, the error in system parameters of the system shown in Figure 5.1 reduces the accuracy of shooter localization. Each error in system parameters can be reduced by means of different mitigation methods. In fact, error in sensor locations can be assumed as least significant since it can be reduced gradually as the sensor is stationary. However, microphone locations, which have a significant impact on shooter localization accuracy, might change due to thermal expansion or shrinkage of rods of the microphone array even if they have been measured with sensitive tools. Furthermore, precise measurement of microphone locations one by one for all sensors deployed in the field is not a feasible way. In addition, the accuracy of speed of sound might be enhanced by utilizing more sensitive devices or by increasing number of devices, but this does not resolve the accuracy problem since shooter localization is sensitive to error in the speed of sound. Thus, this thesis proposes an optimization based system calibration method in terms of microphone locations and speed of sound to enhance shooter localization accuracy and performance (Akman, Sonmez, Ozugur, & Leblebicioglu, 2016).
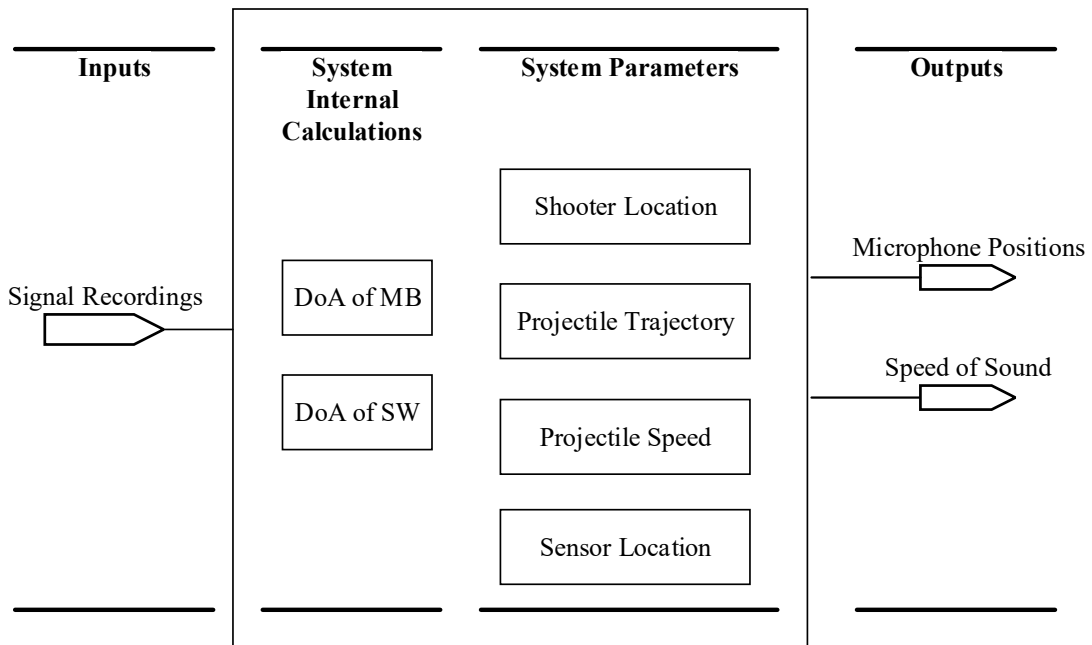

Figure 5.6: Acoustic Shooter Localization System Calibration Model

The system calibration method is based on a system model shown in Figure 5.6 which is derived from the system model shown in Figure 5.1. In detail, the inputs of the system calibration method are signal recordings of each microphone likewise the shooter localization system model. However, outputs of the system calibration model are microphone locations and speed of sound instead of shot specific estimations such as shooter location or projectile trajectory. In fact, the outputs and system parameters, except sensor location, of the shooter location system model are swapped in shooter calibration system model. Furthermore, time dependent parameters and calculation such as ToA and shot time are removed in the system calibration model since shot time cannot be measured precisely even if it is a controlled shot.

The system calibration is performed with a controlled shot and each sensor deployed in the field is calibrated in terms of microphone locations and speed of sound. In detail, a shooter at a known location fires a gun with known muzzle velocity to a known target location. Actual DoA values of muzzle blast and shockwave are calculated as (51) with respect to known parameters namely, shooter location $\vec{x}_0$, target location $\vec{T}_0$, muzzle velocity $\vec{v}_m$ and sensor location $\vec{s}_i$.

$$
\begin{aligned}
\widehat{\vec{u}_i^{MB}} &= \frac{\vec{x}_0 - \vec{s}_i}{\left\| \vec{x}_0 - \vec{s}_i \right\|_2} \\
\widehat{\vec{u}_i^{SW}} &= \frac{\left\| \vec{x}_0 - \vec{s}_i \right\|_2 \cos\left(\theta_M + \phi_i\right) \vec{u}_0 + \left(\vec{x}_0 - \vec{s}_i\right) \cos\left(\theta_M\right)}{\left\| \left\| \vec{x}_0 - \vec{s}_i \right\|_2 \cos\left(\theta_M + \phi_i\right) \vec{u}_0 + \left(\vec{x}_0 - \vec{s}_i\right) \cos\left(\theta_M\right) \right\|_2} \\
\vec{u}_0 &= \frac{\vec{T}_0 - \vec{x}_0}{\left\| \vec{T}_0 - \vec{x}_0 \right\|_2} \\
\phi_i &= \arccos\left(\frac{\vec{s}_i - \vec{x}_0}{\left\| \vec{s}_i - \vec{x}_0 \right\|_2} \bullet \vec{u}_0\right) \quad , \quad 0 < \phi_i < \frac{\pi}{2} \\
\theta_M &= \arcsin\left(\frac{1}{M}\right) \quad , \quad 0 < \theta_M < \frac{\pi}{2} \\
M &= \frac{v_M}{c}
\end{aligned}
\tag{51}
$$

Each sensor deployed in the field also estimate DoA of muzzle blast and shockwave by processing recorded signals as shown in (52). The negative sign is used in (52) for a directional match with actual DoA's calculated in (51). In fact, TDoA based DoA

estimation, described in section 4.2, is used for system calibration purpose since it is fast and provides accurate shooter localization for a single shot.

$$
\begin{aligned}
\vec{u}_i^{MB} &= \tilde{A}\,\vec{\tau}_i^{MB} \\
\vec{u}_i^{SW} &= \tilde{A}\,\vec{\tau}_i^{SW}
\end{aligned}
\tag{52}
$$

$\tilde{A}:$ Moore-Penrose pseudo inverse of $\left(-\dfrac{1}{c}A_{Diff}\right)$

A nonlinear constrained optimization problem is obtained by rearranging actual and estimated DoA of muzzle blast and shockwave signals as (53). The minimization of the objective function (54) leads to calibrated speed of sound and relative microphone locations. The constraint for the microphone relative location array is defined such that norm of the difference of each microphone cannot exceed a maximum limit $err_{\Delta Mic}$. This value can be set according to the thermal expansion coefficient of the material of the microphone array. In addition, the constraint for speed of sound might be set such that it is in a range of $[c_{Min}\ c_{Max}]$ corresponding to a predefined temperature interval or it can be set simply as greater than zero.

$$
\begin{aligned}
f_{1i} &= \widehat{\vec{u}_i^{MB}} - \vec{u}_i^{MB} \\
f_{2i} &= \widehat{\vec{u}_i^{SW}} - \vec{u}_i^{SW}
\end{aligned}
\tag{53}
$$

$$
\min_{A_{Diff},\,c} J = \sum_{i=1}^{N}\left\|f_{1i}\right\|_2^2 + \left\|f_{2i}\right\|_2^2 \quad N:\text{Number of sensors}
$$

subject to

$$
row\left(\left\|A_{Diff} - \hat{A}_{Diff\,(Uncalibrated)}\right\|_2\right) < err_{\Delta Mic}
$$

$$
c_{Min} < c < c_{Max}
$$

(54)

Simulation and test results regarding shooter localization performance enhancement with system calibration method are provided in section 7.5.

CHAPTER 6

SYSTEM DESIGN

6.1   Overview

Acoustic shooter localization systems simply consist of a microphone array, processor unit, and a power unit. Microphone arrays can be used as a separate unit as well as they can be mounted on the sensor board. It is important that microphones on the array should confirm the predefined geometry. Furthermore, microphones can be ordinary electret or they can be MEMS for more sensitive and small-in-size applications. Sensor board should have appropriate peripherals and interfaces for microphones and other supplementary units and it is important that it has computational capability required for the algorithms used in shooter localization.

There are several studies involving system architecture and hardware platform used in acoustic based shooter localization. For example, Lédeczi et al., (2005) have proposed both DSP based and FPGA based sensor board in their studies. Furthermore, Völgyesi et al. (2007) have proposed ad-hoc wireless sensor network based sensor mote in their studies. Raytheon BBN has also developed wearable and vehicle-mounted acoustic shooter localization systems (Raytheon Corp, 2017).

6.2   Hardware Design

This thesis proposes an acoustic shooter localization system architecture and hardware platform corresponding to several application requirements. In fact, the system has a DSP based processing unit which has the capability of processing microphone signals for shooter localization. It has several analog interfaces for microphones and digital interfaces other auxiliary peripheral units. In addition, it has GPS, accelerometer, and magnetometer so that the system has the capability to measure self-location and self-

orientation. It has also wireless communication unit to establish a network oriented shooter localization that can be monitored and controlled from an operation center. Finally, the system can be powered by battery or an electrical adapter. The block diagram of the system architecture and corresponding hardware design with 8 MEMS microphones are illustrated in Figure 6.1 and Figure 6.2, respectively.
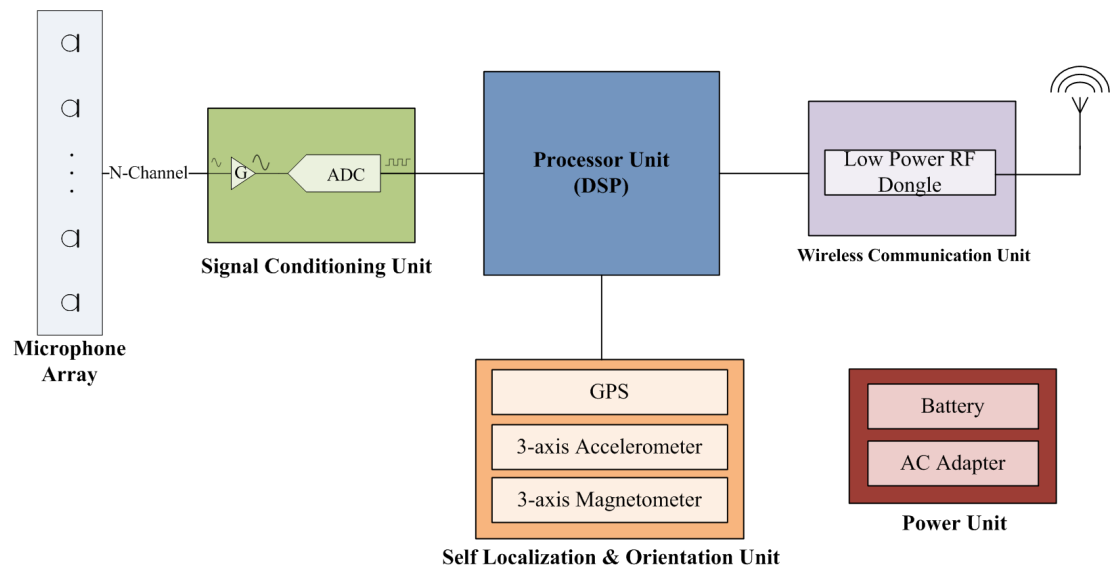

Figure 6.1: Hardware Architecture for Shooter Localization
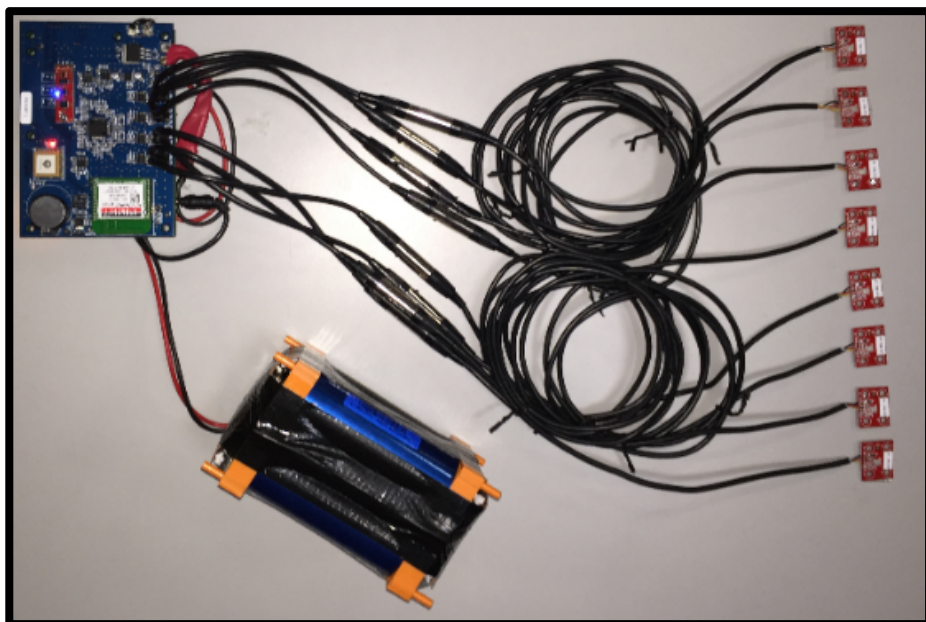
Figure 6.2: Hardware Design for Shooter Localization System

The processing unit is selected as commercial off-the-shelf (COTS) Blackfin® series of Analog Devices®. The processor unit is determined so that it has the capability of processing eight microphones, and auxiliary units such as GPS, accelerometer, magnetometer and wireless unit.

The microphone signals are filtered, amplified and converted to digital signals in the signal conditioning unit. The signal conditioning unit involves Analog-to-digital (ADC) units of Analog Devices® for compatibility with the COTS processor unit. In detail, analog signals are converted to digital signals with 16-bit resolution and the microphones signals are sampled with 400 kSPS (Sample-per-Second).

The conceptual system design is considered not only for stationary applications but also vehicle-mounted and wearable applications. The hardware design is produced as a prototype for the stationary case but it can be easily converted to a vehicle-mounted or a wearable system by hardware optimization and corresponding mechanical design. Hence, the auxiliary units such as GPS (GlobalTop® Ladybird), accelerometer and magnetometer (SPARKFUN® Sensor Stick) are involved within the design so that the system can measure self-location and self-orientation while the platform is in motion.

The design involves a wireless communication unit (Synapse® RF Module) to provide communication between each sensor in the field and the operation center. The wireless network is designed such that each sensor can send data directly to the operation center and the operation center can send data to a single sensor as well as broadcast data to all sensors in the field. Each node can work as a router in the network. For example, if the transmitter node is not within the FOV of the receiver node then the message can be sent to the receiver node by another node which is in the FOV of both the transmitter and the receiver nodes. The communication protocol also uses acknowledgment procedure to ensure that message is sent and received properly. In fact, any message is sent five times within the network until the acknowledgment is sent back by the receiver node otherwise the message is discarded to free communication bandwidth.

When the system starts, each sensor in the field starts sending health status periodically to the operation center so that the operation center can monitor the health of the nodes

deployed in the field. The operation center requests the location and orientation of sensors in the field for the initial setup. After initialization, each sensor updates location and orientation data if there is a change for any reason so that the operation center utilizes correct data in localization.

When a sensor node in the field detects a gunshot, the message sent by the node to the operation center involves available ToA and DoA of muzzle blast and shockwave with sensor ID and proper time tag. Then, the operation center fuses the time labelled data within a proper time interval to estimate corresponding range, azimuth, and elevation for shooter localization. The estimation framework is utilized with respect to the available data as described in Chapter 3. If the system is used for system calibration purpose, the calibrated microphone positions and local speed of sound data is sent by the operation center to all sensor nodes deployed in the field. After calibration is done, the system is switched to normal working state.

6.3   Performance Results

The hardware has been tested in the field as a single sensor with a microphone array of four MEMS microphones in tetrahedral geometrical form. The location estimation framework utilized the method of both muzzle blast and shockwave detection case for shooter localization.

The location estimation performance result of the system is measured as $\pm$ 2.2° error in azimuth angle and maximum detection range of the system is measured as 1000 m for the single sensor case (Akman et al., 2016). This performance result is comparable with the performance results of PILAR systems for single sensor case of both muzzle blast and shockwave detection (Millet & Baligand, 2006).

The further field tests for shooter localization with multi sensor and WBSRPF based multiple shooter localization and reflection elimination will be performed as future work.

CHAPTER 7

SIMULATION AND TEST RESULTS

7.1 Overview

This chapter involves all simulation and test results performed for described work in this thesis. The assumptions, requirements, and models used in these simulations are described in the corresponding sections of this chapter. All the simulations in these chapters are coded and performed in MATLAB® 2015. All simulation software is coded by the author by using basic MATLAB® functions except optimization and statistics. The built-in function "*fmincon*" of MATLAB® Optimization Toolbox is used for constrained nonlinear optimization and the built-in functions "*randn*" and "*unifrnd*" of MATLAB® Statistics Toolbox are used for statistical processes such as noise generation, randomization of parameters in simulations (MATLAB R2015a).

The organization of this chapter is in accordance with the chapter orders in the thesis. Firstly, simulation and test results of estimation framework described in Chapter 3 are provided in section 7.2. The estimation for shooter location, shot time, projectile trajectory and projectile velocity are performed according to the type of signal detection and number of sensors deployed in the field for a single shot.

Detection of simultaneous multiple shooter localization with the WB-SRPBF method described in section 4.3 is provided in section 7.3. Furthermore, elimination of reverberation by using the WB-SRPBF method and common output functions is provided in section 7.4.

Finally, the effects of system parameters on estimation framework and enhancement in performance of the framework depending on the TDoA based system calibration method proposed in Chapter 5 is provided in section 7.5.

7.2 Single Shooter Localization

This section provides simulation and test results for shooter location estimation framework described in Chapter 3. Simulations are performed in the case of detection of only muzzle blast, only shockwave and both of acoustic events for varying number of sensors deployed in the field. All the simulations are performed under appropriate assumptions. The assumptions for the simulation and tests of estimation framework are listed in Table 7.1.

Table 7.1: Assumptions of Simulations for Single Shot Estimation Framework

Assumption Type	Description
Signal Detection	Signals required for estimation process are already detected in signal detection process and corresponding DoA and ToA values are already obtained. All DoA and ToA calculations are subject to timing and microphone location error model described in Table 7.2.
Detection Range	Range from sensor location to an acoustic source is assumed to be appropriate for detection of the signal.
Background Noise	SNR level is assumed to be high enough for detection.
Hindering Obstacles	Any hindering obstacle is avoided. Thus, if a sensor in the field is positioned in the appropriate detection zone, then it detects the corresponding signals.
Far Field Waves.	Muzzle blast and Shockwave signals are assumed to be planar waves
Projectile	Projectile is assumed to propagate at a constant speed on a straight trajectory line
Shot	There is a single shot to be estimated since this section aims to provide the performance of the estimation framework.

The performance of the estimation framework depends on the measurement errors, as described in Chapter 5. Those measurements can be categorized as timing errors, location errors, and the speed of sound error.

First of all, when a sensor detects muzzle blast or shockwave, it measures ToA with an error depending on the sampling frequency. Then, locations of microphone arrays in the field and single microphones on the array are subject to location errors. In fact, sensor locations, reference points in shooter localization, depends on the GPS measurement error. Relative locations of single microphones on the array might also be erroneous because of measurement tool as well as temperature dependent expansion and contraction in rods of the array where microphones are attached. Finally, the estimation of the speed of sound has also error because it is estimated as (6) by a temperature sensor which has a measurement error likewise other measurement tools. While timing error has an effect on ToA estimation, positioning and speed of sound errors have an effect on DoA estimation. Consequently, all estimations performed by the framework are subject to those errors. Error models for corresponding measurements are listed in Table 7.2.

Table 7.2: Error Models of Simulations for Single Shot Estimation Framework

Parameter	Error Model
Timing	ToA measurement error is modelled as uniform distribution over one sampling period (T_s), $U\left(-T_s/2, T_s/2\right)$
Sensor Location	Microphone location measurement error is modelled as a zero-mean normal distribution with a variance of 3 m, $N\left(0,3\right)$.
Microphone Location	Measurement of microphone locations is modelled as a zero-mean normal distribution with a variance of 3 mm, $N\left(0,0.003\right)$.
Speed of Sound	Measurement error of temperature sensor is modelled as a zero-mean normal distribution with a variance of 5°C, $N\left(0,5\right)$.
Note: All types of errors are introduced to simulations at the same time.	

The descriptions of simulation parameters of the estimation framework for a single shot are listed in Table 7.3.

Table 7.3: General Simulation Parameters for Single Shot Estimation Framework

Parameter	Description
Sensors Locations	$s_1 = [\quad -20m \quad -50m \quad 10m \quad]$ $s_2 = [\quad -40m \quad 75m \quad 20m \quad]$ $s_3 = [\quad -50m \quad -50m \quad 50m \quad]$ $s_4 = [\quad 50m \quad 10m \quad 10m \quad]$ $s_5 = [\quad 0m \quad 40m \quad 35m \quad]$ For n-sensor case, s_1 to s_n are used in simulations. Sensor locations are subject to location errors defined in Table 7.2.
Microphone Locations	$$\begin{bmatrix} m_1 \\ m_2 \\ m_3 \\ m_4 \\ m_5 \\ m_6 \\ m_7 \\ m_8 \end{bmatrix} = \begin{bmatrix} 0m & 0m & 0m \\ 0.4m & 0.0m & 0m \\ 0.2m & 0.2m & 0m \\ 0.2m & -0.2m & 0m \\ 0.1333m & 0.0667m & 0.2828m \\ 0.2667m & -0.0667m & 0.2828m \\ 0.1333m & -0.0667m & 0.2828m \\ 0.2m & 0m & 0.4m \end{bmatrix}$$ All sensors have same array configuration. Microphone locations are subject to microphone location errors defined in Table 7.2.
Shot Locations	Shots are randomly distributed in the hemisphere of radius 500m centered at the origin.
Shot Time	There is only single shot at a time and shot time is uniformly distributed in limits of (0, 100 sec).
Sampling Frequency	$f_s = 51200KHz$ Time measurements are subject to timing error defined in Table 7.2.
Speed of Sound	The nominal speed of sound is assumed to be 340 m/s. The speed of sound is subject to temperature error defined in Table 7.2.
Mach Number	Nominal Mach number is assumed to be 2, and Mach numbers are randomly distributed in limits of (1, 7).

7.2.1 Only Muzzle Blast Detection

If a sensor in the field detects only muzzle blast then framework (19) is used to estimate shooter location and shot time in case there is more than one sensor as described in section 3.2.2.

$$
\begin{aligned}
f_{1i} &= \widehat{\vec{u}_i^{MB}} - \vec{u}_i^{MB} &&= \frac{\vec{x}_0 - \vec{s}_i}{\left\| \vec{x}_0 - \vec{s}_i \right\|_2} - \vec{u}_i^{MB} \\[2ex]
f_{2i} &= \widehat{t_i^{MB}} - t_i^{MB} &&= \frac{\left\| \vec{x}_0 - \vec{s}_i \right\|_2}{c} + t_0 - t_i^{MB} \\[2ex]
\min_{x_o, t_0} J &= \sum_{i=1}^{N} \left\| f_{1i} \right\|_2^2 + \left| f_{2i} \right|^2 \quad N \geq 2
\end{aligned}
\tag{19}
$$

subject to
$$
\left\| \vec{x}_0 \right\|_2 < R_{Max}
$$
$$
t_0 > 0
$$

Simulation results of shooter localization by 2 and 3 sensors for 50 shots, randomly distributed in the hemisphere of radius 500m centered at the origin, are shown in Figure 7.1 and Figure 7.2. Shot number is selected low for sake of visualization.
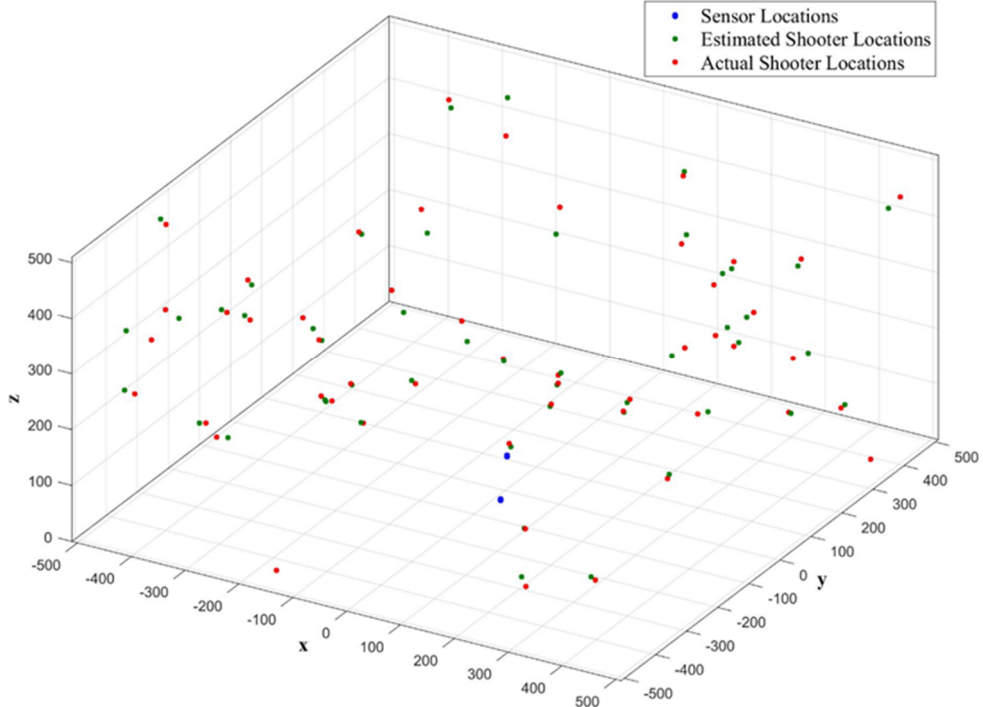
Figure 7.1: Shooter Localization with 2 Sensors – only MB Detection
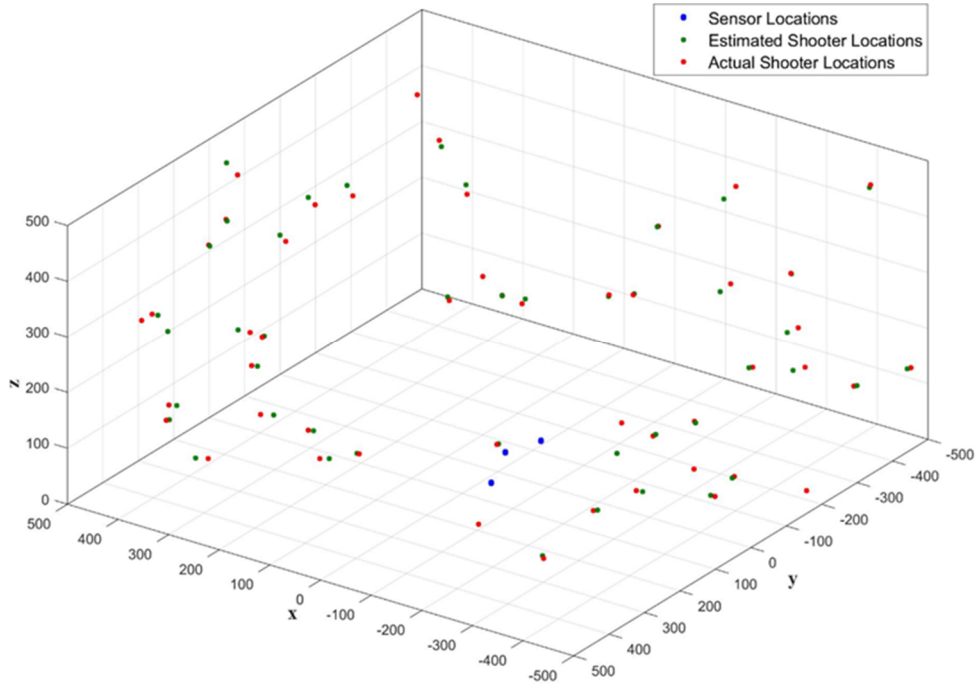
Figure 7.2: Shooter Localization with 3 Sensors – only MB Detection

As it can be realized from Figure 7.1 and Figure 7.2, an increase in the number of sensors enhances the localization performance. If this 50-shot case is generalized for 1000 shots then more comparable results are obtained. Deviation errors for Monte Carlo simulation results of shooter location and shot time estimation with respect to increasing number of sensors are listed in Table 7.4.

Table 7.4: Estimation Results for Shot Location and Time (Only MB)

Number of Sensors	Standard Deviation Errors 1000 Monte Carlo Estimations			
	Shooter Location			Shot Time
	Azimuth	Elevation	Range	
1	No available estimation. Only DoA and ToA of MB are available.			
2	< 1°	< 1.5°	< 8%	< 0.1%
3	< 0.5°	< 1°	< 7%	< 0.06%
4	< 0.4°	< 0.6°	< 6%	< 0.05%
5	< 0.35°	< 0.5°	< 6%	< 0.05%

As shown in Table 7.4, the accuracy of estimation increases with increasing number of sensors. There is a significant enhancement due to the addition of one more sensor to the field in which two sensors are already deployed; nevertheless, increasing number of sensors greater than three has a slight improvement in estimation results. As a result, an optimum number of sensors might be set as three for shooter localization related to only muzzle blast detection case.

7.2.2 Only Shockwave Detection

If a sensor in the field misses muzzle blast and detects only shockwave signal then generalized estimation framework is used as (21) as described in section 3.2.3. In this case, the estimation performed by the framework depends on projectile specific information such as projectile speed and projectile trajectory. If there is a single sensor, then the system outputs only ToA and DoA of shockwave and the framework cannot output any estimation, like only muzzle blast detection case. Hence, the number of sensors in simulations are selected as greater than one.

$$f_{3i} \; = \; \widehat{t_i^{SW}} - t_i^{SW} \;\; = \;\; \frac{\left\| \vec{x}_0 - \vec{s}_i \right\|_2}{c} \sin(\theta_M + \phi_i) + t_0 - t_i^{SW}$$

$$f_{4i} \; = \; \widehat{\vec{u}_i^{SW}} - \vec{u}_i^{SW} \;\; = \;\; \frac{\left\| \vec{x}_0 - \vec{s}_i \right\|_2 \cos(\theta_M + \phi_i)\vec{u}_0 + (\vec{x}_0 - \vec{s}_i)\cos(\theta_M)}{\left\| \left\| \vec{x}_0 - \vec{s}_i \right\|_2 \cos(\theta_M + \phi_i)\vec{u}_0 + (\vec{x}_0 - \vec{s}_i)\cos(\theta_M) \right\|_2} - \vec{u}_i^{SW}$$

$$\phi_i = \arccos(\frac{\vec{s}_i - \vec{x}_0}{\left\| \vec{s}_i - \vec{x}_0 \right\|_2} \bullet \vec{u}_0) \;\;, \;\; 0 < \phi_i < \frac{\pi}{2}$$

$$\min_{\vec{u}_0, M} J = \sum_{i=1}^{N} \left| f_{3i} \right|^2 + \left\| f_{4i} \right\|_2^2 \quad N \geq 2$$

subject to

$$\left\| \vec{x}_0 \right\|_2 < R_{Max}$$
$$t_0 > 0$$
$$\left\| \vec{u}_0 \right\|_2 < 1$$
$$1 < M < \frac{v_{Max}}{c}$$

(21)

Simulation results of single trajectory estimation of the framework (21) for the case of 2 and 3 sensors are illustrated in Figure 7.3 and Figure 7.4, respectively. Simulations

are plotted as unit vectors of actual and estimated trajectory lines. In simulations, shot location, trajectory line passing between sensors, projectile speed, and measurement errors are kept constant for comparison.
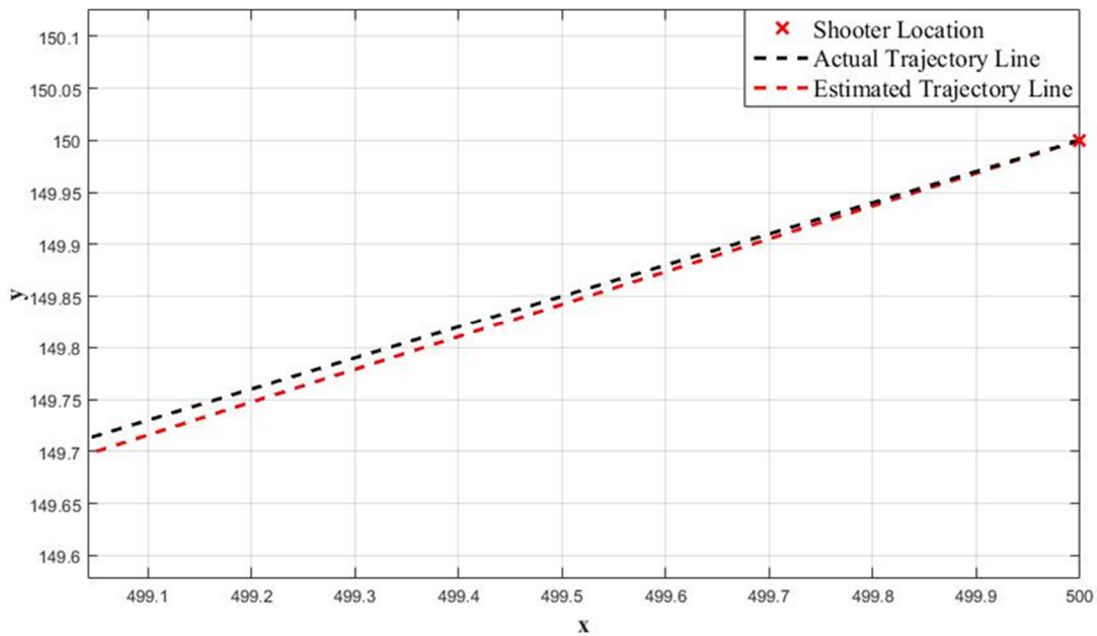
Figure 7.3: Trajectory Estimation with 2 Sensors – only SW Detection
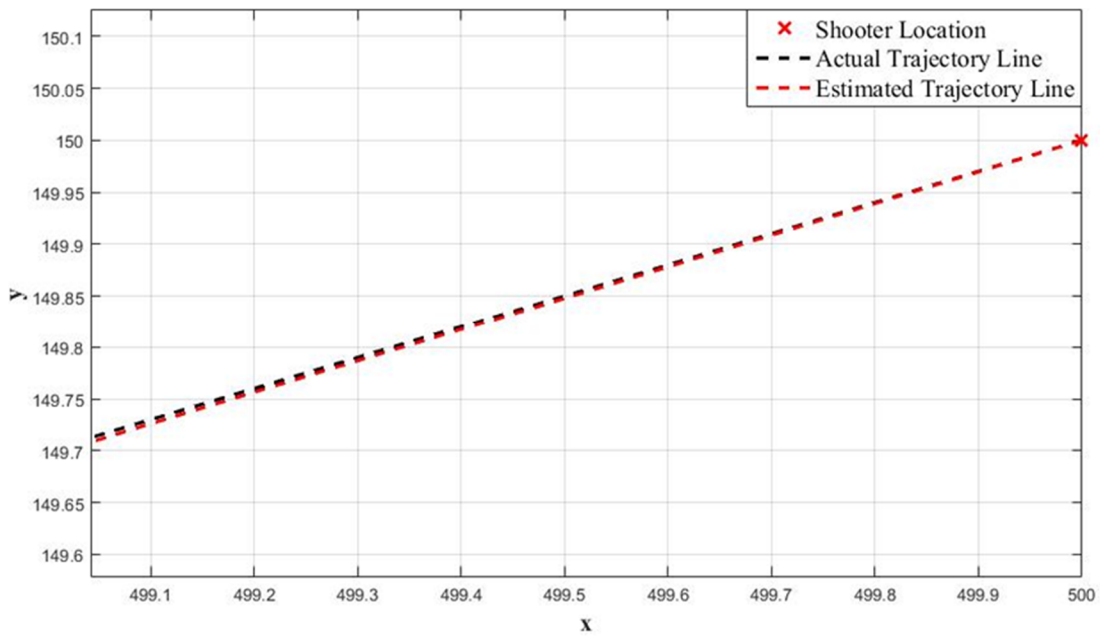

Figure 7.4: Trajectory Estimation with 3 Sensors – only SW Detection

As it can be realized from Figure 7.3 and Figure 7.4, the number of sensors enhance the trajectory estimation accuracy. If this example single shot case is generalized as 1000 shots from different locations with different projectile speeds and varying projectile lines, passing between sensors in the field, then more comparable results are obtained with respect to increasing number of sensors. Deviation errors for Monte Carlo simulation results of projectile trajectory and Mach number estimation with respect to the number of sensors are listed in Table 7.5.

Table 7.5: Estimation Results for Projectile Trajectory and Speed (Only SW)

Number of Sensors	Standard Deviation Errors 1000 Monte Carlo Estimations		Mach Number
	Unit Vector of Projectile Trajectory		
	Azimuth	Elevation	
1	No valid estimation. Only ToA and DoA of SW are available.		
2	$< 1°$	$< 2°$	$< 10\%$
3	$< 0.4°$	$< 1°$	$< 8\%$
4	$< 0.3°$	$< 0.5°$	$< 6\%$
5	$< 0.2°$	$< 0.4°$	$< 5\%$

As shown in Table 7.5, deviation of error decreases as the number of sensors increases in the field. Those error values are valid for trajectory line passing through between sensors with a proper miss distance. Projectile trajectory error is below 1° in azimuth and below 2° in elevation and decreases as the number of sensors deployed in the field increases. Projectile speed error is shown in terms of Mach number in Table 7.5. It can be converted to metric units by multiplying with the speed of sound calculated with ambient temperature, and estimated Mach number (6).

7.2.3 Both Muzzle Blast and Shockwave Detection

If both muzzle blast and shockwave signals are detected then framework (16) is used for shooter location, shot time, trajectory, and projectile speed estimation as described in section 3.2.4. In both muzzle blast and shockwave detection case, there is no restriction on the number of sensors deployed in the field for shooter localization. Shooter localization is possible even if there is a single sensor in the field in case the sensor detects both of muzzle blast and shockwave signals. Nevertheless, there is still need of more than one sensor for estimation of projectile trajectory and speed.

$$f_{1i} = \widehat{\bar{u}_i^{MB}} - \bar{u}_i^{MB} = \frac{\bar{x}_0 - \bar{s}_i}{\left\|\bar{x}_0 - \bar{s}_i\right\|_2} - \bar{u}_i^{MB}$$

$$f_{2i} = \widehat{t_i^{MB}} - t_i^{MB} = \frac{\left\|\bar{x}_0 - \bar{s}_i\right\|_2}{c} + t_0 - t_i^{MB}$$

$$f_{3i} = \widehat{t_i^{SW}} - t_i^{SW} = \frac{\left\|\bar{x}_0 - \bar{s}_i\right\|_2}{c}\sin(\theta_M + \phi_i) + t_0 - t_i^{SW}$$

$$f_{4i} = \widehat{\bar{u}_i^{SW}} - \bar{u}_i^{SW} = \frac{\left\|\bar{x}_0 - \bar{s}_i\right\|_2 \cos(\theta_M + \phi_i)\bar{u}_0 + (\bar{x}_0 - \bar{s}_i)\cos(\theta_M)}{\left\|\left\|\bar{x}_0 - \bar{s}_i\right\|_2 \cos(\theta_M + \phi_i)\bar{u}_0 + (\bar{x}_0 - \bar{s}_i)\cos(\theta_M)\right\|_2} - \bar{u}_i^{SW}$$

$$\phi_i = \arccos(\frac{\bar{s}_i - \bar{x}_0}{\left\|\bar{s}_i - \bar{x}_0\right\|_2}\bullet\bar{u}_0) \quad , \quad 0 < \phi_i < \frac{\pi}{2}$$

$$\min_{x_o,t_0,u_0,M} J = \sum_{i=1}^{N}\left\|f_{1i}\right\|_2^2 + \left|f_{2i}\right|^2 + \left|f_{3i}\right|^2 + \left\|f_{4i}\right\|_2^2 \quad N:\text{Number of sensors}$$

subject to

$$\left\|\bar{x}_0\right\|_2 < R_{Max}$$
$$t_0 > 0$$
$$\left\|\bar{u}_0\right\|_2 < 1$$
$$1 < M < \frac{v_{Max}}{c}$$

(16)

Single Sensor Case:

$$\bar{x}_0 = \bar{s}_i + c\left(\frac{t_i^{MB} - t_i^{SW}}{1 - \left(\bar{u}_i^{MB}\bullet\bar{u}_i^{SW}\right)}\right)\bar{u}_i^{MB} \tag{26}$$

$$t_0 = \frac{t_i^{SW} - t_i^{MB}\left(\bar{u}_i^{MB}\bullet\bar{u}_i^{SW}\right)}{1 - \left(\bar{u}_i^{MB}\bullet\bar{u}_i^{SW}\right)} \tag{27}$$

Shooter localization performed by the framework (16) for 50 shots, randomly distributed in the hemisphere of radius 500m centered at the origin, in the case of a single sensor and 2 sensors are depicted in Figure 7.5 and Figure 7.6, respectively.
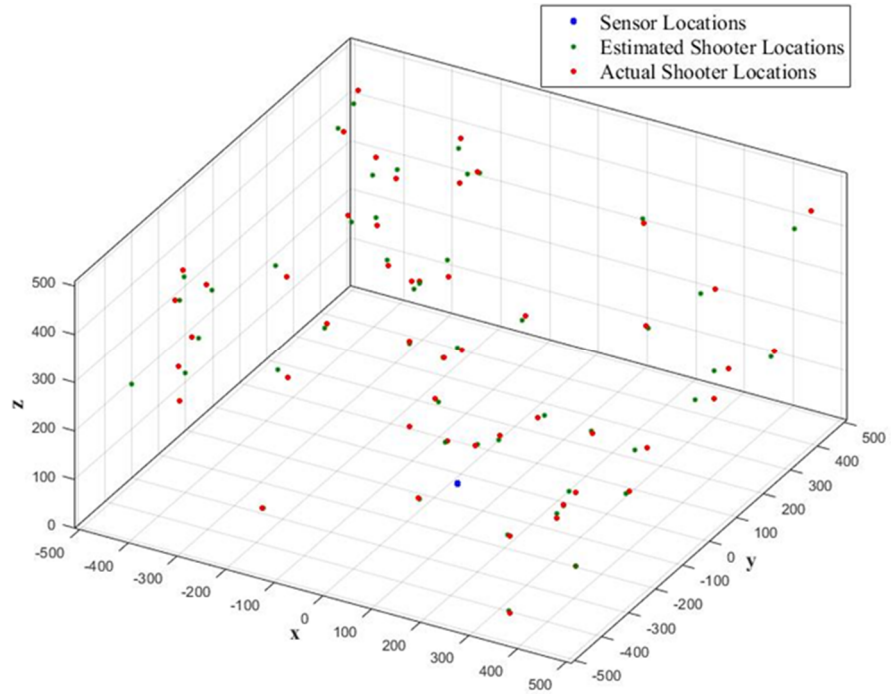

Figure 7.5: Shooter Localization with 1 Sensors – MB-SW Detection
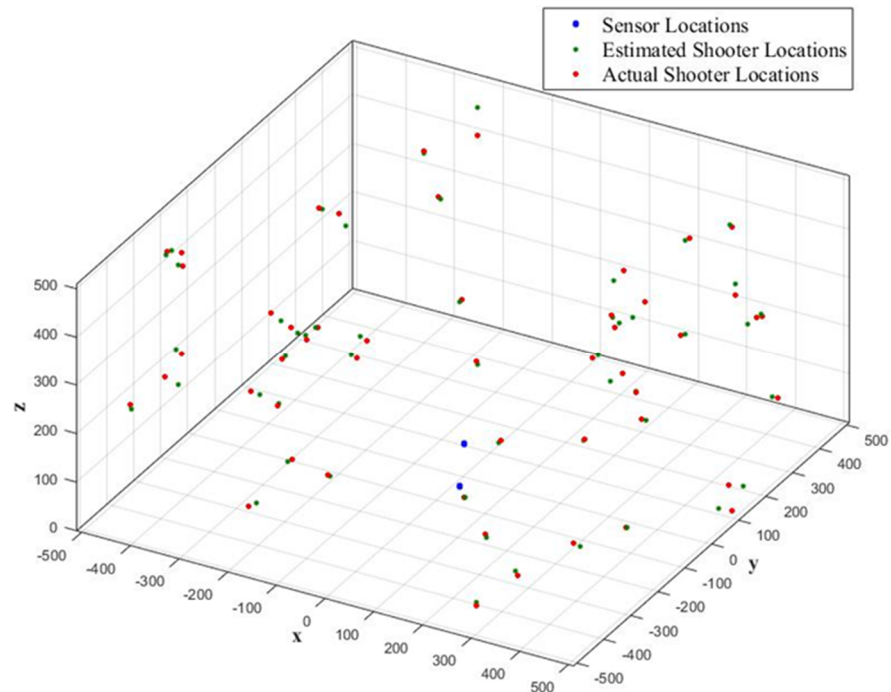

Figure 7.6: Shooter Localization with 3 Sensors – MB-SW Detection

As seen from Figure 7.5 and Figure 7.6, the accuracy of shooter localization increases as the number of sensors increases in the field. Estimation results for the generalized case of 1000 shots are listed in Table 7.6 for shooter location and shot time estimations and Table 7.7 for projectile trajectory and speed estimations. As shown in simulation results, deviation of error decreases as the number of sensors increases in the field.

Table 7.6: Estimation Results for Shot Location and Time (MB-SW)

Number of Sensors	Standard Deviation Errors 1000 Monte Carlo Estimations			
	Shooter Location			Shot Time
	Azimuth	Elevation	Range	
1	< 1°	< 1.2°	< 8%	< 0.10%
2	< 0.8°	< 1°	< 6%	< 0.08%
3	< 0.5°	< 0.6°	< 5%	< 0.06%
4	< 0.4°	< 0.5°	< 4.5%	< 0.05%
5	< 0.3°	< 0.4°	< 4%	< 0.04%

Table 7.7: Estimation Results for Projectile Trajectory and Speed (MB-SW)

Number of Sensors	Standard Deviation Errors 1000 Monte Carlo Estimations		Mach Number
	Unit Vector of Projectile Trajectory		
	Azimuth	Elevation	
1	No valid estimation. Only ToA and DoA of SW are available.		
2	< 1°	< 1.5°	< 9%
3	< 0.5°	< 0.8°	< 8%
4	< 0.35°	< 0.45°	< 6%
5	< 0.3°	< 0.4°	< 5%

7.3   Multi Shooter Localization

This section provides simulation and test results for the WB-SRPBF method described in section 4.3. Simulations are performed for DoA estimation of muzzle blast and shockwave signals with a varying number of acoustic sources at different SNR levels and reverberation levels. All the simulations are performed under appropriate assumptions. The assumptions for the simulation and tests based on WB-SRPBF based DoA estimation are listed in Table 7.8.

Table 7.8: Assumptions of Simulations for WB-SRPBF Based DoA Estimation

Assumption Type	Description
Microphones	Microphones are omnidirectional.
Detection Range	Range from sensor location to an acoustic source is assumed to be appropriate for detection of the signal.
Signal Detection	When the output of beamformer is obtained, it is assumed that the signal is labeled as muzzle blast or shockwave.
Background Noise	Effect of different SNR levels are tested in DoA estimation; however, any SNR level is assumed to be high enough for signal detection. Noise is assumed to be white noise.
Far Field Waves.	Muzzle blast and Shockwave signals are assumed to be planar waves.
Gunshot Acoustics	Shockwave has a bandwidth between 1000–10.000 KHz and the frequency components are intense in 1000–4000 KHz. Muzzle blast has a bandwidth of 300–1000 KHz.
Shot	There are single and multiple shots to be estimated.
Reverberation	Reverberation is simulated as described in APPENDIX C. Each reverberation is assumed as another acoustic source.
Shooter Localization	Each shot in a multi shooter case is processed as a single shot after DoA's and ToA's are obtained. Shooter localization performance is provided in section 7.2.

The performance of DoA and corresponding ToA estimation depend on the geometry of the array, measurement errors, SNR levels, and reflections. Measurement errors can be categorized as timing, location, and speed of sound errors as listed in Table 7.2. Effect of microphone array geometry is provided in 7.3.1. Single and multiple shot detection with respect to varying SNR levels and reverberation are provided in section 7.3.2. The description of general simulation parameters of WB-SRPBF is listed in Table 7.9. Those parameters are common and valid for all simulations in this section.

Table 7.9: Simulation Parameters for WB-SRPBF Based DoA Estimation

Parameter	Description
Microphone Locations	Microphone array consists of some microphones populated on UCA on a horizontal plane and some microphones placed above UCA on a vertical line passing through the center of UCA. Further details are given in section 7.3.1.
Shot Locations	Gunshot acoustic signals arrive at microphone array from a point in the upper hemisphere with respect to the microphone array. Range of azimuth angle of a gunshot: [0 360] Range of elevation angle of a gunshot: [0 90°] The spherical coordinate system is described in APPENDIX D.
Shot Time	If gunshot acoustics do not overlap then they are processed as a single shot. For multi shot case, gunshot acoustic signals arriving from different directions overlap in the time domain.
Beamformer Frequency	$300 \leq f_{BEAM} \leq 4000$
Sampling Frequency	$f_s = 51200 KHz$, $N_s = 1024$ Time measurements are subject to timing error defined in Table 7.2.
Speed of Sound	The nominal speed of sound is assumed to be 340 m/s. The speed of sound is subject to temperature error defined in Table 7.2.

7.3.1 DoA Estimation Depending on Microphone Topology

The performance of WB-SRPBF based DoA estimation method relies on the geometry of microphone array in terms of estimation accuracy and angular resolution of multiple source detection. There are several studies in the literature proposing optimum geometry and microphone placement of microphone arrays for accurate sound source localization (Rabinkin, Renomeron, French, & Flanagan, 1997; Alameda-Pineda, Horaud, & Mourrain, 2013; Ward, 2002).

This thesis utilizes a microphone geometry formed by uniform circular array (UCA) and uniform linear array (ULA) in WB-SRPBF simulations. In detail, the array consists of microphones distributed on (UCA) and microphones populated on a vertical line passing through the center of UCA as shown in Figure 7.7. The horizontal plane is formed as UCA to span 360° in azimuth plane and vertical microphones are used to increase accuracy in elevation angle.
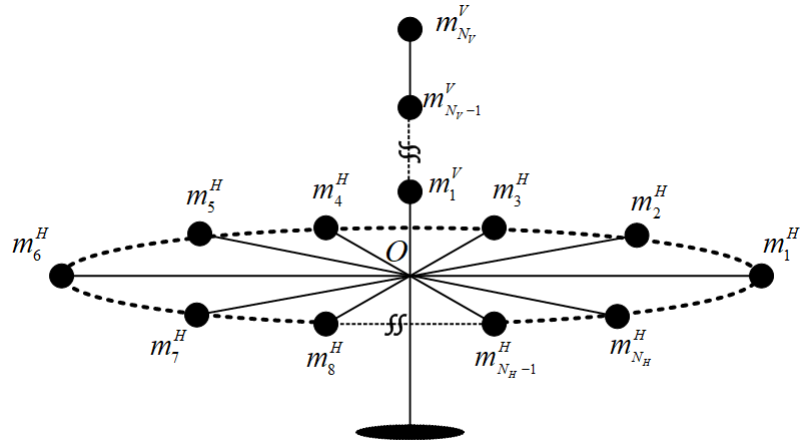

Figure 7.7: Microphone Array Topology for WB-SRPBF Technique

Each successive microphone m_i^H and m_{i+1}^H placed on UCA has a uniform angular displacement with respect to center of circle is uniform and each microphone placed on vertical line with uniform displacement of d^V (55).

$$\angle m_i^H O m_{i+1}^H = \frac{2\pi}{N_H}$$
$$\left| m_i^V m_{i+1}^V \right| = d^V$$

$$(55)$$

In shooter localization concept, there might be a random number of multiple shots occurred from different directions. In detail, muzzle blast signals or shockwave signals due to simultaneous gunshots at different locations might overlap in the time domain. Furthermore, reflected signals of original signals might overlap with the original signal. Each of those signals is assumed as a separate acoustic source with different DoA.

Source separation depends on the directivity of the beamformer and the directivity depends on the beamformer frequency, number of elements and inter-distance between each element (Brandstein & Ward, 2013). As inter-distance between elements increase beamwidth of beamformer becomes narrow but side lobes increases and as the number of elements increases, side lobes decreases.

WB-SRP beamformer has a directivity function (56) as shown in (38) in section 4.3.

$$D\left(f_{BEAM},\phi,\theta\right) = wU^T\left(f_{BEAM},\phi,\theta\right) \tag{56}$$

$$w = \frac{1}{N_M}\mathbf{1}^{N_M \times 1}, \quad U\left(f_{BEAM},\phi,\theta\right) = \begin{bmatrix} e^{j2\pi f_{BEAM}\frac{\left(\bar{m}_1 \cdot \bar{u}(\phi,\theta)\right)}{c}} \\ e^{j2\pi f_{BEAM}\frac{\left(\bar{m}_2 \cdot \bar{u}(\phi,\theta)\right)}{c}} \\ \vdots \\ e^{j2\pi f_{BEAM}\frac{\left(\bar{m}_M \cdot \bar{u}(\phi,\theta)\right)}{c}} \end{bmatrix}$$

Phase shift in beam-steering vector U has a range between $-\pi$ and π as (57). Then, for uniformly distributed microphones, inter-distance between microphones are limited by (58) so that side lobes do not occur.

$$\left| 2\pi f_{BEAM} \frac{\bar{m}_i \cdot \bar{u}}{c} \right| < \pi \tag{57}$$

$$Max(\bar{m}_i \cdot \bar{u}) = d_{max}$$

$$\left| 2\pi \frac{f_{BEAM} d_{max}}{c} \right| < \pi$$

$$d_{max} \leq \frac{c}{2 f_{BEAM}} \tag{58}$$

The problem is to find a proper number of microphones and appropriate microphone locations which satisfy the application requirements. Simulations are performed for 4-8-16-32 microphones. For 4-microphone case, 3 of microphones are distributed on UCA and 1 microphone is positioned above the center of UCA. For 8-16-32 cases, the number of microphones distributed on UCA is much greater than the number of microphones on vertical line because UCA has already capability of elevation span and the microphones on the vertical line are for enhancement in elevation estimation.

Beamwidth of the beamformer is analyzed with respect to different microphone arrays in simulations. Simulations have general parameters described in Table 7.9 and special parameters listed in Table 7.10. Furthermore, the side-lobe peak value less than 0.1 for normalized SRP is allowed so that narrower beamwidth can be obtained with the beamformer.

Table 7.10: Simulation Parameters for Beamwidth Analysis of Arrays

Parameter	Description
Source	Shockwave Signal simulated as described in APPENDIX A. SNR level is 10 dB for each simulation. Reverberation is discarded for each simulation since the aim is to analyze beamwidth of the beamformer.
Shot Location	Shot location is assumed as a single shot for each microphone topology. Azimuth angle of a gunshot: 180° Elevation angle of a gunshot: 45°
Microphone Array	<table><tr><td>N_{Mic}</td><td>N^H</td><td>r^H</td><td>$\angle m_i^H O m_{i+1}^H$</td><td>N^V</td><td>d^V</td></tr><tr><td>4</td><td>3</td><td>0.020 m</td><td>120°</td><td>1</td><td>0.020 m</td></tr><tr><td>8</td><td>6</td><td>0.080 m</td><td>60°</td><td>2</td><td>0.040 m</td></tr><tr><td>16</td><td>14</td><td>0.200 m</td><td>26°</td><td>2</td><td>0.100 m</td></tr><tr><td>32</td><td>30</td><td>0.400 m</td><td>12°</td><td>2</td><td>0.200 m</td></tr></table>

Figure 7.8, Figure 7.9, Figure 7.10, and Figure 7.11 show beamwidth analysis for 4-8-16-32 microphone arrays, respectively.
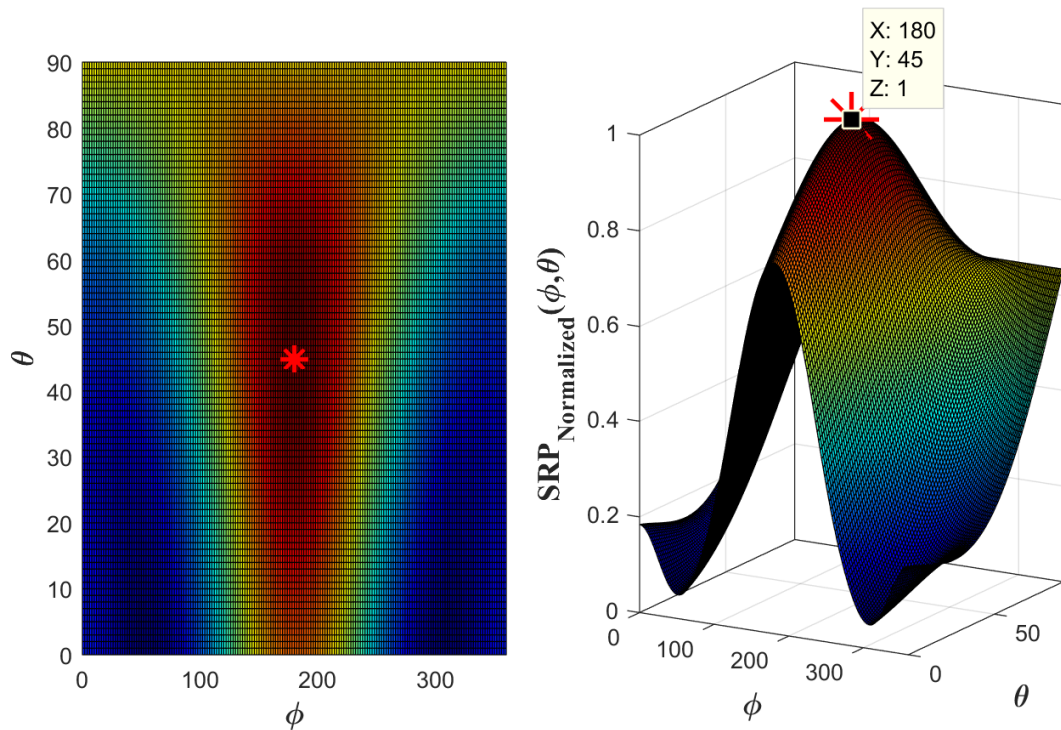
Figure 7.8: Beamwidth of Beamformer the Array of 4 Microphones
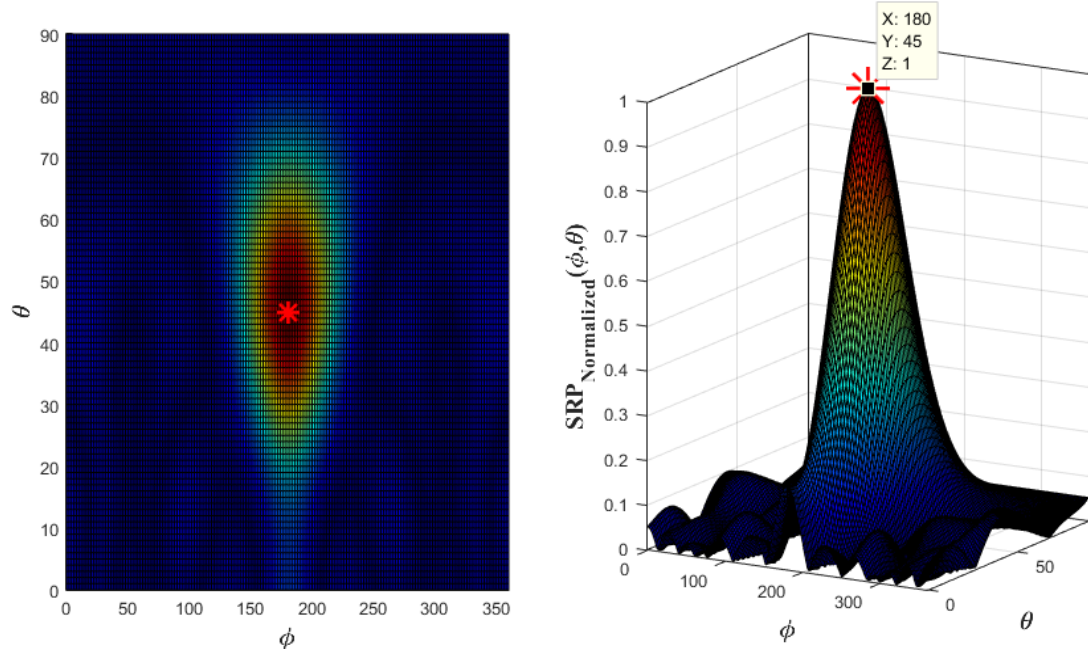
Figure 7.9: Beamwidth of Beamformer for the Array of 8 Microphones
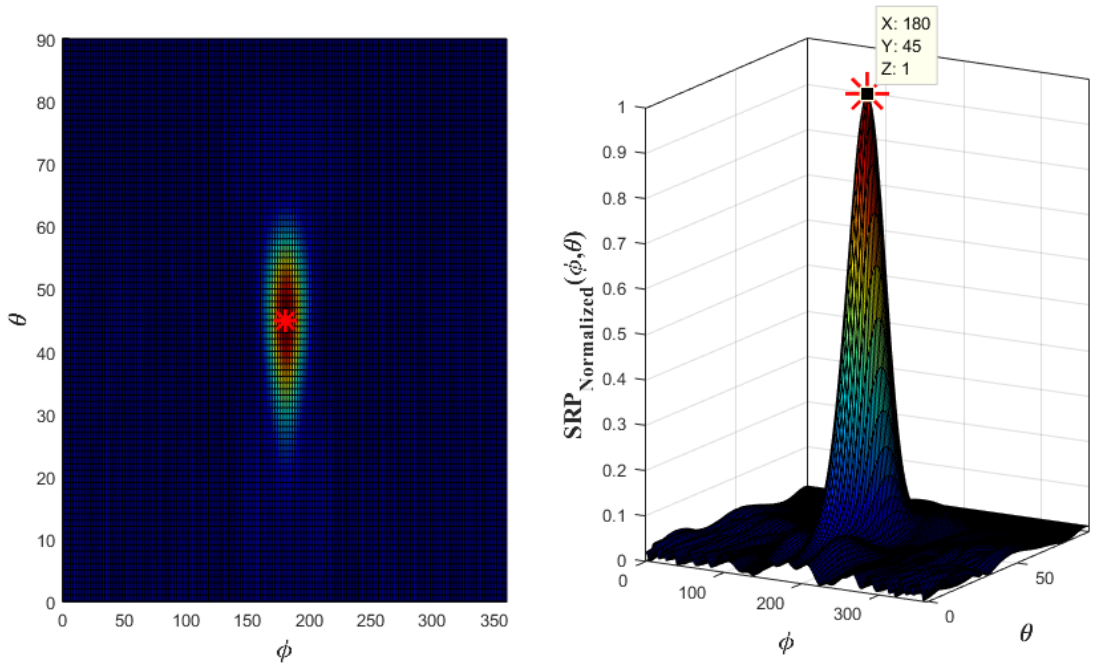
Figure 7.10: Beamwidth of Beamformer for the Array of 16 Microphones
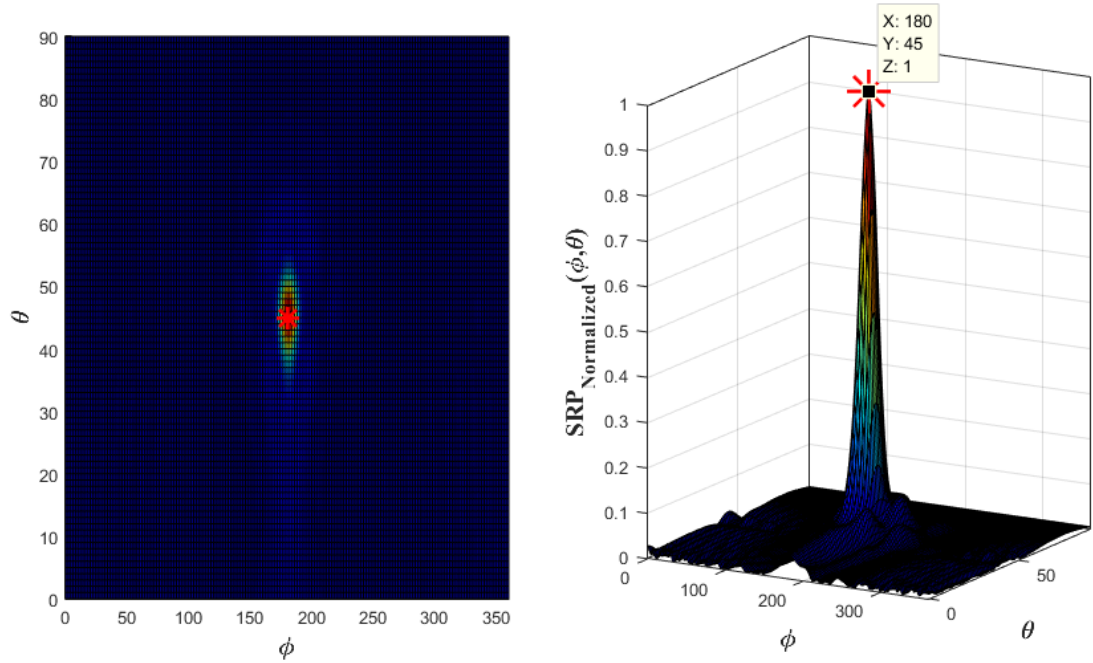

Figure 7.11: Beamwidth of Beamformer the Array of 32 Microphones

According to the SRP output o WB-SRPBF for 4-8-16-32 microphone arrays illustrated as the aperture size increases with increasing number of microphones the beamwidth decreases since beamwidth depends on effective aperture size as (59).

$$BW_\phi = \frac{\lambda}{L_{Azimuth}}$$

$$BW_\theta = \frac{\lambda}{L_{Elevation}} \qquad (59)$$

$$L_{Azimuth} = L_{Elevation} = 2\,r^H \quad \text{for UCA}$$

The microphone arrays consisting of 16 and 32 microphones are appropriate for simultaneous multiple shooter detections since any additional beam in other directions due to other sources can be distributed on SRP map without overlapping. The number of microphones can be selected with respect to application requirement. In fact, the number of microphones and aperture size should increase to separate multiple shots directed from closer angular directions. Besides, each additional microphone results in an increase of hardware and computation requirements such as preamplifiers, analog to digital converters and computation time. Computational time for each configuration is listed in Table 7.11 for simulations performed with MATLAB® on a PC with the configuration of i7-2.4GHz. Those process times can be reduced more by optimizing codes for the embedded system provided in Chapter 6.

Table 7.11: Simulation Time of WB-SRPBF for Varying Array Size

Number of Microphones	Simulation Process Time for WB-SRPF for Single Frequency f_{BEAM}
4	8.962 msec
8	9.166 msec
16	9.640 msec
32	11.293 msec

As a consequence of simulation results, this thesis utilizes microphone arrays consisting of 16 and 32 microphones for DoA estimation and simultaneous multiple shooter detections since those arrays have the capability to detect more simultaneous shot than microphone arrays with 4 and 8 microphones.

7.3.2 Multiple Gunshot Acoustic Event Detection

The simultaneous multi shooter detection problem is defined as the separation of gunshot acoustic events overlapping in the time domain. In detail, the multiple shot case is defined such that muzzle blast or shockwave signals due to shots at different locations are recorded in the same sampling frame. Furthermore, this case is valid not only for simultaneous multiple shots but also for reflected signals overlapping with the original signal in time. Hence, the same approach can be used for separation of acoustic events of different shots and separation of original signal from reflections. Further details of reflection elimination are provided in section 7.4. Figure 7.12 depicts an example of a recording corresponding to of overlapped two identical muzzle blasts which might be caused by multiple gunshots at different locations or reflected signal overlapping with the original signal.
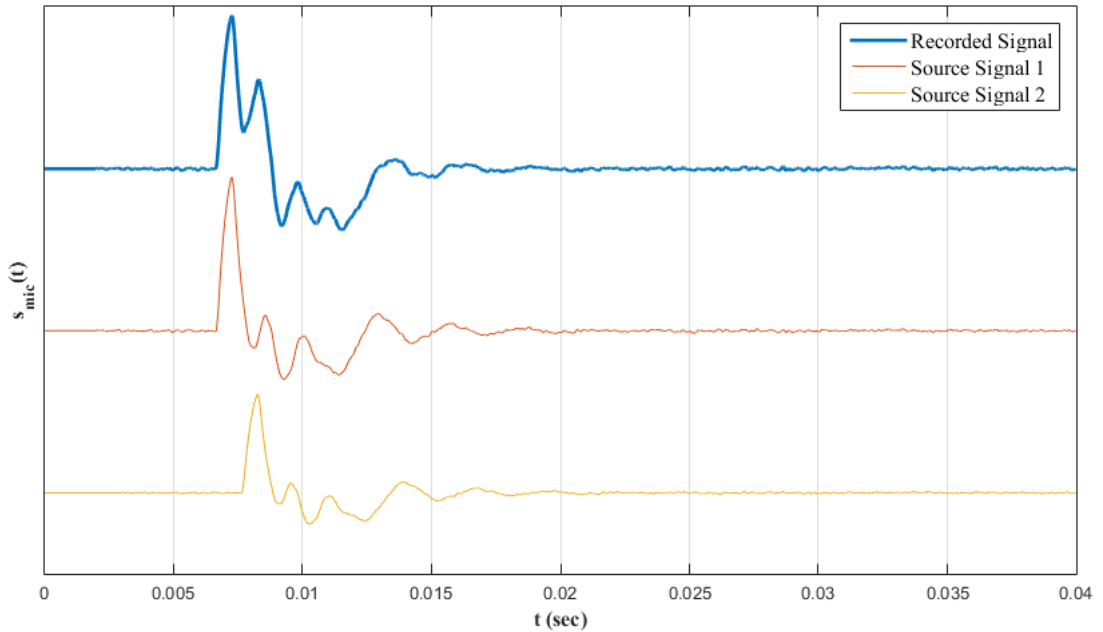

Figure 7.12: An Example Recording of Multi Shot (Muzzle Blast Signals)

WB-SRPBF technique is analyzed for the problem of multiple shooters detection with the arrays of 16–32 microphones described in section 7.3.1. Each simulation has general parameters described in Table 7.9 and special parameters listed in Table 7.12.

Table 7.12: Simulation Parameters for Multiple Shot Detection

Parameter	Description
Source	Sources consist of muzzle blast and shockwave signals simulated as described in APPENDIX A and APPENDIX B. SNR is high enough such that signals are detected without a miss. Reverberation is discarded. All signals have the same power.
Number of Sources	The number of sources is set a maximum value for each geometry such that beamformer detects each signal without a miss.
Shot Locations	Shot locations are uniformly distributed in the upper hemisphere with respect to the microphone array. Range of azimuth angle of a gunshot: [0° 360°] Range of elevation angle of a gunshot: [0 60°]

Figure 7.13, Figure 7.14, Figure 7.15 and Figure 7.16 depict resultant SRP map of microphone arrays consisting of 16 and 32 microphones for uniformly distributed shockwaves and muzzle blasts, respectively.
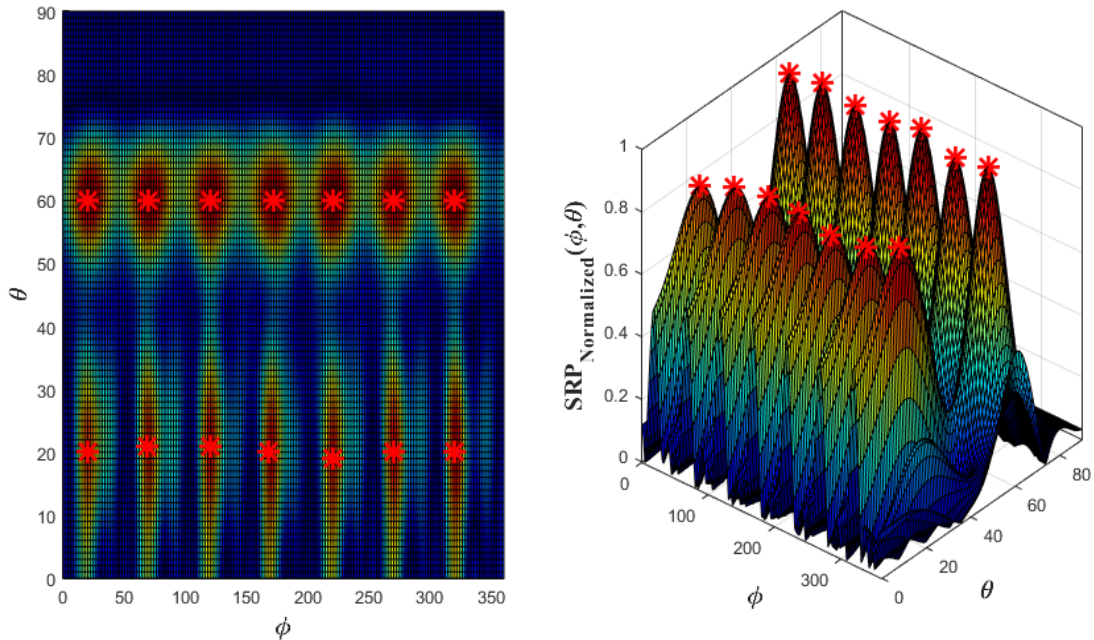
Figure 7.13: SRP Map of Uniformly Distributed Shockwave (16 Microphone)
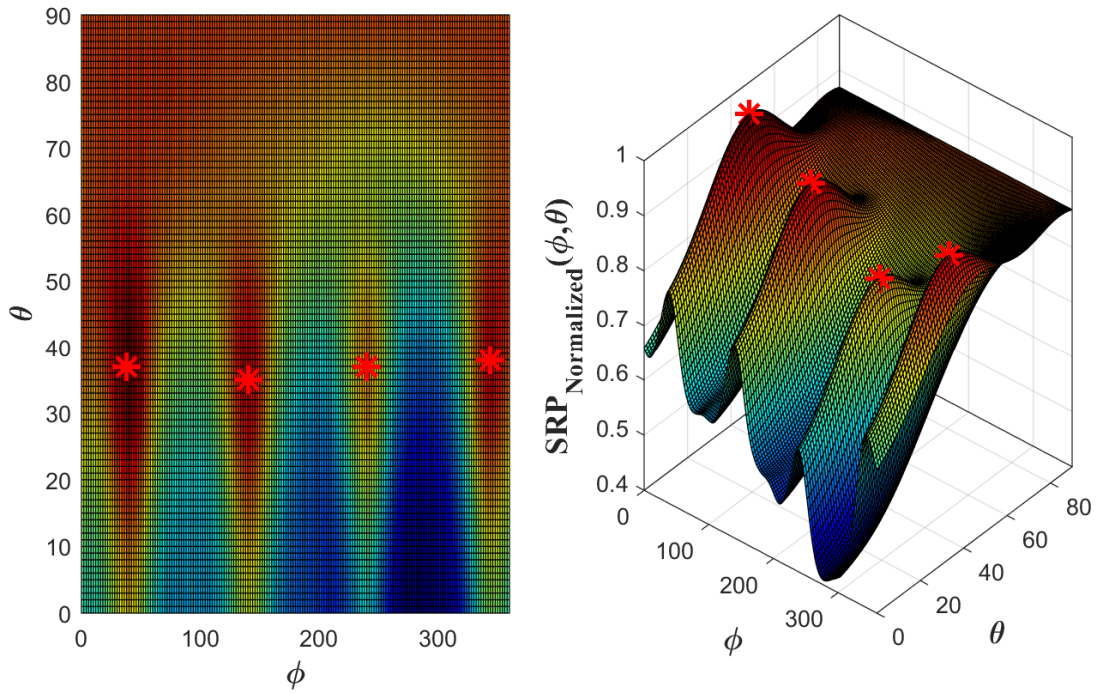
Figure 7.14: SRP Map of Uniformly Distributed Muzzle Blast (16 Microphone)
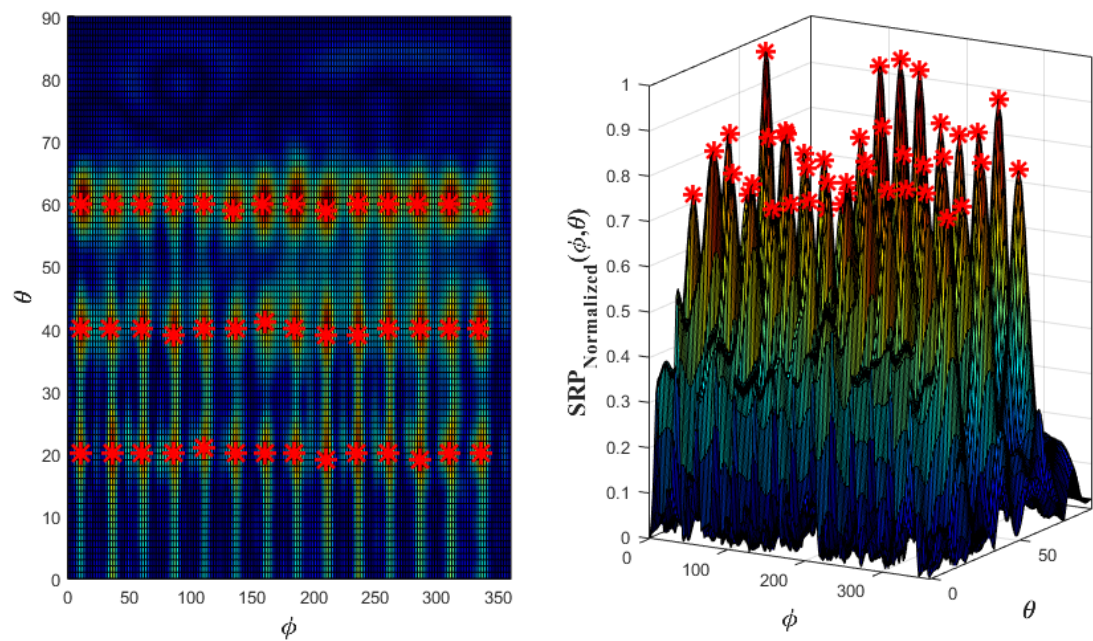
Figure 7.15: SRP Map of Uniformly Distributed Shockwave (32 Microphone)
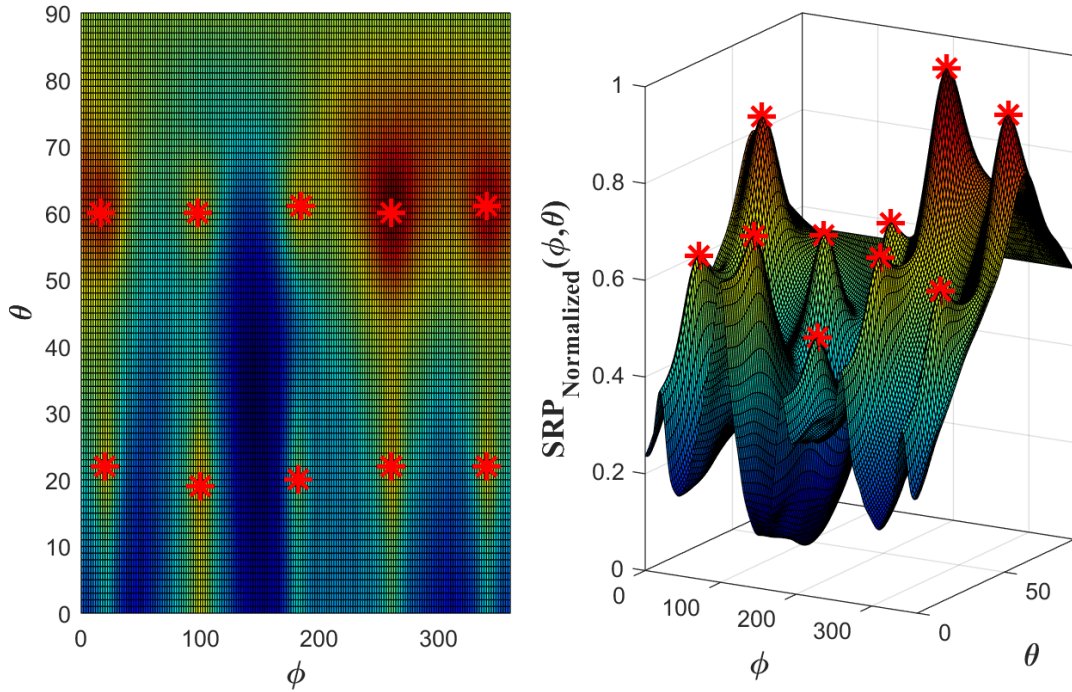
Figure 7.16: SRP Map of Uniformly Distributed Muzzle Blast (32 Microphone)

Table 7.13 shows the maximum number of detected gunshot acoustic events by the arrays of 16 and 32 microphones. The number of detected shockwaves is greater than that of muzzle blast because muzzle blast has a long duration in time than shockwave and as the number of overlapped muzzle blast increases detection capability decreases.

Table 7.13: Maximum Number of Detected Acoustic Events in Single Frame

Acoustic Event	Number of Microphones	Maximum Number of Detection of Same Acoustic Event in Single Frame
Shockwave	16	14
	32	42
Muzzle Blast	16	4
	32	10

Simulations illustrated in Figure 7.13, Figure 7.14, Figure 7.15 and Figure 7.16 are for analyzing the capabilities of the WB-SRPBF method under synthetic conditions such

that there are a maximum number of same acoustic events and there is no reflection. These conditions can be converted to a more realistic case by changing SNR level of each acoustic event and adding reflected signals. The single sampling frame of 1024 samples involving both muzzle blast and its reflection and two shockwaves of different shots is depicted as an example in Figure 7.17. Actual DoA values of each acoustic event are provided in Table 7.14. Figure 7.18, Figure 7.19 illustrates SRP map corresponding to example multi shot for 16 and 32 microphones, respectively.

Table 7.14: DoA of Acoustic Events for Example Multi Shot Detection

Acoustic Event	Actual DoA (Azimuth, Elevation)
Muzzle Blast	(130°, 50°)
Reflected Muzzle Blast	(210°, 30°)
First Shockwave	(30°, 20°)
Second Shockwave	(75°, 20°)
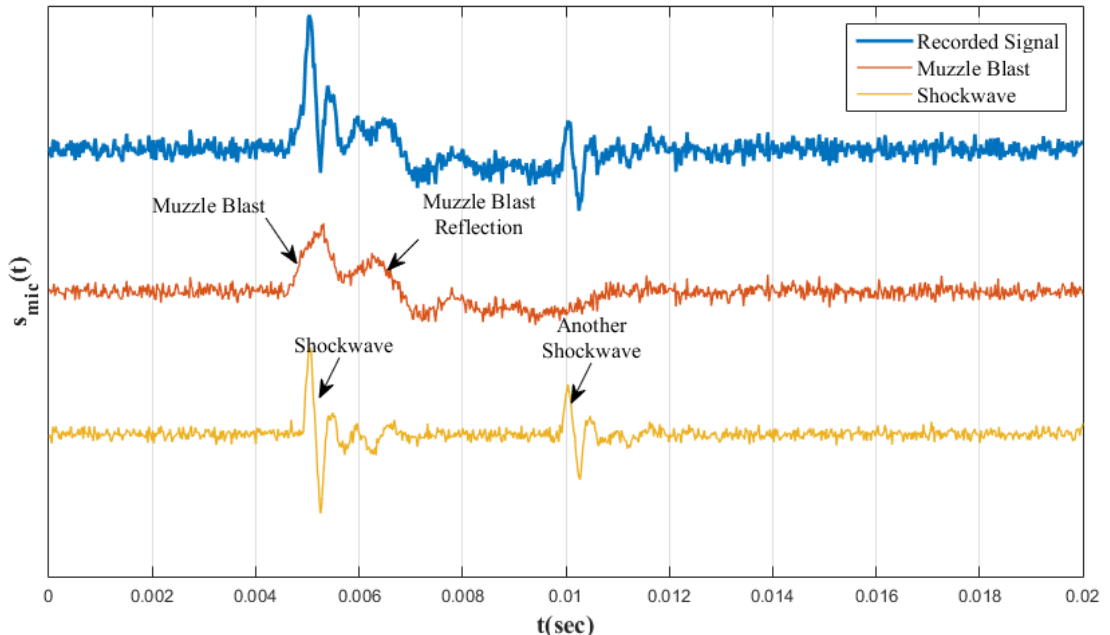
Figure 7.17: Example Recording of Multi Shot in a Single Frame
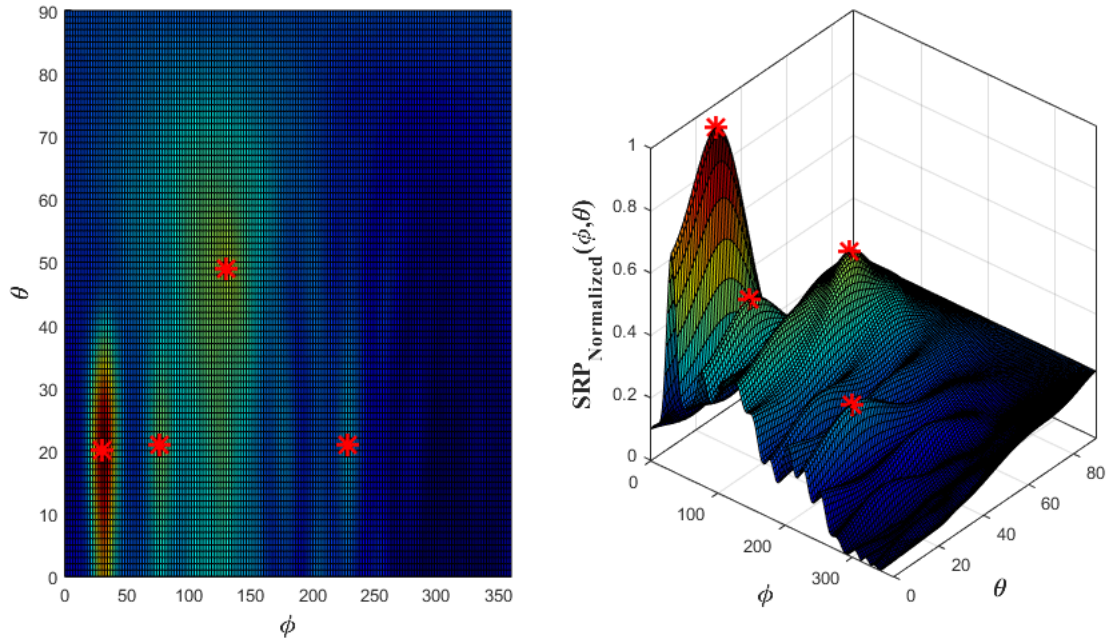
Figure 7.18: SRP Map for Multiple Shots with Reverberation (16 Microphone)
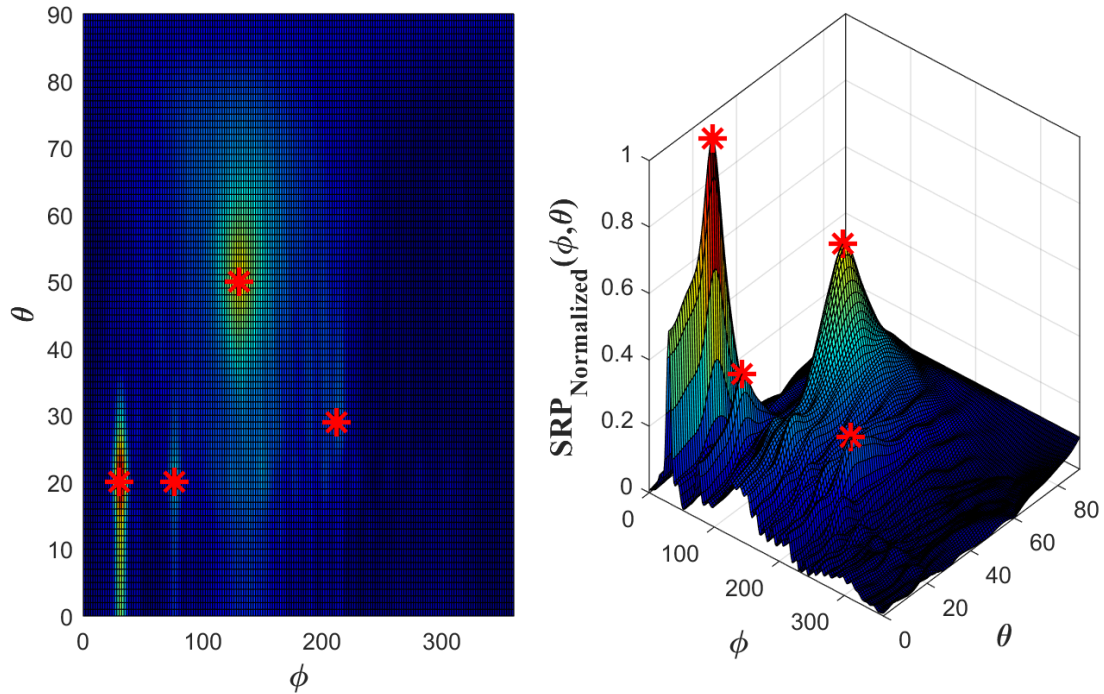
Figure 7.19: SRP Map for Multiple Shots with Reverberation (32 Microphone)

Table 7.15 shows estimation results of the example multi shot detection. If this simulation example is generalized with 1000 Monte Carlo simulations for multiple

shots at different locations then the performance of WB-SRPBF is obtained in terms of estimation errors and angular resolution as shown in Table 7.16. In fact, Table 7.16 lists the performance values for the worst case . If time separation between overlapping signals increases, then the angular resolution enhances up to 10°.

Table 7.15: Performance Results of Multi Shot Detection (Example Simulation)

Number of Microphones	Estimation Error	
	Azimuth $0 \le \phi \le 360$	Elevation $0 \le \theta \le 60$
16	4.00°	2.25°
32	2.75°	1.75°

Table 7.16: Performance Results of Multi Shot Detection (Generalized)

Number of Microphones	Number of Acoustic Events (Mixed)	Standard Deviation of Estimation Error		Angular Resolution	
		Azimuth $0 \le \phi \le 360$	Elevation $0 \le \theta \le 60$	Azimuth $0 \le \phi \le 360$ θ : Same Angle	Elevation $0 \le \theta \le 60$ ϕ : Same Angle
16	Single	< 1°	< 1°	-	-
	Two	< 2°	< 3°	~20°	~35°
	Max	< 4°	< 5°	~45°	~30°
32	Single	< 1°	< 1°	-	-
	Two	< 2°	< 2°	~15°	~25°
	Max	< 2°	< 3°	~30°	~15°
In the maximum number of acoustic events, it is assumed that two muzzle blasts and two shockwaves are recorded in a single frame and all signals overlap in time.					

After DoA is obtained then ToA is computed from the beamformer output as described in section 4.3 and both values are used in shooter location estimation framework

described in Chapter 3. The performance of shooter localization framework is provided in section 7.2.

7.4 Reflection Elimination

Reflected signals overlapping with original signals are handled as if they are another acoustic source directed from different locations. Thus, the problem of the elimination of reverberation is same as the multi shot detection problem. Two different methods might be used to eliminate reverberation. One of the methods is straightforward such that a power threshold is determined to eliminate any peak in SRP map below the threshold; however, this method can cause signals with a low power level to be missed. For example, muzzle blast signals with low SPL can easily be eliminated in such a case. The second method is utilizing multiple sensors in the field with the common output functions described in Chapter 3 and it is better than the former method.

The case in which both muzzle blast and shockwave signals are detected by the sensors in the field is selected as an example for the reverberation elimination. The assumption is that sensors in the field detected DoA's and associated ToA's for muzzle blast and shockwave signals as well as the reflected signals. All pairs of DoA's and ToA's should satisfy the common output functions for the case of both muzzle blast and shockwave detection are (26) and (27) in section 3.2.4.

$$t_0 = \frac{t_i^{SW} - t_i^{MB} \left(\vec{u}_i^{MB} \bullet \vec{u}_i^{SW} \right)}{1 - \left(\vec{u}_i^{MB} \bullet \vec{u}_i^{SW} \right)} \tag{26}$$

$$\boldsymbol{x}_0 = \boldsymbol{s}_i + c \left(\frac{t_i^{MB} - t_i^{SW}}{1 - \left(\vec{u}_i^{MB} \bullet \vec{u}_i^{SW} \right)} \right) \vec{u}_i^{MB} \tag{27}$$

If same locations are detected in a predefined confidence level by each sensor in the field then it is a valid shooter location, but if a shooter location estimation is not confirmed by other sensors then it is most probably a result due to a reflection. However, there is still a probability of missing a real shot because a sensor might not be deployed in the detection zone described in section 3.2.1. This problem might be

resolved by deploying a minimum number of 3 sensors with the overlapping field of views in the field.

An example of reverberation elimination for the case both muzzle blast and shockwave detection by each sensor in the field is simulated according to the simulation properties listed in Table 7.17.

Table 7.17: Simulation Parameters for Reflection Elimination Example

Parameter	Description
Gunshot Acoustic	Each sensor in the field is assumed to detect both muzzle blast and shockwave due to an actual gunshot.
Sensors Locations	$s_1 = [\quad 0m \quad 0m \quad 0m \quad]$ $s_2 = [\quad 30m \quad -40m \quad 20m \quad]$ $s_3 = [\quad 50m \quad 200m \quad 50m \quad]$
Shot Location	$x_0 = [\quad 500m \quad 150m \quad 20m \quad]$
Reflections	Reflections are assumed to be only for muzzle blast signals. Each sensor in the field is assumed to record shockwave, muzzle blast and reflected muzzle blast signals.
DoA of Reflections	Reflections due to the original signal are assumed to be directed from the ground so elevation angle of the original signal is shifted in negative direction. The azimuth angle of reflection is assumed to be in the range of $\pm 10°$. $-10^o \leq \phi_{ORIGINAL} - \phi_{REFLECTION} \leq 10^o$ $-5^o \leq \theta_{ORIGINAL} - \theta_{REFLECTION} \leq 0^o$
ToA of Reflections	Time difference between ToA's of each reflected and the original signal is assumed to be 1 msec as maximum and 0.5 msec as a minimum. $0.0005 \sec \leq ToA_{ORIGINAL} - ToA_{REFLECTION} \leq 0.001 \sec$

Simulation results of reflection elimination are depicted in Figure 7.20. In simulation results, it can be seen that blue colored "+" location estimations are gathered closer, but green colored "+" location estimations are at distant locations with respect to each other. In other words, while the encircled location estimations due to original signals have a consistency, the location estimations due to reflected signals are not within consistent limits. Hence, singular location estimations can be assumed to be occurred due to reflected signals; in turn, discarded. After elimination of reflections, then DoA and associated ToA values can be used in the estimation framework for shooter localization.
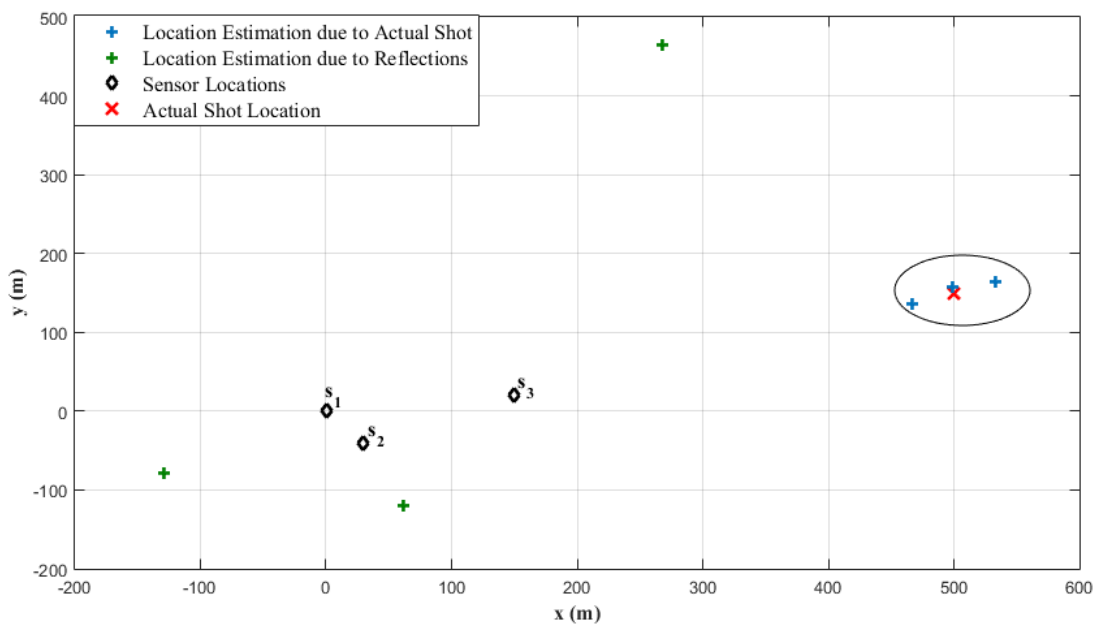
Figure 7.20: Example Reflection Elimination in Shooter Location Estimation

7.5   System Calibration and Performance Enhancement

This section provides simulation and test results for the optimization based system calibration method described in Chapter 5. According to the effects of system parameters in shooter localization described in section 5.2, errors in microphone location and speed of sound have a significant impact on the accuracy of the shooter localization. Shooter localization simulations are performed with uncalibrated and

calibrated microphone locations and speed of sounds to show performance enhancement with the proposed system calibration method.

System calibration simulations are compatible with the simulations of shooter location estimation provided in section 7.2. In detail, simulations are performed according to the same simulation parameters listed in Table 7.3 and errors introduced to microphone location and speed of sound and other internal system errors are assumed same as the error models as listed in Table 7.2.

The error introduced to the speed of sound has a zero-mean normal distribution with standard deviation of approximately 5 m/s, and the error introduced to microphone locations has a zero-mean normal distribution with standard deviation of 3 mm. Furthermore, the constraints of the optimization problem (54) in the system calibration method are assumed such that speed of sound is greater than 0 and microphone location error is limited to 1 cm. Table 7.18 lists the uncalibrated and calibrated microphone location and speed of sound in terms of standard deviation of error. System calibration simulation is performed by Monte Carlo simulation with a number of 500 iterations.

Table 7.18: Estimation Results of Calibrated System Parameters

System Parameter	Estimation Error Standard Deviation
Microphone Positions	$1.637 \ 10^{-3}$ m
Speed of Sound	1.293 m/s

There is still an error in estimated system parameters because there are still measurement errors although it is a controlled shot with known parameters. Sensor, shooter, and target locations in the controlled shot are measured with GPS so actual DoA values and projectile trajectory calculated with respect to those values are also subject to GPS error. In addition, timing error due to sampling frequency still exists in the system so estimations are also subject to the timing error. Nevertheless, the

calibration process fixes the erroneous system parameters significantly, in turn, the accuracy of shooter localization.

Figure 7.21 illustrates the Monte Carlo simulation with 500 iterations for shooter location estimation with respect to uncalibrated and calibrated system parameters for a sample shot at the location of (500m, 400m, 60m). Table 7.19 lists the corresponding errors for uncalibrated and calibrated shooter location estimations, respectively. The results of simulations show that the optimization based system calibration method enhances the accuracy of the shooter localization significantly.

Table 7.19: Uncalibrated and Calibrated Shooter Localization Errors

|	**Shooter Localization Estimation Norm Error Standard Deviation**
Uncalibrated	21.676 m
Calibrated	3.381 m
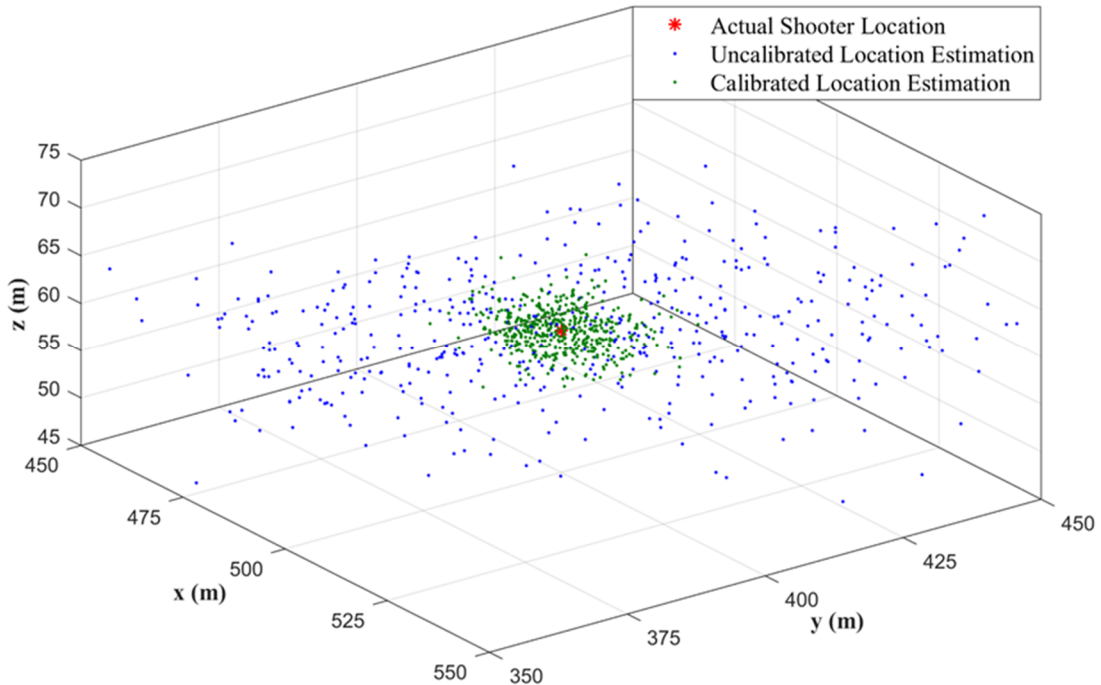
Figure 7.21: Calibrated and Uncalibrated Shooter Localization

CHAPTER 8

CONCLUSIONS AND FUTURE WORKS

8.1 Conclusions

The thesis proposes a generalized shooter location estimation framework which is valid when both gunshot related acoustic events are present or when one of them is absent for some reason. The performance of the framework for detection of only muzzle blast, only shockwave, and both of them are simulated and analyzed separately. Furthermore, the output of estimation related to each case is analyzed. This analysis shows that shooter location and shot time can be estimated if muzzle blast exists and projectile trajectory and projectile speed can be estimated if shockwave exists and trajectory line passes between the sensors. However, if there is a single sensor deployed in the field, it can only provide DoA and ToA of the detected signal. A minimum number of two sensors are required for a gunshot related estimation. However, there is a special case such that even if there is a single sensor in the field, the framework can output shooter location and shot time provided that the sensor detects both muzzle blast and shockwave. The simulations corresponding to each case show that the framework estimate actual values with a high precision.

The thesis also analyzes estimation methods for ToA and DoA of the gunshot acoustic events which are essential information in the shooter estimation framework. The thesis involves two different methods, namely TDoA technique and beamforming technique called WB-SRPBF. TDoA technique is used for single shooter localization and system calibration since it requires low computational time. On the other hand, WB-SRPBF technique is used for simultaneous multiple shooter localization in reverberant environments. Furthermore, reflection elimination method utilizing both WB-SRPBF DoA estimation and common output functions of the localization framework is provided in the thesis. Simulations corresponding to multiple shooter localization and

reflection elimination show that the proposed methods work successfully for simultaneous multiple shooter localization in a reverberant environment.

The thesis proposes a system model for shooter localization framework and defines several system parameters such as microphone positions and speed of sound. The analysis of the relation between system parameters and shooter localization show that measurement errors in system parameters have a significant effect on the accuracy of shooter localization. Thus, a system calibration method which is derived from the system model is proposed to calibrate system parameters to enhance the accuracy of shooter localization. The simulation results of shooter localization with uncalibrated and calibrated system parameters show that the calibration method enhances the accuracy of shooter localization significantly.

The thesis also proposes a system architecture and hardware design for acoustic based shooter localization. This system has the capability of processing analog microphone signals according to shooter localization algorithms. The proposed system can also measure self-location and self-orientation which is important in shooter localization. Furthermore, it can establish a wireless network with other sensors in the field and operational center for sensor-network based shooter localization system.

All the simulations and experiments are provided in this thesis to clarify and verify the methods involved in this thesis. The simulation results show that the proposed methods work with appropriate accuracy.

8.2 Future Works

There are future works related the work involved in this thesis in terms of shooter localization, DoA estimation methods, and system calibration. Future works concern increasing system capabilities and adaptations for different conditions.

Shooter localization concept described in this thesis considers the shooter or shooters are stationary but not in motion. Hence, DoA estimation methods based on TDoA or WB-SRBPF also assume that shooter is stationary. In fact, there might be attacks from a moving vehicle or vehicles. In such a case, the shooter localization system should

not only estimate the location but also track the shooter. Thus, it could be interesting to study localizing and tracking a single shooter or multiple shooters in motion. Such a system is important at least as much as a shooter localization considering stationary shooters.

In addition, WB-SRPBF method is based on conventional delay-and-sum beamformer and phase shift beamformer. This method can be further improved by utilizing different algorithms available in the literature to increase the accuracy of DoA estimation with less number of microphones. In addition, reflection elimination is based on predefined thresholding of WB-SRPBF result and common output functions of the framework. This method can be further improved with adaptive thresholding in run-time so that the problem of missing muzzle blast due to the threshold value is resolved.

The system calibration method is defined such that there is a controlled shot during the system calibration procedure. This is feasible for all time; however, it would be useful if this procedure is converted to a run-time application. In other words, this model could be converted to a runtime calibration method which uses the information gathered by all sensors while there is an attack.

The work related to shooter localization system involved in this thesis has the capability of shooter location and trajectory estimation for both single shooter and simultaneous multiple shooters and it is also able to caliber system parameters for accurate estimations. The future works will enhance the system capabilities and performance so that it will work under different conditions varying from stationary shooters to mobile shooters and it performs calibration runtime even there is a severe attack.

REFERENCES

Adams, R. N., Horowitz, L. L., & Senne, K. D. (1980). Adaptive main-beam nulling for narrow-beam antenna arrays. *IEEE Transactions on Aerospace and Electronic Systems*, *4*, pp. 509-516.

Aguilar, J. R. (2013). Gunshot location systems the transfer of the sniper detection technology from military to civilian applications. *Security Technology (ICCST), 2013 47th International Carnahan Conference on* (pp. 1-6). IEEE.

Agurok, I., Falicoff, W., Alvarez, R., & Shatford, W. (2012). Passive electro-optical projectiles tracker. *Proc. of SPIE, 8359*, pp. 835916-1.

Akman, C., Sonmez, T., Ozugur, O., & Leblebicioglu, M. K. (2016). Shooter localization system calibration and implementation. *Signal Processing and Communication Application Conference (SIU), 2016 24th* (pp. 2025-2028). IEEE.

Alameda-Pineda, X., Horaud, R., & Mourrain, B. (2013). The geometry of sound-source localization using non-coplanar microphone arrays. *Applications of Signal Processing to Audio and Acoustics (WASPAA), 2013 IEEE Workshop* (pp. 1-4). IEEE.

Allen, C. S., Blke, W. K., Dougherty, R. P., Lynch, D., Soderman, P. T., & Underbrink, J. R. (2013). Removal of flow noise. In *Aeroacoustic measurements* (pp. 83-86). Springer Science & Business Media.

Awasthi, V., & Raj, K. (2014). Application of hardware efficient CIC compensation filter in narrow band filtering. *World Academy of Science, Engineering and Technology, International Journal of Electrical, Computer, Energetic, Electronic and Communication Engineering, 8*(9), 1468-1474.

Baker, W. E. (1973). *Explosions in air.* University of Texas press.

Bohn, D. A. (1988). Environmental effects on the speed of sound. *Journal of the Audio Engineering Society, 36*(4), 223-231.

Brandstein, M., & Ward, D. (Eds.). (2013). *Microphone arrays: signal processing techniques and applications.* Springer Science & Business Media.

Brookner, E. (1985). Phased-array radars. *Scientific American, 252*(2), 94-102.

Damarla, T., Kaplan, L. M., & Whipss, G. T. (2010). Sniper localization using acoustic asynchronous sensors. *IEEE Sensors Journal, 10*(9), 1469-1478.

Danicki, E. (2006). The shock wave-based acoustic sniper localization. *Nonlinear analysis: theory, methods & applications, 65*(5), 956-962.

Danicki, E. (2009). Calibration of EM and acoustic antisniper systems. *Biuletyn Wojskowej Akademii Technicznej, 58*(4), 139-147.

Dougherty, R. P. (2008). What is beamforming? *Berlin Beamforming Conference (BeBeC).* Germany Berlin.

Fransler, K. S., Thompson, W. P., Carnahan, J. S., & Patton, B. J. (1993). *A parametric investigation of muzzle blast.*

Kneipfer, R. R. (1992). *Sonar Beamforming-An Overview Of Its History and Status.* NAVAL UNDERSEA WARFARE CENTER NEWPORT DIV NEW LONDON CT NEW LONDON DETACHMENT.

Lédeczi, Á., Nádas, A., Völgyesi, P., György, B., Kusy, B., Sallai, J., . . . Molnár, K. (2005). Countersniper System for Urban Warfare. *ACM Transactions on Sensor Networks, 1*(2), 153-177.

Libal, U., & Spyra, K. (2014). Wavelet based shock wave and muzzle blast classification for different supersonic projectiles. *Expert Systems with Applications, 41*(11), 5097-5104.

Lindgren, D., Olof, W., Fredrik, G., & Habberstad, H. (2010). Shooter localization in wireless microphone networks. *Eurasip journal on advances in signal processing, 2010(1)*, 690732.

Magand, F., Donzier, A., & Molliex, F. (2004). PILAR acoustic gunshot detection & localization system: principles of acoustic localization of small caliber gunshots. *CFA/DAGA, 4*, pp. 563-564. Strasbourg.

Maher, R. C., & Shaw, S. R. (2008). Deciphering gunshot recordings. *Audio Engineering Society Conference: 33rd International Conference: Audio Forensics-Theory and Practice.* Audio Engineering Society.

MATLAB R2015a. (n.d.). *The Mathworks, Inc.* Natick, Massachusetts, United States.

Mays, B. T. (2001). *Shockwave and muzzle blast classification via joint time frequency and wavelet analysis.* Army Research Lab Adelphi MD 20783-1197.

Millet, J., & Baligand, B. (2006). *Latest achievements in gunfire detection systems.* 01DB-METRAVIB LIMONEST (FRANCE).

Moroz, S. A., Pierson, R. B., Ertem, M. C., & Burchick Sr., D. A. (1999). *Airborne deployment of and recent improvements to the viper counter sniper system.* NAVAL RESEARCH LAB WASHINGTON DC.

Mucci, R. (1984). A comparison of efficient beamforming algorithms. *IEEE Transactions on Acoustics, Speech, and Signal Processing, 32*(3), 548-558.

Osborne, R. W., Bar-Shalom, Y., George, J., & Kaplan, L. (2014). Data fusion from multiple passive sensors for multiple shooter localization via assignment. *Proceedings of 17th international conference on information fusion (FUSION)* (pp. 1-7). IEEE.

Ozugur, O., Sonmez, T., Basli, A. B., & Leblebicioglu, M. K. (2015). Atış tespit sistemleri İçin duyarlılık analizi. *Signal Processing and Communications Applications Conference (SIU), 2015 23th* (pp. 1709-1716). IEEE.

Page, E., & Sharkey, B. (1995). SECURES: system for reporting gunshots in urban environments. *Proc. SPIE, 2497*, 160-172.

Penrose, R. (1955). A generalized inverse for matrices. *Mathematical proceedings of the Cambridge philosophical society, 51*(3), 406-413.

Rabinkin, D. V., Renomeron, R. J., French, J. C., & Flanagan, J. L. (1997). Optimum microphone placement for array sound capture. *SPIE, 3162*, 227-239.

Ramos, A. L., Holm, S., Gudvangen, S., & Otterlei, R. (2011). Delay-and-sum beamforming for direction of arrival estimation applied to gunshot acoustics. *SPIE 8019, 8019U.*

Ramos, A. L., Holm, S., Gudvangen, S., & Otterlei, R. (2013). A spectral subtraction based algorithm for real-time noise cancellation with application to gunshot acoustics. *International Journal of Electronics and Telecommunications, 59*(1), 93-98.

Raytheon Corp, C. (2017, May 8). *Boomerang*. Retrieved June 9, 2017, from http://www.raytheon.com/capabilities/products/

Reed, J. W. (1977). Atmospheric attenuation of explosion waves. *The Journal of the Acoustical Society of Americ, 61*(1), 39-47.

Sallai, J., Lédeczi, Á., & Völgyesi, P. (2011). Acoustic shooter localization with a minimal number of single-channel wireless sensor nodes. *Proceedings of the 9th ACM Conference on Embedded Networked Sensor Systems* (pp. 96-107). ACM.

Sallai, J., Völgyesi, P., Lédeczi, Á., Pence, K., Bapty, T., Neema, S., & Davis, J. (2013). Acoustic shockwave-based bearing estimation. *Proceedings of the 12th international conference on Information processing in sensor networks* (pp. 217-228). ACM.

Schroeder, M. R. (1962). Natural sounding artificial reverberation. *Journal of the Audio Engineering Society, 10*(3), 219-223.

Stoughton, R. (1997). Measurements of small-caliber ballistic shock waves in air. *The Journal of the Acoustical Society of America, 102*(2), 781-787.

Svaizer, P., Matassoni, M., & Omologo, M. (1997). Acoustic source location in a three-dimensional space using crosspower spectrum phase. *Acoustics, Speech, and Signal Processing, 1997. ICASSP-97., 1997 IEEE International Conference. 1*, pp. 231-234. IEEE.

Van Veen, B. D., & Buckley, K. M. (1988). Beamforming: A versatile approach to spatial filtering. *IEEE assp magazine, 5(2)*, 4-24.

Völgyesi, P., Balogh, G., Nadas, A., Nash, C. B., & Ledeczi, A. (2007). Shooter localization and weapon classification with soldier-wearable networked sensors. *Proceedings of the 5th international conference on Mobile systems, applications and services* (pp. 113-126). ACM.

Ward, D. B. (2002). Performance of microphone array geometries in a reverberant room. *Transactions on Emerging Telecommunications Technologies, 13*(2), 133-138.

Whitham, G. B. (1952). The flow pattern of a supersonic projectile. *Communications on pure and applied mathematics, 5*(3), 301-348.

APPENDICES

APPENDIX A

ANALYTICAL EXPRESSION OF MUZZLE BLAST

Fransler et al. (1993) have proposed an analytical expression of muzzle blast signal shown in (60). In detail, the total wave muzzle blast signature is divided into two regions namely positive phase for positive values of overpressure and negative phase for negative values of pressure. While positive phase is described by Friedlander wave equation (Baker, 1973), negative phase is described by Reed's (1977) wave equation with a modification so that summation of integral of positive and negative phases is equal to zero (Fransler et al., 1993).

$$p(t) = \begin{cases} P_0 \left(1 - \dfrac{(t - t_a)}{\tau} \right) \exp\left(-\dfrac{(t - t_a)}{\tau} \right) & t_a \leq t \leq t_a + \tau_+ \\ 0.751 P_0 \left(1 - \dfrac{(t - t_a)}{\tau_+} \right) \left(1 - \dfrac{(t - t_a)}{3.67\tau} \right) \left(1 - \left(\dfrac{(t - t_a)}{3.67\tau} \right)^2 \right) & t_a + \tau_+ \leq t \leq \tau \end{cases} \tag{60}$$

$$
\begin{aligned}
p \quad &: \quad \text{Pressure Change in Time} \\
P_0 \quad &: \quad \text{Overpressure Peak} \\
\tau_+ \quad &: \quad \text{Positive Phase Duration} \\
\tau \quad &: \quad \text{Total Wave Duration} \\
t_a \quad &: \quad \text{Time of Arrival (ToA)}
\end{aligned}
$$

The analytical expression of muzzle blast (60) is utilized to perform tests and simulations in Chapter 7. In order to handle more realistic signals instead of ideal ones, measurements such as noise, reverberation and delays are taken into consideration by straightforward mathematical operations and signal processing methods. In detail, reflections and reverberations are simulated by the method described in Appendix C and additive white Gaussian noise is applied to signal to obtain desired SNR.

APPENDIX B

ANALYTICAL EXPRESSION OF SHOCKWAVE

Acoustic shockwave signals generated by supersonic projectile can be described with an analytical expression. Whitham (1952) has studied the properties of "N" shaped shockwave signal. He associated the shockwave wavelength to the caliber and length of the projectile, and the closest distance from the measurement point to the bullet trajectory (Whitham, 1952). In this concept, shockwave signals can be expressed analytically as shown in (61) while taking into account the peak amplitude and period (62) and (63) of shockwave (Libal & Spyra, 2014).

$$p(t) = \begin{cases} A\left(1 - \dfrac{2}{L}(t - t_a)\right) & t_a \leq t \leq t_a + T \\ 0 & o.w. \end{cases} \tag{61}$$

$$A = \frac{0.53 P_0 \left(M^2 - 1\right)^{1/8} \Phi}{d^{3/4} l^{3/4}} \tag{62}$$

$$T = \frac{1.82 M d_{MP}^{1/4} \Phi}{c\left(M^2 - 1\right)^{3/8} l^{1/4}} \approx \frac{1.82 \Phi}{c}\left(\frac{M d_{MP}}{l}\right)^{1/4} \tag{63}$$

p	:	Pressure Change in Time	Φ	:	Caliber
A	:	Shockwave Peak Amplitude	l	:	Length of Projectile
T	:	Shockwave Period	d_{MP}	:	Distance of Miss Point
t_a	:	Time of Arrival (ToA)	M	:	Mach Number
P_0	:	The Atmospheric Pressure	c	:	Speed of Sound

The analytical expression of shockwave in (61) which is relied on the amplitude and period shown in (62) and (63), is used to perform tests and simulations in Chapter 7. Equation (61) leads to theoretical shockwave signal, thus, effect of reverberation and reflection, described in Appendix C, and additive white noise is applied to ideal signal to obtain more realistic shockwave signal likewise muzzle blast signals described in Appendix A

APPENDIX C

MODEL OF REFLECTION AND REVERBERATION

Acoustic signals are subject to reflection due to surrounding physical obstacles or solid surfaces since it is a physical phenomenon. Hence, solid surfaces cause multipath reflections and reverberation in urban or open terrains for gunshot acoustic events. In other words, gunshot related recorded signals involve not only the original signals but also the reflections with delays according to the path. This phenomenon is applied to muzzle blast and shockwave signals generated ideally, described in Appendix A and Appendix B, for simulation and test purpose in Chapter 7.

The reflected signal is another signal which has a similar waveform of an original signal with a delay depending on the difference between the path of the original signal and the reflected signal. Furthermore, it has lower frequency components more than higher frequency components since higher frequencies are absorbed much more than lower frequencies. In addition, multipath reflections cause continuous stream with decaying amplitude which is called reverberation. A reflected signal can be simply expressed with a gain factor α less than 1 and time delay D as shown in (64).

$$x_R[n] = \alpha \, x[n - D] \tag{64}$$

Equation (64) can be used to simulate single reflected signal but it lacks real conditions such as decaying multiple reflections and reverberation. Schroeder (1962) has proposed a method for simulating the effect of reflection and reverberation by using a combination of comb filters. Infinite impulse response (IIR) and all pass comb filters shown in Figure C.1 are applied to ideal muzzle blast and shockwave signals to obtain decaying multiple reflection effects. In detail, Multipath reflection IIR filters are used to simulate multiple decaying reflected signals adjusted by delay and gains. Then, cascaded all-pass reverberator filters are applied to the sum of outputs of those filters

to obtain more natural reverberation. Finally, the output of all-pass filters is summed with the original signal. The overall block diagram is illustrated in Figure C.2. The delays of IIR filters can be set according to arbitrary reflection path lengths by (65) and delays of all-pass filters are set among the same set since all-pass filters are used for reverberation. Decay factors can be set randomly providing it is less than 1.

$$H = \frac{Z^{-D}}{1 - \alpha Z^{-D}}, \quad |\alpha| < 1$$

(a)

$$H = Z^{-D} \frac{1 + \alpha Z^{D}}{1 + \alpha Z^{-D}}, \quad |\alpha| < 1$$

(b)
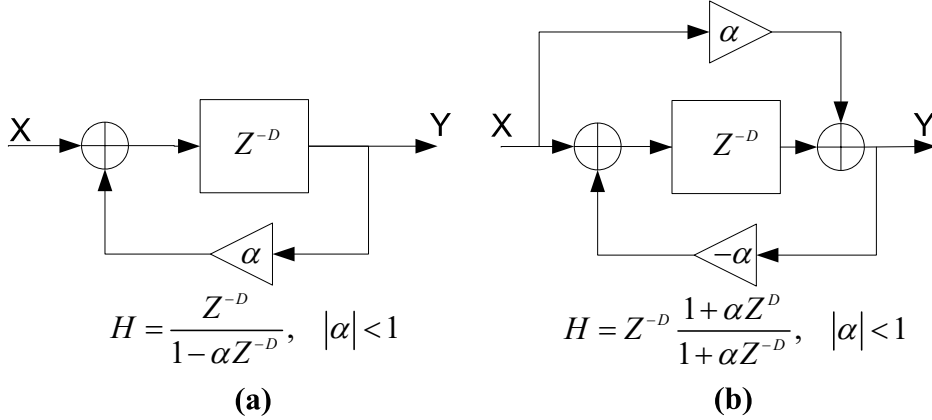
Figure C.1: Multiple Reflection IIR Filter (a) and All Pass Reverberator (b)
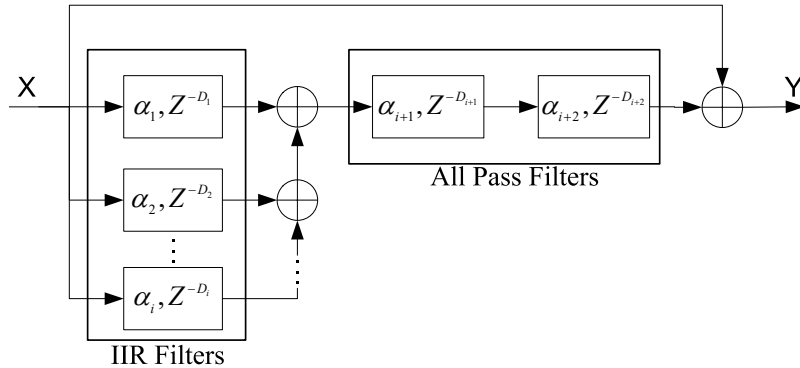
Figure C.2: Overall Block Diagram for Reverberation

$$D_i = \frac{R_i}{c} \times f_s \tag{65}$$

R_i :Length of ith Reflection Path
f_s :Sampling Freqeuncy
c :Speed of Sound

Muzzle blast and shockwave depicted in Figure 2.3 and Figure 2.6 in Chapter 2 are obtained with the topology shown in Figure C.2 with proper delays and gain factors.

102

APPENDIX D

SPHERICAL COORDINATE SYSTEM

This section describes the spherical coordinate system used throughout this thesis as depicted in Figure D.1. All angular representations, notations, and DoA represented in the spherical coordinate system are subject to descriptions in this section.
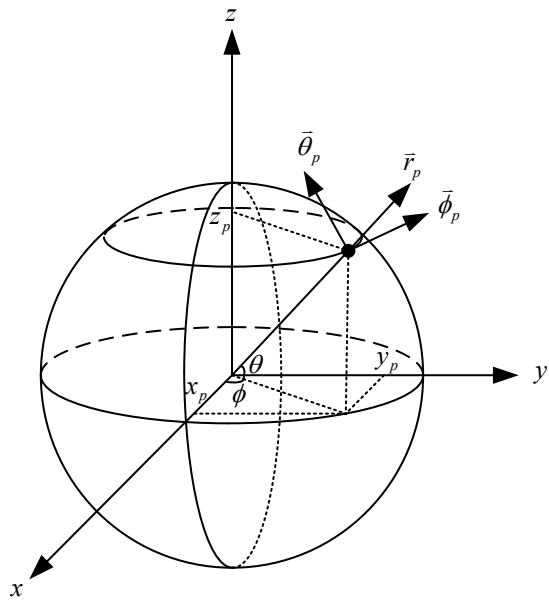

Figure D.1: Spherical Coordinate System

In the spherical coordinate system illustrated in Figure D.1, the azimuth angle is denoted by ϕ, defined in the x-y plane from the x axis with range of $[0 \; 2\pi]$ and elevation angle is denoted by θ defined from the projection line in the x-y plane to the z axis in the range of $[-\pi/2 \; \pi/2]$. Radius R is defined as the distance from the origin to a point on the sphere.

This thesis uses the spherical coordinate system to describe DoA unit vectors which have a radius equal to 1; thus, all DoA vectors in the spherical coordinate system are denoted with azimuth and elevation angles. In other words, directional information is

described with (ϕ, θ) and the range is described with R as a conventional representation in the order shown in (66).

$$u_{SPH}(\phi, \theta, R) = u_{SPH}(\phi, \theta), \quad R = 1 \tag{66}$$

DoA unit vectors are also represented in the Cartesian coordinate system throughout the thesis. The coordinate conversions from the spherical to Cartesian and Cartesian to spherical are shown in (67) and (68) for a point p, respectively.

$$
\begin{aligned}
\bar{P}(\phi_p, \theta_p, R_p) &\rightarrow \bar{P}(x_p, y_p, z_p) \\
x_p &= R \cos(\theta_p) \cos(\phi_p) \\
y_p &= R \cos(\theta_p) \sin(\phi_p) \\
z_p &= R \sin(\theta_p)
\end{aligned}
\tag{67}
$$

$$
\begin{aligned}
\bar{P}(x_p, y_p, z_p) &\rightarrow \bar{P}(\phi_p, \theta_p, R_p) \\
\phi_p &= \arctan\left(\frac{y_p}{x_p}\right), \quad \phi_p \in [0 \quad 2\pi] \\
\theta_p &= \arcsin\left(\frac{z_p}{\sqrt{x_p^2 + y_p^2 + z_p^2}}\right), \quad \theta_p \in \left[-\frac{\pi}{2} \quad \frac{\pi}{2}\right] \\
R &= \sqrt{x_p^2 + y_p^2 + z_p^2} \\
R &= 1, \quad \text{for unit vectors}
\end{aligned}
\tag{68}
$$

There is a conventional representation for DoA and propagation direction of acoustic sources throughout the thesis. For example, direction of propagation of acoustic waves denoted by $\vec{u}_S(\phi, \theta)$ as shown in Figure 4.2 means that the waves move toward the location of sensor from the direction defined by azimuth angle of ϕ and elevation angle of θ. On the other hand, this is not the DoA of source, DoA is equal to opposite direction of $\vec{u}_S(\phi, \theta)$ as shown in Figure 3.1, as an assumption. Those assumptions are made for sake of simplicity in sign operations.